EFFECT OF CONFINEMENT ON DUCTILITY OF RC HOLLOW CIRCULAR COLUMNS

A DISSERTATION

Submitted in partial fulfilment of the requirements for the award of the degree of

MASTER OF ENGINEERING

in

EARTHQUAKE ENGINEERING

(With Specialization in Structural Dynamics)

By

M. LAKSHMI NARASIMHA RAO

DEPARTMENT OF EARTHQUAKE ENGINEERING
UNIVERSITY OF ROORKEE
ROORKEE–247 667 (INDIA)

JANUARY, 2000

CANDIDATE'S DECLARATION

I hereby declare that the work which is being presented in this dissertation titled, **"EFFECT OF CONFINEMENT ON DUCTILITY OF RC HOLLOW CIRCULAR COLUMNS"**, in partial fulfilment of the requirements for the award of degree of **MASTER OF ENGINEERING IN EARTHQUAKE ENGINEERING,** with specialisation in **STRUCTURAL DYNAMICS,** submitted in the Department of Earthquake Engineering, University of Roorkee, Roorkee, India, is an authentic record of my own work carried out during the period from July, 1999 to January, 2000, under the supervision of **Dr. DURGESH C. RAI,** Lecturer, Department of Earthquake Engineering, University of Roorkee, Roorkee.

The matter embodied in this dissertation has not been submitted by me for the award of any other degree.

Dated: January 31st, 2000
Place: Roorkee

M. Lakshmi Narasimha Rao

This is to certify that the above statement made by the candidate is correct to the best of my knowledge.

Dr. Durgesh C. Rai
Lecturer
Department of Earthquake Engineering
University of Roorkee
Roorkee

ACKNOWLEDGEMENTS

I wish to express my deepest and sincere gratitude to Dr. Durgesh C. Rai, Assistant Professor, Department of Earthquake Engineering, for his invaluable professional guidance, continuous encouragement, valuable suggestions and inspiration through out my course of study.

Special thanks are due to Prof. N.C. Nigam, Ex-Vice Chancellor, University of Roorkee and Prof.S. Basu, Department of Earthquake Engineering, who encouraged me a lot in successfully completing my studies in this department ,with their tutorial classes and teaching efficiency .

I would like to take this opportunity to express my thanks to Santosh Kumar Thakur and Venkatesh, who provided the PC at nights in the intial stage of this dissertation work and helped me to complete in time. I would like to express thanks to all my friends DSR,Venku and others with whom I enjoyed my one and half year life in Roorkee far from my native.

I know there is no adequate words to express my gratitude to my parents and my brothers Ramu, Chanti, Goutham and my sister Preethi for their love, understanding and support given by them throughout my studies here at Roorkee. I am mostly grateful to my friends Anil, Kiran and Kalyan for their invaluable love and encouragement.

M. L. Narasimha Rao

(LAKSHMI NARASIMHA RAO MADDALI)

ABSTRACT

EFFECT OF CONFINEMENT ON DUCTILITY OF RC HOLLOW CIRCULAR COLUMNS

Generally the hollow concrete members are used in locations where the cost of concrete is relatively high or in situations where the weight of concrete is to kept minimum. In the case of columns, i.e., the hollow circular columns are used as bridge piers, staging for elevated water tanks, power poles and sign posts. In earthquake prone areas, these members are subjected to large seismic or lateral forces and expected to undergo large inelastic deformations. To sustain these inelastic deformations the member should have good ductility, i.e., the ability to dissipate energy with out degradation of strength. The widely usage of these hollow circular columns forced to study their available curvature ductility and flexural strength.

It has well established that well confined concrete members can sustain large inelastic strains without significant loss of strength. ~~In the case of~~ hollow circular column members having sufficient thickness to ~~provide~~ two layers of longitudinal and transverse reinforcement on the ~~both~~ inside and outside faces of the cross-section, behaves in ductile manner and sustain large inelastic strains due to proper confinement of core concrete. However in the case of hollow circular sections with small cross-sectional size, it may not be convenient to provide two layer of steel. In such situations only one layer of steel is provided ~~at~~ near the outside face of the column cross section. Though it is simple arrangement , it behaves in brittle manner.

In this study ~~only~~ the behaviour of the hollow circular columns with small thickness, provided with one layer of steel near the outside face is considered and analysed. For that purpose ~~we need~~ the complete stress-strain behaviour of confined concrete , unconfined concrete and steel ~~which~~ are used in moment-curvature analysis to know available curvature ductility and derive design charts for circular hollow columns section with different thickness. The confined concrete model of Hoshikuma et al. (1997) of solid column (circular)sections is considered and modified for hollow circular sections with

appropriate modification factors to match experimental results taken from the paper (Zahn,Park and Prestley 1990), though it is giving reasonable results with experimental results in the case of solid circular sections, because in the case of hollow circular sections the stresses are biaxial in nature as contrast to solid which are triaxial.

A computer program is developed for moment-curvature analysis and change in ductility with different factors like transverse reinforcement ratio, longitudinal reinforcement ratio, the axial force on the column, the yield strength of longitudinal steel and strength of the concrete. Design charts are derived for different thickness hollow circular sections. A design procedure is given for the ductility design of columns using these design charts.

In this study it is observed that the hollow circular columns showing less ductility capacity due to improper confinement of inside face ~~concrete~~ as described earlier. However, the curvature ductility of hollow circular column sections mainly effected by axial load ratio on the column, longitudinal reinforcement ratio and transverse reinforcement ratio.

TABLE OF CONTENTS

LIST OF TABLES

Table

LIST OF FIGURES

FIGURE

CHAPTER 1.

INTRODUCTION

1.1. GENERAL

Generally hollow reinforced concrete members are preferred in locations where the cost of concrete is relatively high or in situations where the weight of concrete is to be kept minimum. As in the case of columns, hollow columns which are used as bridge piers, power poles and staging for elevated tanks. If these members are subjected to seismic or lateral forces during large earthquakes they are expected to undergo large inelastic deformations. To sustain such inelastic deformations, they should behave in ductile manner. It has been well established that, concrete well confined by proper transverse reinforcement behave in ductile manner and can sustain large deformations without significant loss of strength.

Previously Mander, Prestly, Park and Carr have investigated the flexural strength and available ductility of rectangular, square and circular hollow reinforced concrete column sections, providing with layers of longitudinal and transverse reinforcement near both inside and outside faces of the section and tied through the wall thickness by transverse reinforcement. These type of columns perform in ductile manner during cyclic loading due to proper confinement of core concrete in between the inside and outside reinforcement layers.

For the columns sections whose thickness is small, it is not convenient to provide layers of reinforcement at both faces of the column section. In such cases it may be possible to provide longitudinal and transverse reinforcement at the outside face of the cross section only. This leads to the simple arrangement of reinforcement. But these columns behave in brittle manner due to insufficient confinement of core concrete.

This study, only deals with hollow circular columns having small thickness. In this case, the spiral or circular hoop reinforcement placed near the outside face of the cross-section restrains the growth of the tube diameter caused by longitudinal compression. The resulting spiral bar stress applies a radial pressure f_r to the outside face of the core of the tube, which in turn causes a circumferential compressive stress, σ_2 in the curved tubular wall. This situation is shown in Fig. 1.1. (a),(b) and (c). The circumferential compressive stress, σ_2 puts a concrete element cut out of the curved wall, into biaxial compression with the primary stress, σ_1 arising from axial load and flexure (Zahn, Park & Prestley 1990).

In contrast to the situation in a solid confined concrete section, there is no compressive confining stress in hollow column sections, acting on the inside face of the curved wall in the radial direction. Therefore in the case of solid confined columns, the state of stresses is triaxial and in the case of hollow confined columns it is biaxial.

1.2. NECESSITY OF DUCTILITY IN EARTHQUAKE RESISTANT DESIGN

To minimise major damage and to ensure the survival of reinforced concrete members with moderate resistance with respect to lateral forces, these members must be

capable of sustaining a high proportion of their initial strength when a major earthquake imposes large inelastic deformations. These deformations may be well beyond the elastic limit. The ability of the structure or member or of the materials used to offer resistance in the inelastic domain of response, is described by the general term "Ductility". It includes the ability to sustain large deformations and a capacity to absorb energy by hysteric behaviour without significant loss of strength. This ductility may be defined in different terms like strain ductility, curvature ductility and displacement ductility. For this reason, it is the single most important property sought by the designer of structures located in regions of significant seismicity.

Ductility in structural members can be developed only if the constituent material itself is ductile. Thus, it is relatively easy to achieve the desired ductility if resistance is to be provided by steel in tension. Concrete is inherently a brittle material. But with proper confinement of transverse reinforcement, these concrete members become capable of meeting the inelastic deformation demands imposed by severe earthquakes.

1.3. OBJECTIVE AND SCOPE OF THE STUDY:

The primary objective of the study is to review the effect of confinement on ductility of hollow circular column sections with small thickness provided with only one layer of longitudinal and transverse reinforcement near the outside face of the cross-section only. To prepare design charts for available curvature ductility of hollow circular column sections of different thickness (i.e., the variation of curvature ductility with longitudinal reinforcement ratio and axial load ratio on the column). Modifying the stress-strain model of confined concrete of Hoshikuma et al. (1997) to apply for hollow

circular sections. Giving the appropriate modification factors for the above model, which satisfy the experimental results of moment and curvature of column sections given in the technical paper(Zahn, Park & Pristley 1990). The data used for the moment curvature analysis of column section described above is shown in Table. 1.1. Estimation of available curvature ductility and displacement ductility factors of typical hollow circular staging for elevated water tanks. Analytical study of factors effecting the curvature ductility of hollow circular column sections was done. A brief design procedure is given for the design of hollow circular columns for ductility based on design charts.

CHAPTER 2.

BEHAVIOUR AND MODELLING OF CONFINED CONCRETE

2.1. STRESS-STRAIN MODELLING

Generally the strain distribution corresponds to a simple diagram as shown in the Fig. 2.1. However the stress distribution is considerably more complicated. The general stress-strain diagram for concrete can be assumed to have the appearance as shown in Fig. 2.2.(a). A characteristic feature of this diagram is that the stress-strain curve reaches a maximum value, f_{cc} and then continues downward beyond this maximum value. The diagram can be considered to be fairly typical for normal structural concrete and corresponds to the general conditions. This behaviour is more or less pronounced for various types of concrete.

The stress-strain diagram generally consists of three parts.: the ascending branch, the descending branch and the sustaining branch. The ascending branch is from zero stress to the peak compressive stress. The descending branch is from peak compressive stress to the residual stress. The sustaining branch is from strain corresponding to residual stress to large strains.

Attempts have been made to represent the three parts of stress-strain curve shown in Fig. 2.2.(b) by means of mathematically defined expressions. A number of models have been proposed to represent the behaviour of concrete. In these models, most

of them described the ascending branch as second order parabola, the descending and the sustaining branches as straight lines.

2.1.1. UNCONFINED CONCRETE MODEL:

Unconfined concrete means concrete, which is not reinforced with transverse reinforcement i.e., plain concrete. To know the actual stress-strain relationship of unconfined concrete, many investigators developed different models to satisfy the experimental results as shown in Fig. 2. 4. Generally speaking, for unconfined concrete the maximum stresses occur at a compressive strain varying between 0.0015 and 0.002. A limiting value for the maximum strain in practical cases is 0.003 to 0.004. In Indian code IS: 456-1978, the maximum strain for unconfined concrete is 0.0035 and maximum stress occurs at 0.002 strain. Among many proposed models, the well-approved model for unconfined concrete is Hognestad model which is shown in Fig. 2.2.(a). It has the ascending branch as second order parabola and the descending branch as straight line. In practice it is not possible to utilise the unconfined concrete up to large compressive strains i.e., up to 0.008 as shown in Fig. 2.3. The unconfined concrete cannot sustain up to large strains, due to that reason, there is no sustaining branch in unconfined concrete models.

2.1.2. NECESSITY OF CONFINED CONCRETE

Concrete restrained in the directions at right angle to the applied stress by transverse reinforcement, is usually referred as confined concrete. In earthquake prone areas, the reinforced concrete members subjected to seismic or lateral forces undergo large inelastic deformations. These inelastic deformations cannot be sustained by

unconfined concrete due to small ultimate stain (i.e., up to 0.003 to 0.004). It is well known fact that the confinement of concrete by suitable arrangement of transverse reinforcement in the form of spiral or hoop increases the energy absorption capacity (toughness), ductility of the members and can sustain large strains. Confinement of the core concrete is essential if the member is to have a reasonable plastic rotational capacity in plastic hinge regions.

At low level of axial compressive stress, the transverse reinforcement is barely stressed and thus the concrete is unconfined. The concrete becomes confined when the axial stress approaches the uniaxial strength of concrete. At this stage the volume of the concrete increases due to progressive internal fracturing and bears out against the transverse reinforcement which then applies a confining reaction to the concrete which is given by f_l ,as shown in Fig. 2.5. f_l is known as confining force due to transverse reinforcement , it is given by the following equation,

$$f_l = \frac{2 f_{yh} A_{sp}}{d_s s_h} \tag{2.1}$$

In the above equation, f_{yh} is the yield strength of the transverse reinforcement, d_s is the diameter of the transverse reinforcement A_{sp} is the area of the bar and s_h is the longitudinal spacing of the transverse reinforcement. Due to this confinement the stress-strain characteristics of concrete can be improved considerably. The increase in concrete strength due to confinement f_{cc} is given by the equation (Paulay & Prestley 1992),

$$f_{cc} = f_{co} + 4f_l \tag{2.2}$$

In the above equation f_{co} is unconfined concrete strength, f_l is confining force.

2.1.3. FACTORS EFFECTING THE CONFINEMENT

2.1.3.1. Hoop Reinforcement Ratio

It should be noted that the initial stiffness is independent of hoop reinforcement ratio. As the volumetric ratio of hoop reinforcement increases, both the peak stress and the strain at peak stress increase and severe deterioration of concrete after the peak stress prevented. The hoop reinforcement ratio increases the confining force, is described in Eqn. 2.1 increases the confinement of concrete i.e., the strength of concrete as shown in Eqn. 2.2.

2.1.3.2. Spacing of Hoop Reinforcement

With increase in spacing of hoop reinforcement spacing, maintaining the same volumetric ratio of hoop reinforcement, it is seen that the deterioration after the peak stress is considerable. Though the spacing does not increase the confining force in the case of same volumetric ratio of hoop reinforcement, it decreases the unconfined portion of concrete and it increases the strength of concrete.

2.1.3.3. Hoop Reinforcement Configuration

Spiral or circular hoops, because of their shape, are placed in hoop tension by the expanding concrete and thus provide a continuous confining force around the circumference, as shown in Fig. 2.5. Square or rectangular hoops can only apply full confining reactions near the corners of the hoops because the pressure of the concrete

against the sides of the hoops tends to bend the sides outward as shown in Fig. 2.5. The confinement provided by the square or rectangular hoops can be significantly improved by the use of overlapping hoops or hoops with cross-ties, which results in several legs crossing the section. The better confinement resulting from the presence of a number of transverse bar legs is shown in Fig.2.5. The arching action is more efficient since the arches are shallower and hence more of the concrete area is effectively confined. The presence of a number of longitudinal bars well distributed around the perimeter of the section, tied across the section, will also aid the confinement of concrete (Sheikh & Uzumeri 1982).

2.1.3.4. Aspect Ratio of the Section

Aspect ratio of the section is defined as ratio of breadth to depth of the section. It can be seen that when a constant amount of hoop reinforcement is provided, the peak stress and the ductility deteriorate as the aspect ratio of the section increases.

2.1.4. CONFINED CONCRETE MODEL

It is essential to know the complete stress-strain relationship of confined concrete for moment-curvature analysis of reinforced concrete members to derive design charts and indicate the flexure strength and ductility of the member. These design charts also gives the required transverse reinforcement to achieve particular curvature-ductility and displacement ductility factors in the plastic hinge regions of reinforced concrete members. Confined concrete stress-strain model contains three parts as described earlier, i.e., an ascending branch, falling branch and sustaining branch as shown in Fig. 2.2.(b). In the most of the stress-strain models of confined concrete proposed previously, the

ascending branch has been formulated by a second-order parabola. This is because a second-order parabola is a simple mathematical expression and it represents well the stress-strain relation. The falling branch has been formulated by a straight line, which is given by the parameters on which confinement depends. The sustaining branch also has been formulated as a straight line.

2.1.5. DIFFERENT MODELS OF CONFINED CONCRETE

Various studies on the confinement effects of lateral reinforcement in reinforced concrete members have already been conducted and proposed. Different models as shown in Table.2.1.

2.1.5.1. Kent and Park Model (1971)

Kent and Park (1971) proposed a stress-strain model for confined concrete as shown in Fig. 2.6, consisting of a second order parabola for ascending branch and a straight line for descending branch. According to this model there is no increase in strength of concrete due to confinement, however, the confinement effects the slope of the descending branch. Park et.al.(1982) revised the model to introduce the increase in concrete strength caused by confinement. It was assumed that the confinement effect was proportional to the volumetric ratio of transverse reinforcement and yield strength of hoop reinforcement. Ascending branch equation is given by

$$f_c = f_c'\left[\frac{2\varepsilon_c}{\varepsilon_o} - \left(\frac{\varepsilon_c}{\varepsilon_o}\right)^2\right] \qquad (2.3)$$

In the above equation ε_c is concrete strain, ε_o is strain in concrete at peak stress,

f_c' that is assumed to 0.002, f_c' is compressive strength of confined concrete in member and f_c is confined concrete stress. Descending branch equation is given by,

$$f_c = f_c'\left[1 - Z(\varepsilon_c - \varepsilon_o)\right] \tag{2.4}$$

where, Z is a coefficient defined by Kent and Park (1971). The sustaining branch has a stress $0.2 f_c'$ from ε_{20c} to infinity because concrete can sustain some stress at indefinitely large strains (Kent & Park 1971).

2.1.5.2. Sheikh and Uzumeri Model (1982)

Sheikh and Uzumeri (1980,1982) proposed a stress-strain model as shown in the Fig. 2.7 that reflects the confinement effect by adjusting the peak stress and a confinement effectiveness coefficient. The confinement effectiveness coefficient depends on the configuration of hoop reinforcement. The deterioration rate of the falling branch is similar to that in the model of Park et al. (1982). This is the only model which gives a broad peak stress as shown in Fig. 2.7. The ascending branch equation is given by,

$$f_c = K_s f_{cp}\left[\frac{2\varepsilon_c}{\varepsilon_{s1}} - \left(\frac{\varepsilon_c}{\varepsilon_{s1}}\right)^2\right] \tag{2.5}$$

In the above equation f_c is confined concrete stress, f_{cp} is unconfined concrete compressive strength, K_s is confinement effectiveness coefficient, ε_c is confined concrete strain, ε_{s1} minimum strain corresponding to maximum stress. The descending branch equation is given by,

$$f_c = f_{cp}\left(1 - Z(\varepsilon_c - \varepsilon_{s2})\right) \tag{2.6}$$

The coefficient Z is the same as in the Kent and Park (1971). In the above equation ε_{s2} is the maximum strain at the maximum stress. The sustaining branch has the stress of $0.3\,f_{cp}$ from ε_{s30} to infinite strains (Sheikh & Uzumeri 1982).

2.1.5.3. Mander et al Model (1988)

Mander et al. (1988) proposed a stress-strain model as shown in Fig. 2.8. This is the only model that gives a fractional expression to represent both the ascending and descending branches of the stress-stain curve. To evaluate the peak stress, a confinement effectiveness coefficient for circular, square and wall-type sections was introduced based on a theory similar to Sheikh et al. (1980-1982). The only equation for the both ascending and descending branches as shown below.

$$f_c = \frac{f_{cc} x r}{r - 1 + x^r} \tag{2.7}$$

In the above equation f_c is the confined concrete stress, f_{cc} is confined concrete compressive strength, x is the ratio of concrete strain to strain at peak stress, r is a factor depends on tangent and section modulus of concrete. There is no sustaining branch according to this model. This model gives directly ratio of confined compressive strength, f_{cc} and unconfined compressive strength, f_{co} when the concrete core is placed in triaxial compression with equal effective lateral confining force, f_l' from spirals or circular hoops by the following equation,

$$f_{cc}/f_{co} = \left[-1.254 + 2.254\sqrt{1 + \frac{7.94 f_l'}{f_{co}}} - \frac{2 f_l'}{f_{co}} \right] \quad \textbf{(2.8)}$$

For rectangular sections this ratio of confined and unconfined compressive strength can get from the graph as shown in Fig. 2.9 after knowing f_{l1}' and f_{l2}' (Mander et al. 1988).

2.1.5.4. Saatcioglu and Razvi Model(1992)

Saatcioglu and Razvi proposed a model in 1992 as shown in Fig. 2.10. This model consists of a parabolic ascending branch, followed by a linear descending segment without sustaining branch. The falling branch is a function of the strain corresponding to 85% of the peak stress. This model is based on the computation of confinement pressures starting from the material and geometric properties of columns. Different distributions of pressures resulting from different arrangements of reinforcement are expressed in terms of equivalent uniform pressures. The actual, average and equivalent pressures are as shown in Fig. 2.11. The equation of the ascending branch is given by,

$$f_c = f_{cc}\left[2\left(\frac{\varepsilon_c}{\varepsilon_{cc}}\right) - \left(\frac{\varepsilon_c}{\varepsilon_{cc}}\right)^2 \right]^{\frac{1}{1+2K}} \quad \textbf{(2.10)}$$

In the above equation f_c is the confined concrete stress, f_{cc} is the confined concrete compressive strength, ε_c is the strain in confined concrete, ε_{cc} is strain at peak stress, K is a coefficient which depends on equivalent effective lateral pressure and unconfined concrete compressive strength. The falling branch equation is given by

$$f_c = f_{cc} - \frac{0.15 f_{cc}}{\varepsilon_{85} - \varepsilon_{cc}}(\varepsilon_c - \varepsilon_{cc}) \tag{2.11}$$

$$f_{cc} = f_{co} + k_1 f_l \tag{2.12}$$

In the above Eqn 2.11, ε_{85} is the strain at 85% of the peak stress, in Eqn 2.12 f_{co} is the unconfined concrete compressive strength, k_1 is the coefficient given below, f_l is the confining force described in Eqn.2.1.

$$k_1 = 6.7(f_l)^{-0.17} \tag{2.13}$$

2.1.5.5. Hoshikuma et al. Model(1997)

Hoshikuma et al. proposed a model for confined concrete in 1997. This model also consists of parabolic ascending branch followed by linear descending branch without sustaining branch. According to this model, the main factors for controlling the stress-strain relation of confined concrete are the peak stress, the strain at the peak stress and the slope of the falling branch, i.e., the deterioration rate. In this model all these factors are expressed in terms of one coefficient known as confinement effectiveness factor. The confinement effectiveness factor mainly depends on the volumetric ratio of transverse reinforcement ρ_s, the yield strength of transverse reinforcement f_{yh} and the unconfined compressive strength of concrete f_{co}.The ascending branch equation is given by Eqn. 2.13 and the falling branch branch equation given by Eqn. 2.15,

$$f_c = E_c \varepsilon_c \left[1 - \frac{1}{n} \left(\frac{\varepsilon_c}{\varepsilon_{cc}} \right)^{n-1} \right] \tag{2.13}$$

$$n = \frac{E_c \varepsilon_{cc}}{E_c \varepsilon_{cc} - f_{cc}} \tag{2.14}$$

$$f_c = f_{cc} - E_{des} (\varepsilon_c - \varepsilon_{cc}) \tag{2.15}$$

In the above Eqn. 2.13, f_c is confined concrete stress, E_c is the initial stiffness as shown in the Table 2.2, ε_c is the strain in the concrete, ε_{cc} is the strain corresponding the peak stress and n is the coefficient given by the Eqn. 2.14, f_{cc} is the confined concrete compressive strength. In the Eqn. 2.15 E_{des} is the deterioration rate.

2.1.6. COMPARISON OF DIFFERENT MODELS

For the comparison of different models, the experimental results of stress-strain curve of the confined column section are taken from the paper of Hoshikuma et al.(1997). The properties of the column section: 500 mm x 500 mm section with volumetric ratio of transverse reinforcement is 4.10% (16 mm diameter at spacing of 40 mm), the longitudinal reinforcement ratio is 0.95% and unconfined compressive strength of concrete is 24.3 MPa and yield strength of the transverse reinforcement steel is 295 MPa and height of the column member is 1000mm (Hoshikuma et al. 1997).

Kent and Park (1971) and Sheikh and Uzumeri (1982) models are only applicable to square sections. Mander et al.(1988), Saatcioglu and Razvi (1992) and Hoshikuma et al.(1997) models are applicable to circular, square, rectangular and wall-type sections. As shown in the Fig. 2.12, all other models except Hoshikuma et al.(1997) are predicting the slope of the ascending branch to be larger than the experimental results and at the

same time it can be seen that the peak stress f_{cc}, the strain at the peak stress ε_{cc} and deterioration rate i.e., the slope of the descending branch E_{des} also predicted more reasonable to experimental results.

As shown in Fig. 2.6, Kent and Park (1971) model is the first model for the confined concrete. According to this model there is no increase in strength of the concrete due to confinement, which is not a realistic behaviour of the confined concrete.

Mander et al.(1988) proposed a fractional expression given by Eqn. 2.7 for both the ascending branch and the descending branch of the stress-strain curve of the confined concrete unlike other models which are having two equations. In this model the ratio of confined compressive strength and unconfined compressive strength for circular members is given be the Eqn. 2.8. The elaborate procedure is there for other shape of members. At the same time the compressive strength ratio for the members other than circular members obtained only from graph which may cause some error in determining the strength of confined concrete.

Both Sheikh and Uzumeri (1982) and Saatcioglu and Razvi (1992) models predicted higher values for stresses than the experimental results. Shiekh and Uzumeri and Hoshikuma et al. (1997) models can not be used for unconfined concrete. The values for stresses given by Hoshikuma et al. (1997) model is reasonable agreement with the experimental results.

CHAPTER 3.

DUCTILITY

3.1. DUCTILITY OF REINFORCED CONCRETE MEMEBRS

As described in section 1.2, ductility is defined as the ability of the member and the constituent materials of the member to offer resistance in the inelastic domain of response. It includes the ability to sustain large deformations and a capacity to absorb energy by hysteric behaviour. Due to that it is the primary design aspect for the structures located in regions of significant seismicity. It is known that the ductility in the member can be developed only if the constituent material itself ductile. Concrete members are brittle in nature, i.e., the strength degradation is high as compared to ductile nature members like steel members, which is shown in Fig. 3.1. However the concrete members cab be rendered ductile by providing proper transverse reinforcement.

The limit of ductility, as shown in Fig. 3.2 by the displacement of Δ_u, typically corresponds to a specified limit to strength degradation. Although attaining this limit is sometimes termed as failure, significant additional inelastic deformations may still be possible without structural collapse. Hence a ductile failure must be contrasted with brittle failure, represented in the Fig. 3.2, by dashed curves. Brittle failure implies complete loss of resistance, often complete disintegration of strength in absence of adequate warning. For obvious reasons, brittle failure, which may be said to be other

overwhelming cause for the collapse of members in earthquakes, and the consequent loss of lives, must be avoided. Ductility is defined by the ratio of the total imposed displacements Δ at any instant to that at the onset of yield Δ_y.

$$\mu = \frac{\Delta}{\Delta_y} > 1 \tag{3.1}$$

The displacements Δ_y and Δ in Eqn. 3.1 and Fig. 3.2 may represent strain, curvature, rotation or deflection. The ductility developed when failure is imminent is, from Fig. 3.2, $\mu_u = \Delta_u / \Delta_y$. There are ~~so many~~ several ways to represent ductility.

- Strain Ductility
- Curvature Ductility
- Displacement Ductility

3.1.1. STRAIN DUCTILITY

The fundamental source of ductility is the ability of the constituent materials to sustain plastic strains without significant reduction of stress. By similarity to the response shown in Fig. 3.2 if the response is strain, strain ductility is simply defined as

$$\mu_\varepsilon = \frac{\varepsilon}{\varepsilon_y} \tag{3.2}$$

Where ε is the total strain imposed and ε_y is the yield strain. The strain imposed should not exceed the dependable maximum strain capacity ε_m.

The unconfined concrete exhibits very limited strain ductility in compression as compared to confined concrete. However, this can be significantly increased by

appropriately confining the concrete. A strain ductility of $\mu_\varepsilon = \varepsilon_m / \varepsilon_y > 20$, available for reinforcing bars as shown in Fig. 3.1.

Significant ductility in a structural member can be achieved only if inelastic strains can be developed over a reasonable length of that member. If inelastic strains are restricted to a very small length, extremely large strain ductility demands may arise, even during moderate inelastic structural response.

3.1.2. CURVATURE DUCTILITY

The most common and desirable sources of inelastic structural deformations are rotations in potential plastic hinge regions. Therefore, it is useful to relate section rotations per unit length (i.e., curvature) to causative bending moments. By similarity of Eqn. 3.1, the maximum curvature ductility is expressed as:

$$\mu_\phi = \phi_m / \phi_y \tag{3.4}$$

where ϕ_m is the maximum or ultimate curvature expected to be attained or relied on and ϕ_y is the yield curvature as shown in Fig. 3 3.

3.1.3. DISPLACEMENT DUCTILITY

The most convenient quantity to evaluate either the ductility imposed on a structure by an earthquake μ_m, or the structure's capacity to develop ductility μ_u, is displacement ductility. For the example cantilever in Fig. 3.4, the displacement ductility is

$$\mu_\Delta = \Delta / \Delta_y \tag{3.6}$$

where $\Delta = \Delta_y + \Delta_p$. The yield($\Delta_y$) and fully plastic($\Delta_p$) are components of the total lateral tip deflection Δ are defined in Fig. 3 4.

The yield deflection of the cantilever Δ_y, as defined in Fig. 3.4 for most reinforced concrete and masonry structures, is assumed to occur simultaneously with the yield curvature ϕ_y at the base. Its realistic estimate is very important because absolute values of maximum deflections $\Delta_m = \mu_\Delta \Delta_y \leq \Delta_u$ also need to be evaluated and related to the height of the structure over this displacement occurs.

3.1.4. RELATIONSHIP BETWEEN CURVATURE AND DISPLACEMENT DUCTILITY

For a simple structural element, such as the vertical cantilever of Fig. 3.4, the relationship between curvature and displacement ductilities can simply be expressed by integrating the curvatures along the height. Thus

$$\mu_\Delta = \frac{\Delta_m}{\Delta_y} = \frac{\int \phi(x) x dx}{\int \phi_e(x) x dx} = \frac{K_1 \phi_m}{K_2 \phi_y} = K \mu_\phi \tag{3.7}$$

where $\phi(x)$ and $\phi_e(x)$ are the curvature distributions at maximum response and at yield respectively. K,K_1 and K_2 are constants and x is measured down from the cantilever tip.

3.1.4.1. Yield Displacement:

The actual curvature distribution at yield, $\phi_e(x)$, will be non-linear as a result of the basic non-linear moment curvature relationship as shown in Fig. 3 4 and because of local tension stiffening between cracks. However, adopting the linear approximation suggested in Fig. 3.3 and shown in Fig. 3.4, the yield displacement may be estimated as

$$\Delta_y = \phi_y l^3 / 3 \tag{3.8}$$

3.1.4.2. Maximum or Ultimate Displacement:

The curvature distribution at maximum displacement Δ_m is represented by Fig. 3.4, corresponding to a maximum curvature ϕ_m at the base of the cantilever. For convenience of calculation, an equivalent plastic hinge length l_p is defined over which the plastic curvature $\phi_p = \phi - \phi_e$ is assumed equal to the maximum plastic curvature $\phi_m - \phi_y$. The plastic hinge length l_p is chosen such that the plastic displacement at the top of the cantilever Δ_p, predicted by the simplified approach is the same as that derived from the actual curvature distribution. The plastic rotation occurring in the equivalent plastic hinge length l_p is given by

$$\theta_p = \phi_p l_p = (\phi_m - \phi_y) l_p \tag{3.9}$$

This rotation is an extremely important indicator of the capacity of a section to sustain inelastic deformation. Assuming the plastic rotation to be concentrated at mid height of the plastic hinge, the plastic displacement at the cantilever tip is thus

$$\Delta_p = \theta_p\left(l - 0.5l_p\right) = \left(\phi_m - \phi_y\right)l_p\left(l - 0.5l_p\right) \tag{3.10}$$

The displacement ductility factor in Eqn. 3.6 is given by,

$$\mu_\Delta = \frac{\Delta}{\Delta_y} = \frac{\Delta_y + \Delta_p}{\Delta_y} = 1 + \frac{\Delta_p}{\Delta_y} \tag{3.11}$$

Substituting Eqn. 3.8 and Eqn. 3.10 in Eqn. 3.11 and rearranging yields the relationship between displacement and curvature ductility:

$$\mu_\Delta = 1 + 3\left(\mu_\phi - 1\right)\frac{l_p}{l}\left(1 - 0.5\frac{l_p}{l}\right) \tag{3.12}$$

or conversely,

$$\mu_\phi = 1 + \frac{\left(\mu_\Delta - 1\right)}{3\left(\frac{l_p}{l}\right)\left[\ - 0.5\frac{l_p}{l}\right]} \tag{3.13}$$

3.1.4.3. Plastic Hinge Length

Theoretical values for the equivalent plastic hinge length l_p based on integration of the curvature distribution for typical members would make l_p directly proportional to l. Such values do not, however, agree well with experimentally measured lengths. This is because, as shown in Fig. 3.4.(c) and (d) show, the theoretical curvature distribution ends abruptly at the base of the cantilever, while steel strains continue, due to finite bond stress, for some depth into the footing. The elongation of bars beyond the theoretical base leads to additional rotation and deflection. The phenomenon is referred to as tensile strain penetration. It is evident that the extent of strain penetration will be related to the reinforcing bar diameter, since large-diameter bars will require greater development

lengths. A second reason for discrepancy between theory and experiment is the increased spread of plasticity resulting from inclined flexure-shear cracking.

A good estimate of the effective plastic hinge length may be obtained from the expression (Park & Paulay 1990)

$$l_p = 0.08l + 0.022 d_b f_y \tag{3.14}$$

where d_b is diameter of longitudinal reinforcing bar and f_y is yield strength of longitudinal reinforcing bar in MPa.

CHAPTER 4.

MOMENT CURVATURE ANALYSIS OF REINFORCED CONCRETE MEMBERS

4.1. MOMENT CURVATURE ANALYSIS

Moment curvature analysis is needed to derive the design charts of the reinforced concrete members, from which we can know how much transverse or longitudinal reinforcement is needed in plastic hinge regions of the members for required curvature ductility corresponding to the displacement ductility factor. Theoretical moment-curvature curves for reinforced concrete sections with flexure and axial load can be derived on the basis of assumptions similar to those used for the determination of the flexural strength. It is assumed that plane sections before bending remain plane after bending and that the stress-strain curves for unconfined concrete, confined concrete and steel are known. The curvatures associated with a range of bending moments and axial loads may be determined using these assumptions and from the requirements of strain compatibility and equilibrium of forces.

Typical stress-strain curves for steel ,unconfined concrete and confined concrete are shown in Fig. 4.1 to 4.3. In this study for the moment curvature analysis taken the steel stress-strain curve as shown in Fig. 4 1 with strain hardening, stress-strain curve for the confined concrete is Hoshikuma et al.(1997) model as shown in the Fig. 4.2 and stress-strain curve for the unconfined concrete is taken form IS:456-1978 as shown in the

Fig. 4.3. A computer program is developed for moment curvature analysis of hollow circular sections by using these stress-strain curves.

4.1.1. STRESS-STRAIN MODEL FOR STEEL REINFORCEMENT

Stress-Strain curves for typical reinforcing steel measured during monotonic loading tests, such as shown in Fig. 3.1 can be idealised into an elastic region, a yield plateau, and a strain-hardening region, as shown in Fig. 4.1.The Stress-Strain curve up to elastic region is given by,

$$f_S = \varepsilon_S E_S \tag{4.1}$$

The Stress-Strain curve in the yield region is given by,

$$f_S = f_y \tag{4.2}$$

The Stress-Strain curve in the strain hardening region ($\varepsilon_{Sh} \le \varepsilon_S \le \varepsilon_{Su}$) can be predicted with good accuracy by,

$$f_S = f_{Su} - \left(f_{Su} - f_y\right)\left(\frac{\varepsilon_{Su} - \varepsilon_S}{\varepsilon_{Su} - \varepsilon_{Sh}}\right)^P \tag{4.3}$$

where E_S is modulus of steel, ε_S is steel strain, ε_{Sh} is steel strain at commencement of strain hardening, ε_y is steel strain at commencement of yielding, ε_{Su} is steel strain at the ultimate tensile strength of steel, f_S is steel stress at any instant, f_{Su} is the ultimate tensile strength of steel, f_y yield strength of the steel, P is the coefficient given below,

$$P = E_{Sh}\left(\frac{\varepsilon_{Su} - \varepsilon_{Sh}}{f_{Su} - f_y}\right) \tag{4.4}$$

where E_{Sh} is the strain-hardening modulus of steel.

4.1.2. STRESS-STRAIN MODEL FOR CONFINED CONCRETE

In this study for the moment-curvature anlaysis we taken Hoshikuma et al.(1997) confined concrete model, which is giving reasonable values compared to experimental results as shown in Fig. 2.12.

It can be seen in Fig. 2.2.(b) that the stress-strain curve consists of three parts ,i.e., an ascending branch, falling branch and sustaining branch. The ascending branch equation is given by,

$$f_c = E_c\varepsilon_c\left[1 - \frac{1}{n}\left(\frac{\varepsilon_c}{\varepsilon_{cc}}\right)^{n-1}\right] \tag{4.5}$$

where n is a coefficient given by

$$n = \frac{E_c\varepsilon_{cc}}{E_c\varepsilon_{cc} - f_{cc}} \tag{4.6}$$

where E_c is the initial stiffness is shown in the Table.2.2, ε_{cc} is the strain at the peak stress, f_c is concrete stress at any instant, ε_c is strain of concrete, f_{cc} confined concrete compressive strength. The falling branch equation is given by,

$$f_c = f_{cc} - E_{des}(\varepsilon_c - \varepsilon_{cc}) \tag{4.7}$$

where E_{des} is deterioration rate i.e., the slope of the falling branch of the stress-

strain curve. The ultimate strain of the concrete is given by,

$$\varepsilon_{cu} = \varepsilon_{cc} + \frac{f_{cc}}{2E_{des}} \tag{4.8}$$

According to this model factors controlling the stress-strain relation of confined concrete are the peak stress, the strain at peak stress and the slope of the falling branch, which are dependent on confinement effectiveness coefficient R. This confinement effectiveness coefficient depends on volumetric ratio, yield strength of transverse reinforcement and the unconfined compressive strength of concrete. The confinement effectiveness coefficient R is given by,

$$R = \frac{\rho_s f_{yh}}{f_{co}} \tag{4.9}$$

where f_{yh} is yield strength of transverse reinforcement, ρ_s is volumetric reinforcement of transverse reinforcement and f_{co} is the unconfined concrete compressive strength. Relation between the peak stress, the strain at peak stress and deterioration rate with confinement effectiveness coefficient R is follows.

4.1.2.1. Relation between Peak Stress and R:

In the case of circular and square sections, the peak stress f_{cc} of the confined concrete sections was normalised by the strength of unconfined concrete f_{co}. It can be seen that f_{cc}/f_{co} is directly proportional to the confinement effectiveness coefficient R. The relation may be approximated by a linear function, with the slope depending on the cross-sectional shape. It is noted that the slope of the linear approximation for the square section is approximately 20% of that for the circular section. This clearly shows the

dependence of confinement on the cross-sectional shape and the efficiency of circular hoops in confining the core concrete. The relations for the circular and square sections are given below,

$$\frac{f_{cc}}{f_{co}} = 1.0 + 3.83\frac{\rho_s f_{yh}}{f_{co}} \tag{4.10}$$

$$\frac{f_{cc}}{f_{co}} = 1.0 + 0.73\frac{\rho_s f_{yh}}{f_{co}} \tag{4.11}$$

4.1.2.2. Relation between Strain at Peak Stress and R

The strain at the peak stress ε_{cc} is directly proportional to the confinement effectiveness coefficient ,R. The relation approximated by a linear function. The confinement effectiveness on ε_{cc} for square sections is approximately 40% of that for circular sections. The relations are shown below,

for circular sections,

$$\varepsilon_{cc} = 0.00218 + 0.0332\frac{\rho_s f_{yh}}{f_{co}} \tag{4.12}$$

for square sections,

$$\varepsilon_{cc} = 0.00245 + 0.0122\frac{\rho_s f_{yh}}{f_{co}} \tag{4.13}$$

4.1.2.3. Relation between Deterioration Rate and R

The Deterioration Rate E_{des} is directly proportional to unconfined concrete compressive strength f_{co} and inversely proportional to the confinement effectiveness coefficient R. It is found from the data that the effect of cross-sectional shape does not

significantly influence the deterioration rate. Therefore a single expression approximated for the both circular and rectangular sections and the approximated relation is written as,

$$E_{des} = \frac{11.2 f_{co}}{R} = \frac{11.2}{\rho_s f_{yh} / f_{co}^2} \tag{4.14}$$

Finally in this model proposed only one equation for the peak stress f_{cc}, the strain at the peak stress ε_{cc} and deterioration rate E_{des} of both circular and square section section with modification factors:

$$\frac{f_{cc}}{f_{co}} = 1.0 + 3.8\alpha \frac{\rho_s f_{yh}}{f_{co}} \tag{4.15}$$

$$\varepsilon_{cc} = 0.002 + 0.033\beta \frac{\rho_s f_{yh}}{f_{co}} \tag{4.16}$$

$$E_{des} = 11.2 \frac{f_{co}^2}{\rho_s f_{yh}} \tag{4.17}$$

in which α and β are modification factors depending on confined concrete cross-sectional shape; for circular α = 1.0 and β = 1.0 ; for square α = 0.2 and β= 0.4.

4.1.2.4. Modification of Hoshikuma et al.(1997) Model for Circular Hollow Sections

The Hoshikuma et al. (1997) confined concrete model is giving good results as compared to experimental. However this model not given any information about hollow column sections. In the case of solid column sections as described above the modification factors α and β for solid circular column sections are 1.0 and,1.0 respectively. For solid square or rectangular sections 0.2 and 0.4 respectively. As described earlier the nature of stresses in hollow circular is biaxial as compared to solid

circular column which is triaxial in nature. Due to this reason in the hollow circular column the concrete near to inside is not confined properly, as in the case of square section the concrete at the corner only confined properly So, it can be assumed that the hollow circular column behaves as square column and modification factors are taken nearly same as for the square sections. In this study to apply Hoshikuma et al. Model (1997) to hollow circular sections, the equations are modified by appropriate modification factors α and β. Values for α and β as 0.20 and 0.45, respectively resulted in close match with (Zahn,Park & Prestley 1990) the experimental results of moment-curvature of hollow circular column sections whose data is given Table. 1.1.

4.1.3. STRESS-STRAIN MODEL FOR UNCONFINED CONCRETE

The stress-strain model for the unconfined concrete is taken from IS: 456-1978 as shown in Fig. 4.2. The peak stress is considered as 0.447 f_{ck} ,the strain at the peak stress is taken as 0.002 and the ultimate strain of unconfined concrete is taken as 0.0035. where f_{ck} is cube strength of concrete or characteristic strength of concrete.

4.2. THEORETICAL PROCEDURE FOR MOMENT CURVATURE ANALYSIS OF HOLLOW CIRCUALR COLUMN SECTIONS

The moment-curvature relationships are best calculated using a digital computer only. For that purpose here in this study a computer program is developed to give moment corresponding to curvatures values considering the stress-strain curves of unconfined concrete, confined concrete and steel as described earlier. In this study, as shown in the Fig. 4.4 the concrete outside the spiral as taken as unconfined concrete and the concrete inside the spiral is taken as confined concrete.

To determine the moment-curvature curves associated with different axial load levels, it is convenient to divide the section into a number of discrete laminae parallel the neutral axis as shown in the Fig. 4.4. The longitudinal steel reinforcement is replaced by an equivalent thin tube with the appropriate wall thickness as shown in Fig. 4.4. Then each lamina contains a quantity of cover concrete or unconfined concrete, core concrete or confined concrete and steel. For a given concrete strain in the extreme compression fibre ε_{cm} and neutral axial depth kd,where d is effective depth of tension steel, the strains in the each lamina ε_i can be determined from similar triangles of the strain diagram as shown in Fig. 4.5. For example, a i th lamina at depth d_i from extreme compression fibre, the strain in the lamina ε_i is given by,

$$\varepsilon_i = \varepsilon_{cm} \frac{kd - d_i}{kd} \tag{4.18}$$

After knowing the strain in the lamina, considering the unconfined concrete, confined concrete and steel in this lamina have the same strain as ε_i. Then the unconfined concrete strain ε_{ui},confined concrete strain ε_{ci} and the steel strain ε_{si} are given by,

$$\varepsilon_{ui} = \varepsilon_{ci} = \varepsilon_{si} = \varepsilon_i \tag{4.19}$$

Knowing the strain in unconfined concrete, confined concrete and steel strains the stresses in unconfined concrete f_{ui},confined concrete f_{ci} and steel f_{si} are given by the above described stress-strain models. Knowing the stresses, quantities(area) of unconfined concrete, confined concrete and steel for the extreme fibre strain ε_{cm} the actual neutral axis depth kd is found which satisfies the force equilibrium equation

$$P = \sum_{i=1}^{n} f_{ci} A_{ci} + \sum_{i=1}^{n} f_{ui} A_{ui} + \sum_{i=1}^{n} f_{si} A_{si} \qquad (4.20)$$

where P is the axial load on the member, n is the total number of laminae, i is the lamina number , f_{ui}, f_{ci}, f_{si} are the stresses in unconfined concrete, confined concrete and steel respectively, A_{ui}, A_{ci}, A_{si} are the quantities (areas) of unconfined concrete, confined concrete and steel respectively.

Then the moment M corresponding to that value of strain in extreme compression fibre ε_{cm} and axial load on the member P is determined by taking the moments of the internal forces corresponding to internal stresses about the extreme compression fibre is given by,

$$M = \frac{Ph}{2} - \left(\sum_{i=1}^{n} f_{ui} A_{ui} d_i + \sum_{i=1}^{n} f_{ci} A_{ci} d_i + \sum_{i=1}^{n} f_{si} A_{si} d_i \right) \qquad (4.21)$$

where h is the outer diameter of the section and d_i is the distance of the centroid of ith lamina from extreme compression fibre.

Then the curvature ϕ corresponding to extreme compression fibre ε_{cm}, the axial load on the member P and moment M is given by,

$$\phi = \frac{\varepsilon_{cm}}{kd} \qquad (4.22)$$

The general moment-curvature diagram of hollow circular column is as shown in Fig. 3.3. The comparison of experimental and analytical values of three column sections as shown in Fig. 4.6 to Fig. 4.8. The data used for the graph is shown in the Table 1.1

CHAPTER 5.

DUCTILITY OF HOLLOW CIRCUALR COLUMNS

5.1. CURVATURE DUCTILITY OF HOLLOW CIRCULAR COLUMN SECTIONS

As described earlier in section 3.1.2, in this study the curvature ductility of hollow circular column section is defined as the ratio of the ultimate curvature to the yield curvature. The definition of the ultimate and yield curvatures is described below.

5.1.1. DEFINITION OF YIELD CURVATURE

It is essential that when assessing the ductility capacity presented in terms of the moment-curvature characteristic as shown in Fig. 3.3 be approximated by an elasto plastic or bilinear relationship. This means that the yield curvature ϕ_y will not necessarily coincide with the first yield of tensile reinforcement, which will generally occur at a some what lower curvature ϕ'_y as shown in Fig. 3.3, particularly if the reinforcement is distributed around the section as would be the case for a column. It is appropriate to define the slope of the elastic portion of the equivalent elastoplastic response by the secant stiffness at first yield. For this typical case, the first-yield curvature ϕ'_y is given by,

$$\phi_y' = \varepsilon_y / (d - c_y) \tag{5.1}$$

where $\varepsilon_y = f_y / E_S$ and c_y is the corresponding neutral-axis depth. Extrapolating linearly to the ideal moment M_i, as shown in Fig. 3.3, the yield curvature ϕ_y is given by,

$$\phi_y = \frac{M_i}{M_i'} \phi_y' \tag{5.2}$$

If the section has a very high reinforcement ratio, or is subjected to high axial load, high concrete compression strain may develop before the first yield of reinforcement occurs. For such cases the yield curvature should be based on the compression strains

$$\phi_y' = \varepsilon_c / \varepsilon_y \tag{5.3}$$

where ε_c is taken as 0.0015. In this study an approximation is made that $\phi_y = \phi_y'$.

5.1.2. DEFINITION OF ULTIMATE CURVATURE

The maximum allowable curvature of a section, ultimate curvature as it is generally termed, is normally controlled by the maximum compression strain ε_{cm} at the extreme fibre, since steel strain ductility capacity is typically high. With reference to Fig. 3.3 this curvature is expressed as ,

$$\phi_u = \frac{\varepsilon_{cm}}{kd} \tag{5.4}$$

where *kd* is the neutral-axis depth at ultimate curvature or at the extreme

compression fibre strain ε_{cm}.

For the purpose of estimating curvature ductility, the maximum concrete compression strain in the extreme fibre of unconfined beam, column or wall sections may be assumed to be 0.004. However much larger strains may be possible to attained when the confined concrete (i.e., concrete reinforced by proper transverse reinforcement) is used. In such situations the contribution of any concrete outside a confined core, which may be subjected to compression strains in excess of 0.004, should be neglected. This generally implies to spalling of the cover concrete. In this study the ultimate curvature is taken as that corresponding to a critical inside-face compression strain is 0.005 and the strain at which cover concrete spalls is 0.0035. The ultimate strain of confined concrete is given by the confined concrete model.

5.2. FACTORS EFFECTING THE CURVATURE DUCTILITY OF HOLLOW CIRCULAR COLUMN SECTIONS

5.2.1. THICKNESS OF THE COLUMN SECTION

The curvature ductility decreases with decreasing the thickness of the section as shown in Fig.5.1 to 5.7. However, at large axial loads the curvature ductility increases with longitudinal reinforcement, decreases with the decrease in thickness of the section as shown in Fig. 5.6 and 5.7.

5.2.2. AXIAL FORCE ON THE COLUMN SECTION , *P*

Axial force on the column section is the important governing factor for available curvature ductility. In this study the axial force is considered as axial load ratio given by

$P/f_c' A_g$,where P is the axial force on the column, f_c' is concrete compressive cylinder strength, A_g is gross area of the cross section of the hollow circular column. As the axial force on the column section increases at constant longitudinal reinforcement ratio, it decreases the both ultimate curvature and yield curvature, thus decreases the curvature ductility. It is observed from the Fig.5.8 to Fig.5.13, that for a given longitudinal reinforcement ratio (A_{st}/A_g) and Diameter ratio (D_i/D), where D_i is the internal diameter and D is the outer diameter, (i.e., thickness of the hollow circular column section) the curvature ductility increases as axial force decreases. The percentage decrease of curvature ductility at low axial forces from 0.05 and 0.10 is very high as compared to high axial forces from 0.3 and 0.35. It is also observed that for a given axial force, which is less than 0.30, the curvature ductility decreases with longitudinal reinforcement ratio increases as shown in Fig.5.8 to 5.13. For high axial force, which is greater than 0.30, the curvature ductility increases with longitudinal reinforcement ratio. The increase in curvature ductility at high axial force with longitudinal reinforcement is less as compared to degradation of curvature ductility at low axial force.

5.2.3. COMPRESSION STRENGTH OF CONCRETE, f_C

It is observed from the Fig.5.14 to 5.22, that at low level of axial forces $P/f_c' A_g <$ 0.15, the high strength concrete is giving more ductility than low strength concrete. Contradictory to this, irrespective of thickness of the hollow section, at high levels of axial force $P/f_c' A_g$ >0.30, the low strength concrete is giving more ductility than high strength concrete as shown in Fig.5.16, Fig.5.19 and Fig.5.22.

5.2.4. YIELD STRENGTH OF LONGITUDINAL STEEL, f_Y

As the yield strength of longitudinal steel increases, the curvature ductility decreases. Because as the yield strength increases it increases the yield curvature, due to increase in yield strain. Due to that reason the yield strength of steel decreases the curvature ductility as shown in Fig. 5.23 to 5.34. It is observed from the Fig. 5.30 and 5.34 at high axial load ratio i.e., greater than 0.30, the high yield strength bars are giving more ductility than the low yield strength bars in the case of the thin hollow sections only.

5.2.5. TRANSVERSE REINFORCEMENT RATIO ρ_S

As the transverse reinforcement ratio increases it increases the confinement and strength of the concrete increases the ultimate curvature thus increases the curvature ductility. It is observed from the Fig.5.35, 5.38 and 5.41 that at the curvature ductility increases with transverse reinforcement ratio up to one level and later again decreases with increase in transverse reinforcement ratio. At low level of axial load ratio i.e., $P/f_c' A_g$ = 0.05 the curvature ductility increasing with increase in transverse reinforcement ratio up to transverse reinforcement ratio 0.018 (i.e., 1.8 %). At the same time as the thickness of the hollow section decreases , the transverse reinforcement ratio up to which the curvature ductility increases also decreases as shown in Fig.5.38 and 5.40. That is for the case of 0.90 diameter ratio the transverse reinforcement ratio up to which the curvature ductility increases is 0.14, for the case of 0.94 it is 0.10.

As shown in the Fig.5.37, 5.40 and 5.43, irrespective of thickness of the hollow section at high axial load ratio i.e., 0.30 the curvature ductility is increasing with transverse reinforcement ratio up to 0.010 transverse reinforcement ratio only. At the same time at low longitudinal reinforcement ratio less than 0.035 the curvature ductility is increasing with transverse reinforcement ratio up to large level.

As shown in the Fig.5.35 to 5.43, irrespective of thickness of the hollow section, as the axial load ratio on the column increases it decreases the level of transverse reinforcement ratio up to which curvature ductility increases. As for the case of the 0.84 diameter ratio at axial load ratio 0.05 the curvature ductility increases with transverse reinforcement ratio up to 0.018,at axial load ratio 0.15 the curvature ductility increases with transverse reinforcement up to 0.014, at axial load ratio 0.30 the curvature ductility increases with transverse reinforcement ratio up to 0.01.

5.2.6. EXTREME COMPRESSION FIBRE STRAIN , ε_{cm}

The effect of considered value of extreme compression fibre strain ε_{cm} for the calculation of ultimate curvature is shown in Fig.5.44 to 5.52. As the considered value of extreme compression fibre strain ε_{cm} for ultimate curvature increases it increases the ultimate curvature thus increases the curvature ductility. It is observed from the Fig.5.44 to 5.52 that at low axial force i.e., $P/f_c' A_g$ < 0.15 and low longitudinal reinforcement ratio less than 0.02, low extreme compression fibre strain is giving more ductility than high extreme compression fibre strain. As the axial load is high $P/f_c' A_g$ > 0.20 and longitudinal reinforcement ratio is more than 0.01 the ductility is increasing rapidly with

extreme compression fibre strain. So it is important to consider the extreme compression fibre strain ε_{cm} assumed for the caluculation of ultimate curvature at high axial loads.

5.3. DESIGN CHARTS FOR HOLLOW CIRCULAR COLUMNS

Design chart is defined as the relation of curvature ductility factor with longitudinal reinforcement ratio at different levels of axial load on the column section Design charts for hollow circular columns with varying thickness (i.e., the diameter ratio D_i / D, where D_i is internal diameter and D is the external diameter of the hollow circular column section) and transverse reinforcement ratio are shown in Fig.5.53 to 5.70. The data used to derive these design charts is the yield strength of longitudinal steel * f_Y is 250.0 MPa, the yield strength of transverse reinforcing steel f_{Yh} is 415.0 MPa, the cylinder compressive strength of concrete f_C is 30.0 MPa ** and outside diameter of the hollow column section D is 3000.0 mm. These design charts are derived assuming the ultimate curvature is corresponding to a particular critical inside face compression strain is 0.005 as shown in Fig. 4.4. The corresponding extreme compression fibre strain is calculated by using the critical inside face compression strain 0.005 and used for the calculation of the ultimate curvature The curvature ductility factor ϕ_u/ϕ_y derived for different sections with diameter ratio D_i / D= 0.84,0.86,0.88,0.90,0.92 and 0.94 and assuming the critical inside-face ultimate compression strain as described earlier. The curvature at first yield ϕ_y is taken as first yield of the longitudinal steel or the extreme fibre concrete compression strain reaches 0.002 , whichever is smaller.

By using these design charts a designer can primarily assess the amount of longitudinal reinforcement ratio and transverse reinforcement ratio required to achieve a

* Why Fe 250? Commonly Used steel is Fe 415 ?

** Where Used? Too Small for Bridge piers / OHR etc.

certain level of curvature ductility for a given axial load ratio and thickness of the column section.

5.3.1. DESIGN PROCEDURE BASED ON DESIGN CHARTS

In this section, a comprehensive design procedure is given for the ductility of reinforced concrete hollow circular columns based on the design charts. In the procedure, the designer chooses the level of curvature ductility factor needed for the column. The required displacement ductility factor at the plastic-hinge locations in the columns is then calculated from the geometry of the column and imposed curvature ductility factor. For example, for the cantilever column shown in Fig. 3.4, the relation ship between the curvature ductility factor ϕ_u/ϕ_y and the displacement ductility factor μ may be approximated (Priestley and Park, 1987) as

$$\frac{\phi_u}{\phi_y} = 1 + \frac{C(\mu - 1)}{3\frac{L_P}{L}\left(1 - 0.5\frac{L_P}{L}\right)} \qquad \textbf{(5.5)}$$

where C = ratio of the elastic flexibility of the system due to the column, foundation and bearings to the elastic flexibility due to the column alone; L = height of the column above the ground; and L_P = equivalent plastic-hinge length. For a solid column from the test data (Priestley and Park 1987) has shown the value for plastic-hinge length

$$L_P = 0.08L + 6d_b$$

where d_b = diameter of the longitudinal reinforcing bars. A good approximation for L_P is half of one column depth (0.5D or 0.5h).To know the equivalent plastic-hinge

length of hollow circular columns a large set of test data is needed. However in this study, due to the absence of test data of hollow circular columns, for different assumed values of L_P and coefficient C for hollow circular columns, the displacement ductility corresponding to the curvature ductility factors are shown in Fig.5.71 to 5.75.

The change in displacement ductility factor with transverse reinforcement ratio at various levels of longitudinal reinforcement ratio are shown in Fig.5.76 to 5.93. By using these figures, one can get required longitudinal reinforcement ratio and transverse reinforcement ratio and thickness of the section for a given axial load and displacement ductility factor for given curvature ductility, coefficient C and L_P, equivalent plastic hinge length of the hollow circular column sections.

CHAPTER 6.

DISCUSSIONS

6.1. MOMENT CURVATURE ANALYSIS

6.1.1. STRESS-STRAIN MODEL FOR CONFINED CONCRETE FOR HOLLOW CIRCULAR COLUMNS

The stress-strain model for confined concrete proposed by Hoshikuma et.al.(1997) giving reasonable results as compared to experimental results than other proposed models as shown in Fig. 2.12. It is not applicable to use for hollow circular sections. Since in contrast to the solid circular column, there is no compressive confining stress acting on the inside face of the curved wall in the radial direction. Due to that reason the concrete near to the inside face is not confined properly as compared to solid circular column concrete inside the spiral due to uniform confining force given by the Eqn. 2.1. As described earlier in section 1.2, the hollow circular column wall undergoes only biaxial compression though it is triaxial compression in the case of solid circular column.

As explained above, it is not possible to get good confinement in hollow circular sections like solid circular sections. Due to that reasons, the peak compressive strength of confined concrete, f_{cc} and strain at peak compressive strength of confined concrete ε_{cc} of hollow circular sections always smaller than the solid circular sections. So it is needed to modify the confined concrete model of the Hoshikuma et.al., (1997) to apply for

hollow circular sections and to do moment curvature analysis as described earlier. Here in this study the confined concrete model of Hoshikuma et.al.,(1997) is modified by the approximate modification factors $\alpha = 0.20$ and $\beta = 0.45$. These modification factors are used in the equations of the peak confined concrete strength and strain at the peak confined concrete strength. The modified model is used in the moment curvature analysis of three column units and results are shown in Fig. 4.6,Fig. 4.7 and Fig. 4.8.

The modification factors are taken as above, because due to biaxial nature the hollow circular column section behaves nearly as same as square section, whose modification factors are $\alpha = 0.20$ and $\beta = 0.40$. In square section also the concrete at the corners is confined properly due to high confining forces.

6.2. DUCTILITY OF HOLLOW CIRCULAR COLUMNS

As the axial force on the column section increases, the curvature ductility decreases with increase in longitudinal reinforcement ratio. But this behaviour is true for the column sections with low axial load ratio, $P/f_c' A_g$ < 0.30 and in the case of the columns with high axial load ratio, $P/f_c' A_g$. > 0.30 and small thickness, the curvature ductility increases with longitudinal reinforcement ratio. Because at high axial load ratio, the extreme concrete compression fibre reaches 0.002 earlier to the first yield of the longitudinal reinforcement ratio. So the curvature ductility gradually increases with the longitudinal reinforcement ratio.

At low level of axial load ratio, $P/f_c' A_g$ < 0.15, the high strength concrete is

giving more ductility than low strength concrete. At high level of axial load ratio, $P/f_c' A_g$ > 0.30, the low strength concrete is giving more ductility than high strength concrete.

In general, as the yield strength of longitudinal steel increases, the curvature ductility decreases due to increase in yield curvature and yield strain. At high axial load ratio, $P/f_c' A_g$ > 0.30,for small thickness hollow circular sections, the curvature ductility increases with yield strength of longitudinal steel.

The transverse reinforcement increases the confining force and confinement of concrete, which increases the curvature ductility. But it is observed that as the transverse reinforcement increases, the curvature ductility increases up to one level and later the curvature ductility decreases with increase in transverse reinforcement ratio. This level of transverse reinforcement ratio up to which the curvature ductility increases, depends upon the thickness of the section and axial load on the section. As the axial load on the section increases, the level of transverse reinforcement ratio up to which curvature ductility increases is decreased. As the thickness of the section increases the level of transverse reinforcement ratio increases.

CHAPTER 7.

SUMMARY AND CONCLUSIONS

7.1. SUMMARY

This study mainly deals with ductility of hollow circular columns of small thickness having only one layer of longitudinal and transverse reinforcement on the outside face of the cross-section of the column. Evaluation of the effect of confinement on ductility of RC hollow circular columns and analytical study of different factors effecting the curvature ductility of circular hollow columns has been done. To know the curvature ductility, moment-curvature analysis is done by using a program developed in this study. Those factors that affecting the available curvature ductility of hollow circular column section are as follows

- Axial load on the column, P
- Thickness of the hollow circular section
- Concrete compressive cylinder strength, $f_c^{'}$
- Yield strength of longitudinal bars, f_y
- Extreme compression fibre strain, ε_{cm}
- Transverse reinforcement ratio, ρ_s

To know the curvature ductility and to derive design charts for the hollow circular column section with different diameter ratios D_i/D, where D_i is the internal

diameter and D is the outer diameter, moment-curvature analysis is needed. For moment-curvature analysis the complete stress-strain behaviour of unconfined concrete, confined concrete and steel to be known. In this study in the hollow circular section as shown in Fig. 4.2, the concrete outside the spiral is taken as unconfined concrete the concrete inside the spiral is taken as confined concrete. For unconfined concrete the stress-strain model is used as given in the IS code IS: 456-1978 as shown in Fig. 4.2, for steel the stress-strain model is used as shown in Fig. 4.1. For confined concrete, the confined concrete model of Hoshikuma et.al., (1997) as shown in Fig. 4.3 which is giving reasonable results with experimental results than other previously proposed models is taken and modified with approximate assumed modification factor $\alpha = 0.2$ and $\beta = 0.45$, applied in moment curvature analysis and results are compared with experimental results (Zahn,Park and Presetley,1990)as shown in Fig.4.6 to 4.8.

A computer program was developed to do the moment-curvature analysis and gives the curvature ductility with various value of diameter ratio, longitudinal reinforcement ratio transverse reinforcement ratio.

A design procedure is given for the ductility design of reinforced concrete hollow circular columns based on design charts. Using the Fig 5.71 to 5.75, one can get the value of displacement ductility factor for the equivalent plastic hinge length, coefficient, C and the corresponding curvature ductility factor. Here C is the ratio of the elastic flexibility of the system due to the column foundation and bearings to the elastic flexibility due to the column alone with respect to curvature ductility.

7.2. CONCLUSIONS

The major findings and conclusions from this study can be summarised as follows:

- The stress-strain model of confined concrete of solid sections of Hoshikuma et al. (1997) gives reasonable agreement with experimental data than other previously proposed models. However, it is not applicable as proposed to hollow circular sections because nature of stresses, is biaxial for hollow sections which is in contrast with solid column sections where stresses are triaxial.

- The solid circular column sections always have more ductility than hollow circular column sections.

- The important factors that effect the ductility of hollow circular column sections are

  1. The thickness of the hollow circular section,
  2. The axial load ratio on the section,
  3. The longitudinal reinforcement ratio of the section
  4. The transverse reinforcement ratio of the section.

- The curvature ductility increases with increase in thickness of the section . Moreover, the curvature ductility decreases with the axial load on the column and longitudinal reinforcement ratio increases.

- Generally, the hollow circular columns with low longitudinal reinforcement ratio, high diameter ratio D_i/D(i.e., the thickness of hollow circular section),low axial load ratio $P/f_c' A_g$ and moderate transverse reinforcement ratio will have high ductility.

- In the case of hollow circular column section having high diameter ratio, i.e., more than 0.94 at large axial load ratio, is more than 0.30 the curvature ductility increasses with increase in longitudinal reinforcement.

- The curvature ductilty of hollow circular column section increases with increase in transverse reinforcement ratio up to a certain level and again decreases with increase in transverse reinforcement ratio. However this level of transverse reinforcement ratio up to which curvature ductility increases depends upon the axial load on the column and thickness of the column section. Generally, this optimum level is between 1% to 1.4% of transverse reinforcement ratio.

- In the case of very small thickness hollow circular column sections the effect of transverse reinforcement on curvature ductility is insignificant.

7.3. SUGGESTIONS FOR FUTURE STUDY

In this study, the appropriate modification factors to modify the stress-strain model of confined concrete of Hoshikuma et al. (1997) for hollow circular sections are assumed to match the experimental results. However with experimental data of stress-

strain behaviour of hollow circular sections, we may get good results than these. To determine the displacement ductility factor for corresponding curvature ductility factor, the value of equivalent plastic hinge length is needed. Due to the absence of test data for hollow circular sections, the analysis is done for a range of plastic hinge length ratio(i.e., the ratio of plastic hinge length and height of the column) values from 0.01 to 0.04. This value can also be calculated by doing experiments and therefore we may get better value of displacement ductility factor.

language is not clear

(2) Ph.D. Thesis of Prof. K.K Singh, CED

BIBLIOGRAPHY

Ang, B.G., Priestley, M.J.N., and Paulay, T., "Seismic Shear Strength of Circular Reinforced Concrete Columns", ACI *Journal of Structural Engineering,* V. 86, No. 1, Jan.-Feb. 1989, pp. 45-59.

BIS(1978).IS:456-1978 General Construction in Plain and Reinforced concrete-Code of practice, Bureau of Indian Standards, New Delhi.

Hjalmar Granholm, " A General Flexural Theory of Reinforced Concrete",John Wiley&Sons, New York,N.Y.,1965.

Hognestad. E., Hanson. N. W., and Mc Henry. D., (1955) "Concrete Stress Distribution in Ultimate Strength Design", *ACI Struct. J, Proceedings Vol.52.4. pp.455-480.*

Hoshikuma, J., Kawashima, K., Nagaya, K., and Taylor, A. W. (1994). " Stress-Strain model for confined reinforced concrete in bridge peirs.", *J. Struct. Div.,* ASCE, 123 (5), pp.624-633.

Kent,D.C., and Park,R. (1971)., "Flexural members with confined concrete",*Journal .Strct.Div.,* ASCE,97(7),1969-1990.

Lakshmi Narasimha Rao,M.,"A seminar report on stress strain modelling of confined concrete",Unicersity of Roorkee, Roorkee.

Mander, J.B., Priestley, M.J.N., and Park, R., "Observed Stress Strain Behaviour of Confined Concrete", ASCE *Journal of Structural Engineering,* Vol. 114, No. 8, Aug. 1988, pp. 1827-1849.

Mander, J. B., Priestley, M.J.N., and Park, R.(1988 a), "Theoretical stress-strain behaviour of confined concrete." *J.Struct.Div.,* ASCE,114(8),1804-1826.

Mander, J. B., Priestley, M.J.N., and Park, R.(1988 b), "Observed stress-strain behaviour of confined concrete", *J. Struct. Div.,* ASCE, 114(8),1827-1849.

Park, R., Priestley, M. J. N., and Gill, W. D. et al. (1982), "Ductility of square-confined concrete columns", *J. Struct. Div.,* ASCE, 108(4), 929-950.

Paulay, T and M.J.N. Priestly., "*Seismic Design of Reinforced concrete and Masonry Buildings*", John Wiley & Sons, Inc, New York, N.Y., 1992.

Priestley, M.J.N., and Park, R., "Strength and Ductility of Concrete Bridge Columns Under Seismic Loading", ACI *Structural Journal,* V. 84, No. 1, Jan.-Feb. 1987, pp. 61-76.

Rai, D.C. (1999), "Earthquake Damage Assesment & Seismic Strengthening Gulaotal Overhead Water Reservoir", *Int.Report, Dept. of Earthquake Engrg.,* University of Roorkee, Roorkee, Feb.

Razvi, S. R., and Saatcioglu, M. (1989). "Confinement of reinforced concrete columns with welded wire fabric", *ACI Struct. J.,* 86(6), 615-623.

Saatcioglu, M., Razvi, S.R., and Salmat, A. H. (1995). "Confined Columns under eccentric loading." *J. Struct. Div.,* ASCE, 121(11), pp.1547-1556.

Saatcioglu, M., and Razvi, S. R. (1992). "Strength and ductilty of confined concrete." *J. Struct. Div.,*ASCE, 118(6), pp. 1590-1607.

Sheikh, S. A.,and Uzumeri, S.M. (1982). "Analytical model for concrete confinement in ties columns." *J. Struct. Div.,* ASCE, 108(2), pp.2703-2722.

Zahn,F.A., R. Park, and M.J.N. Priestley. (1990), "Flexural strength and ductility of circular hollow reinforced concrete columns without confinement on inside face", ACI *Structural Journal,* 87(2),156-166.

TABLES

Column Unit	Diameter Ratio D_i/D	Cover to spiral, co mm ?	Axial Load Ratio P/f'_cA_g	Compressive cylinder strength of concrete (MPa)??	M_{ACI} Moment Units ?	Longitudinal Reinforcement		Transverse Reinforcement	
						Percent, ρ'_S	Yield Strength, f_Y (MPa)	Percent, ρ_S	Yield Strength, f_{yh} (MPa)
Unit 2	0.53	18	0.40	29.6	204.0	3.67	306	2.02	318
Unit 3	0.63	18	0.10	29.6	165.0	4.20	306	2.08	318
Unit 5	0.73	18	0.12	27.3	156.0	5.40	306	2.94	340

Table. 1.1 Data of Column units used for moment-curvature analysis

Units

Researcher	Stress-Strain Model for Confined Concrete			Applicable Cross-sectional shape
(1)	Ascending branch (2)	Descending branch (3)	Residual stress (4)	(5)
Kent and Park (1971)	$f_c = f_c'\left[\frac{2\varepsilon_c}{\varepsilon_o} - \left(\frac{\varepsilon_c}{\varepsilon_o}\right)^2\right]$	$f_c = f_c'\left[1 - Z(\varepsilon_c - \varepsilon_o)\right]$	20% of Kf_{co}	Square
Sheikh and Uzumeri (1982)	$f_c = K_s f_{cp}\left[\frac{2\varepsilon_c}{\varepsilon_{s1}} - \left(\frac{\varepsilon_c}{\varepsilon_{s1}}\right)^2\right]$	$f_c = f_{cp}\left(1 - Z(\varepsilon_c - \varepsilon_{s2})\right)$	30% of f_{cc}	Square
Mander etal. (1988)	$f_c = \frac{f_{cc} xr}{r - 1 + x^r}$	$f_c = \frac{f_{cc} xr}{r - 1 + x^r}$	-	Circular, Square and Wall-type
Saatcioglu and Razvi (1992)	$f_c = f_{cc}\left[2\left(\frac{\varepsilon_c}{\varepsilon_{co}}\right) - \left(\frac{\varepsilon_c}{\varepsilon_{co}}\right)^2\right]^{\frac{1}{1+2K}}$	$f_c = f_{cc} - \frac{0.15 f_{cc}}{\varepsilon_{85} - \varepsilon_{cc}}(\varepsilon_c - \varepsilon_{cc})$	20% of f_{cc}	Circular, Square, Wall-type
Hoshikuma et al. (1997)	$f_c = E_c \varepsilon_c\left[1 - \frac{1}{n}\left(\frac{\varepsilon_c}{\varepsilon_{cc}}\right)^{n-1}\right]$	$f_c = f_{cc} - E_{des}(\varepsilon_c - \varepsilon_{cc})$	-	Circular, Square, Wall-type

Table. 2.1 Stress-Strain Models for Confined Concrete

Strength of unconfined concrete (Mpa) (1)	**Intial Stiffness (Mpa) X10^4 (2)**
20.6	2.30
23.5	2.45
26.5	2.60
29.4	2.75
39.2	3.04
49.0	3.24

Table 2.2 Intial Stiffness

FIGURES

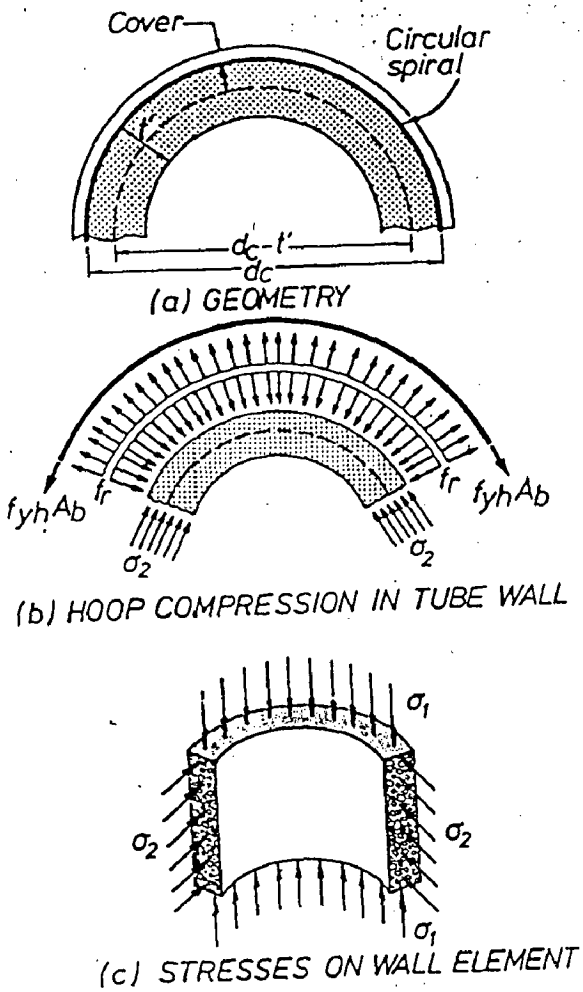

Fig. 1.1 **Geometry and stresses in wall of circular hollow column**
(Zahn,F.A., R. Park, and M.J.N. Priestley. 1990,)

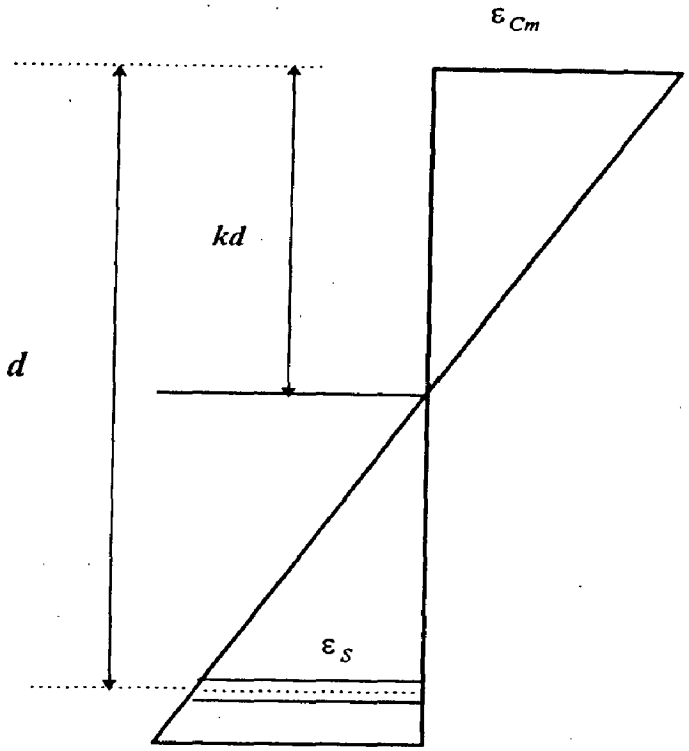

Fig. 2.1 General Strain Distribution

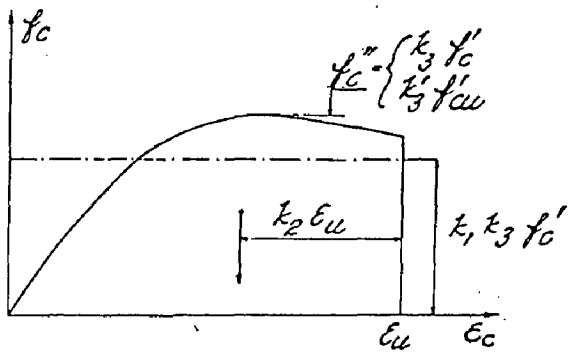

Fig. 2.2 (a) General Stress Distribution (Hognestad,1955)

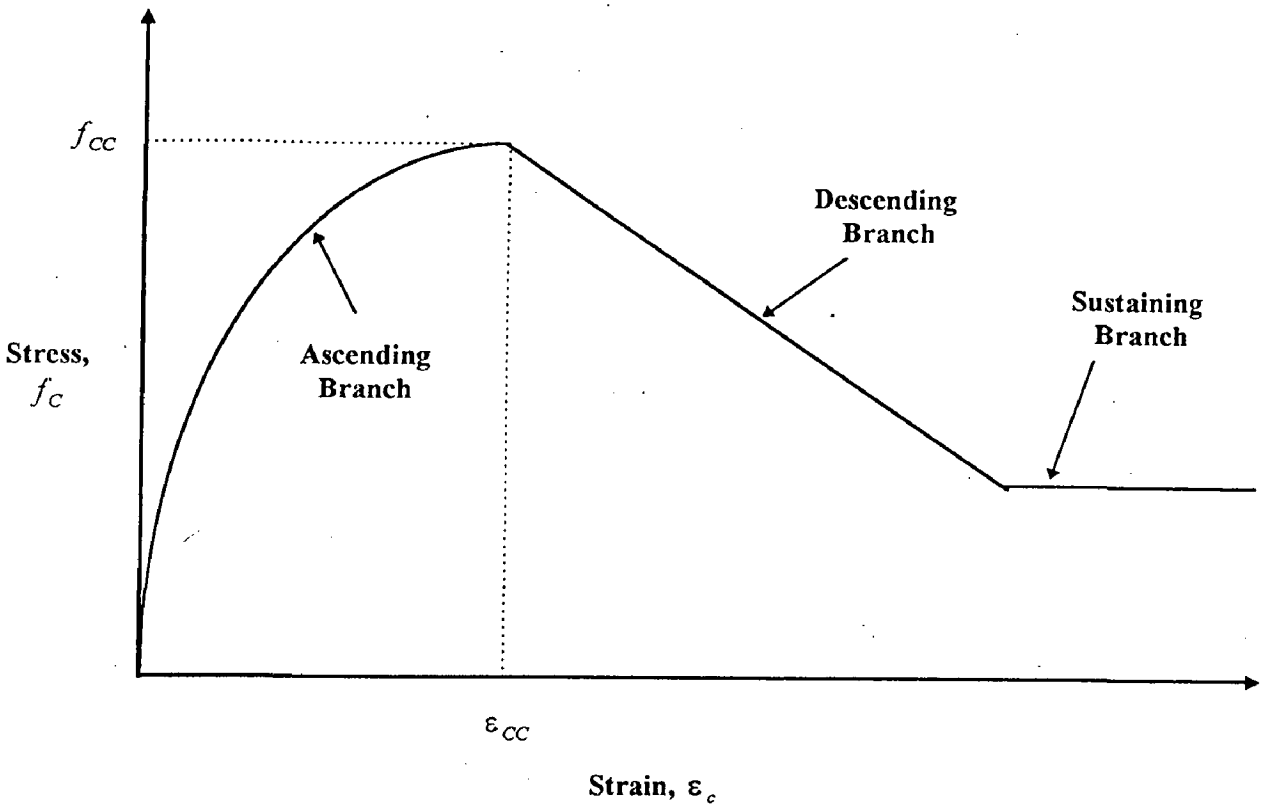

Fig. 2.2.(b) Stress-Strain Model

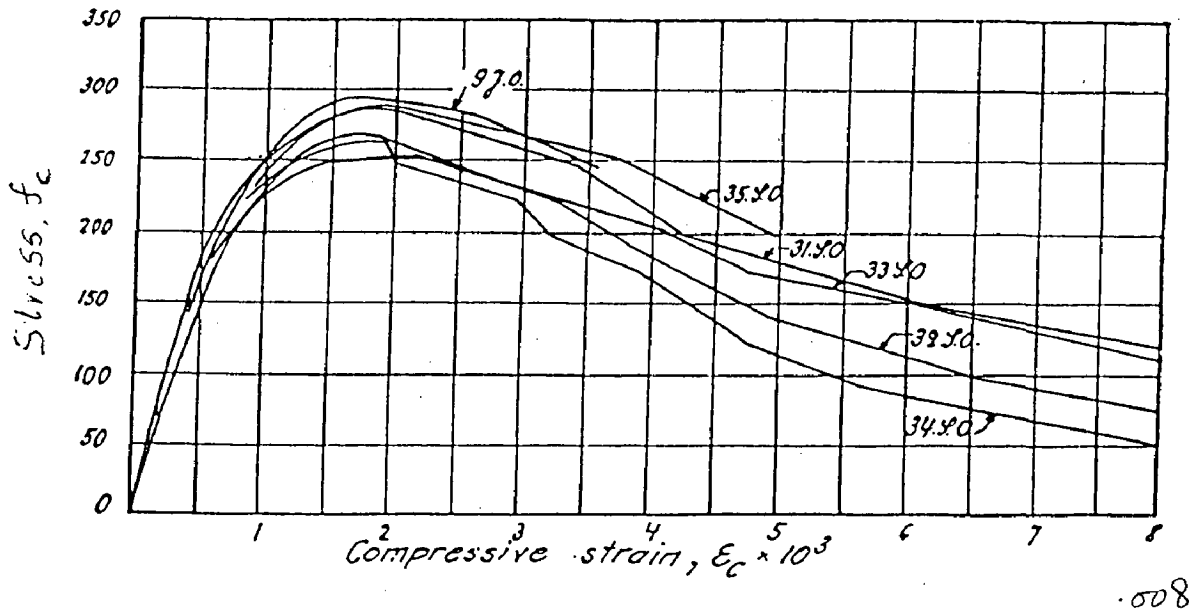

Fig. 2.3 Stress-Strain curves for concrete from tests on cylinders (Hjalmar Granholm 1965)

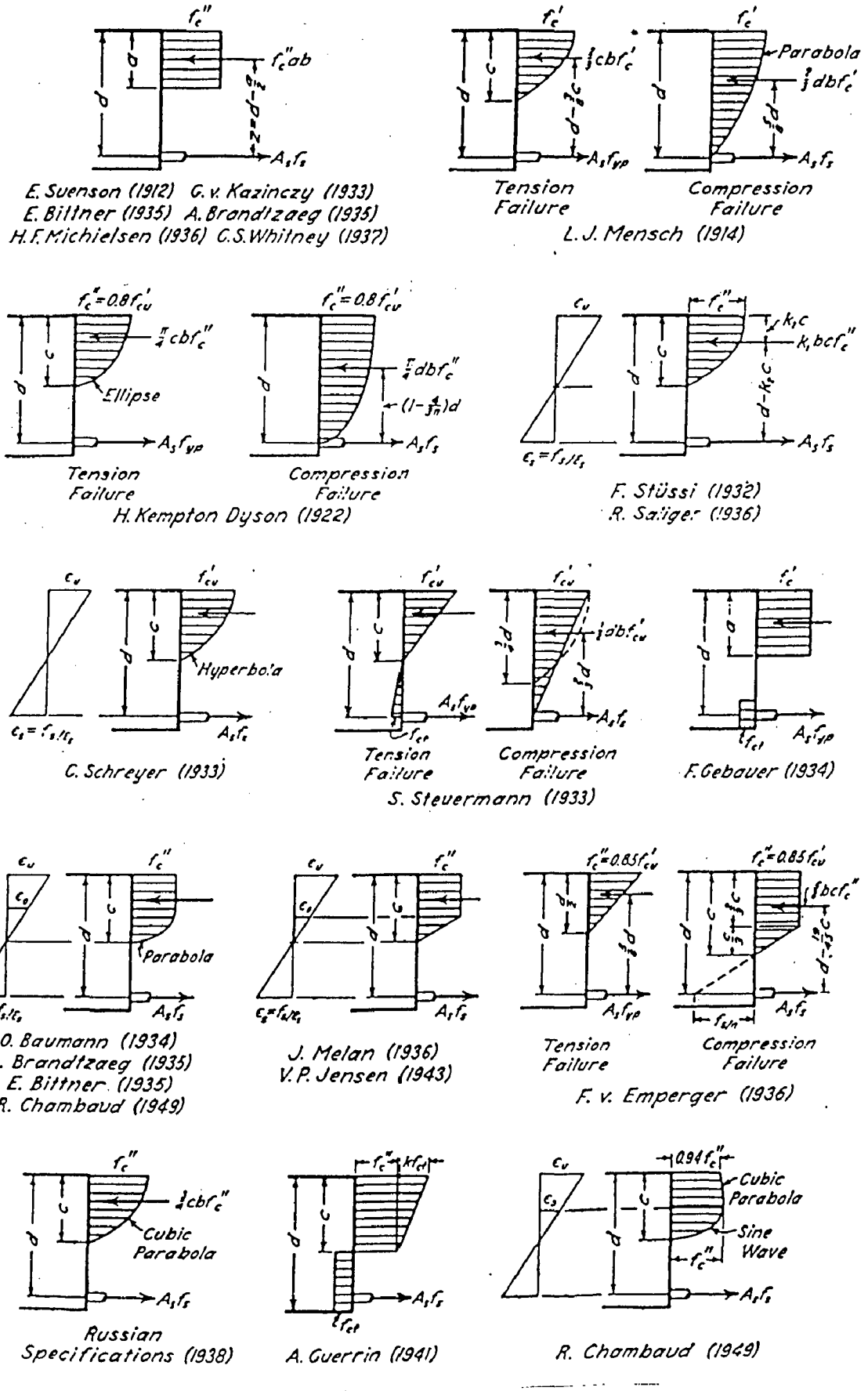

Fig. 2.4 **Different Stress-Strain Models of Unconfined Concrete (Hognestad,1955)**

Fig. 2.5 Confining force

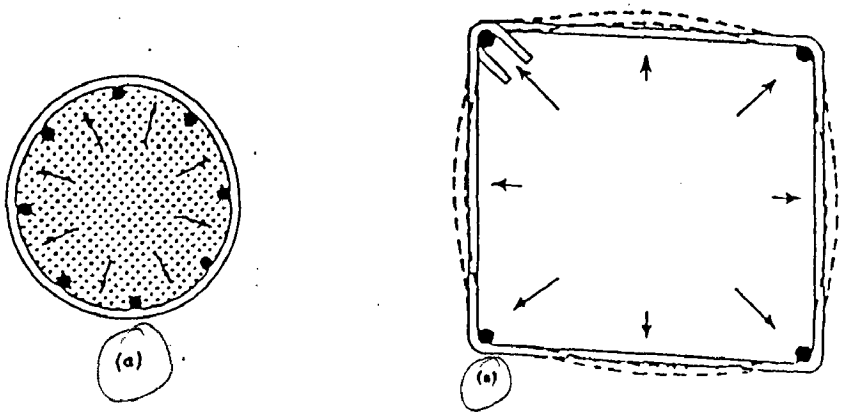

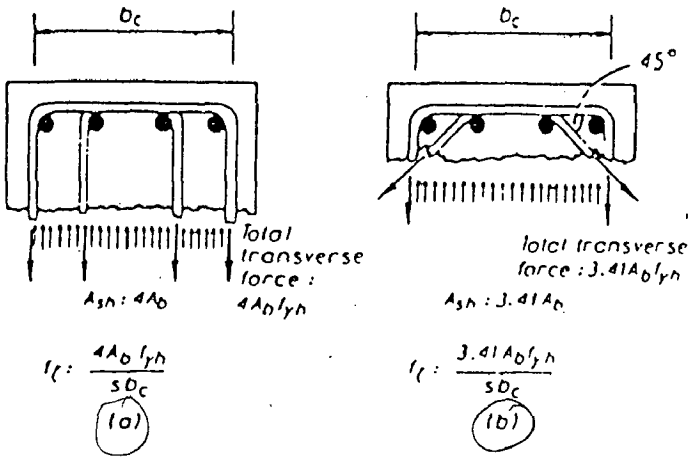

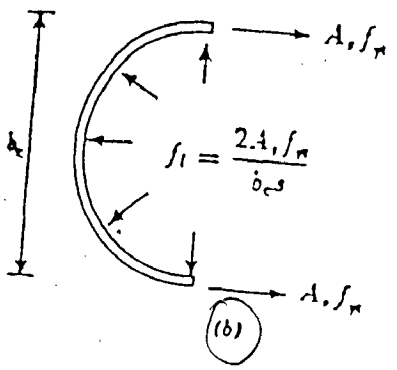

① Figure not properly labelled.

② Lettering illegible

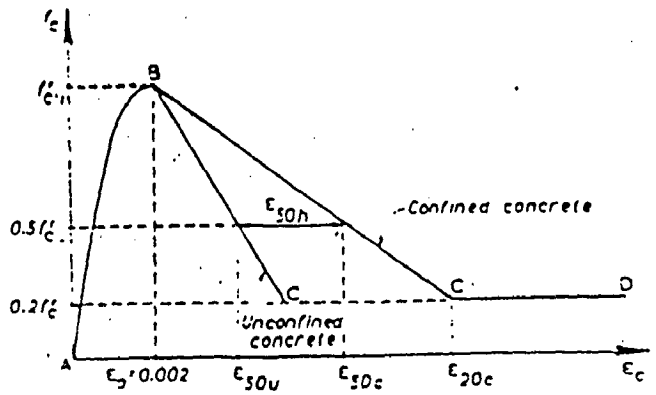

Fig. 2.6 Kent & Park stress-strain model for unconfined and confined Concrete (Kent and Park 1971)

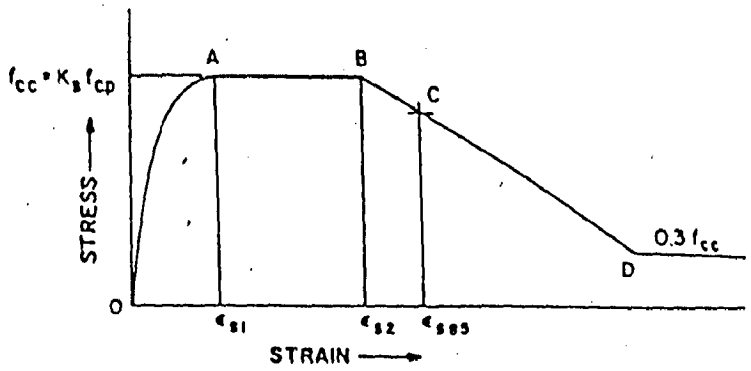

Fig. 2.7 Sheikh and Uzumeri (1982) stress-strain model for confined Concrete

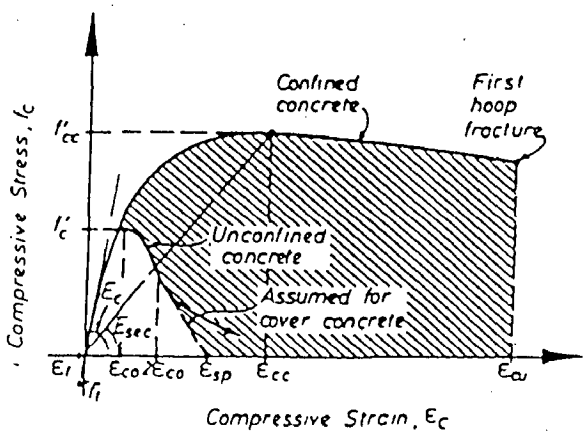

Fig. 2.8 **Mander et al. (1988) stress-strain model for unconfined and confined Concrete**

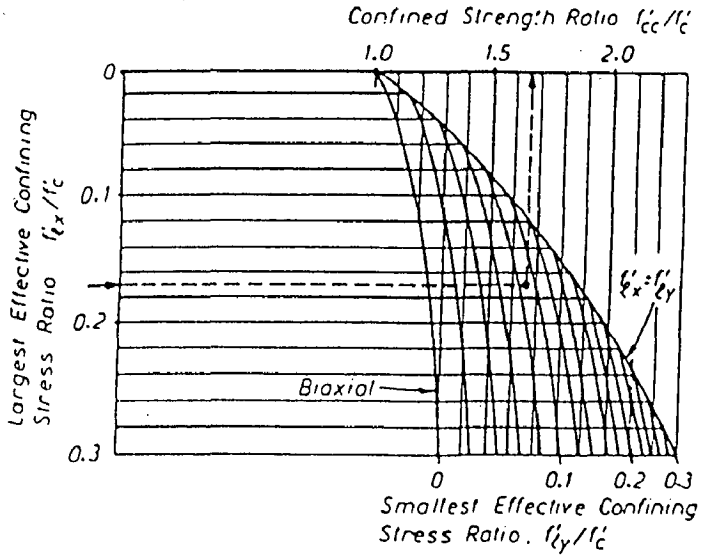

Fig. 2.9 **Confined strength determination from lateral confining stresses for rectangular section.**

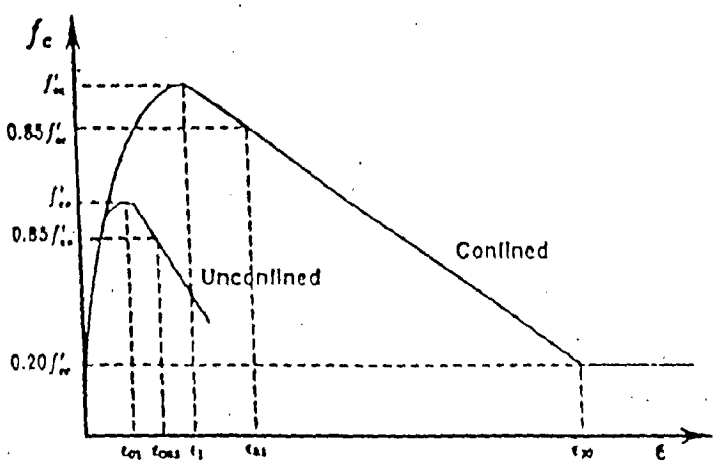

Fig. 2.10- Saatcioglu & Razvi (1992) stress-strain model for confined and unconfined concrete

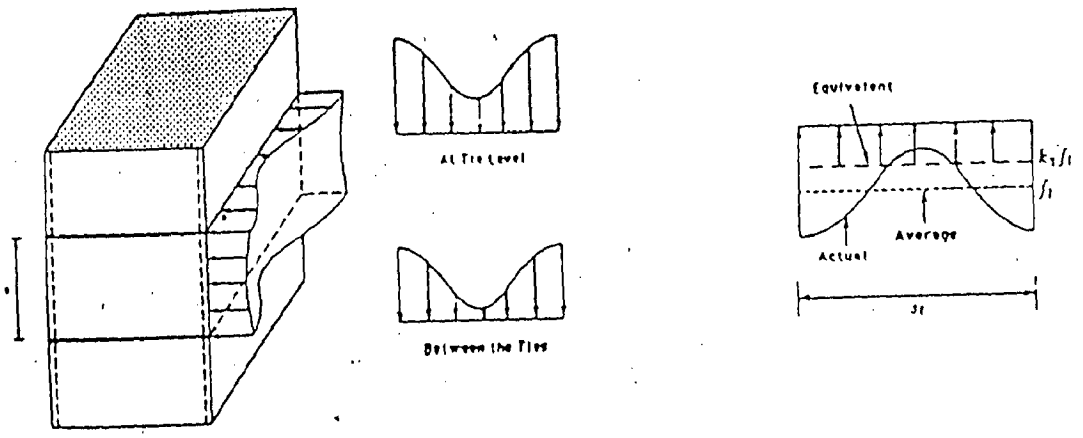

2.11 Distribution of Lateral Pressure along member length and Actual, Average and Equivalent Lateral Pressure

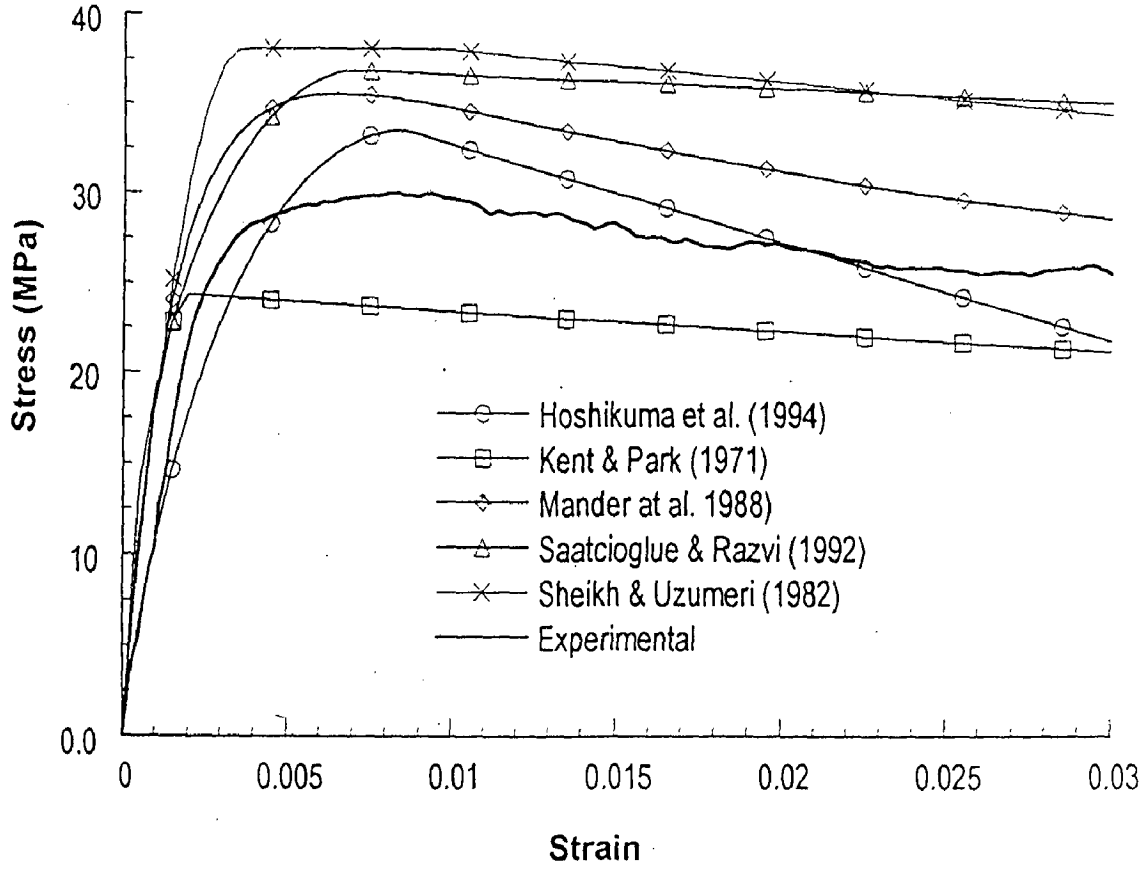

Fig. 2.12 Comparison of Different models

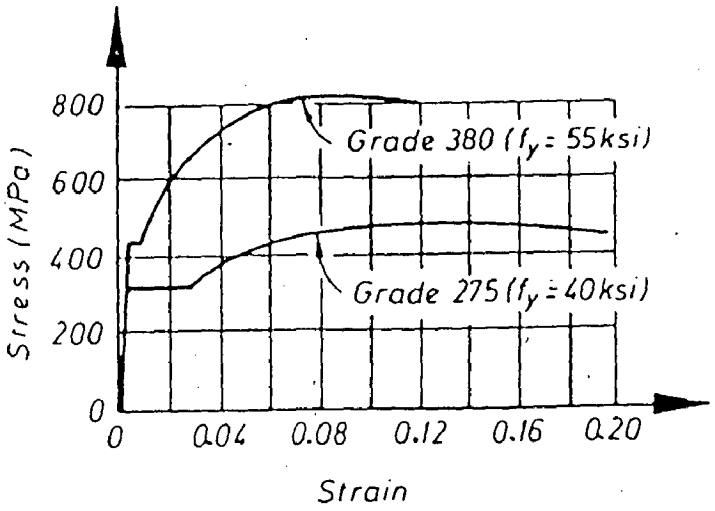

Fig. 3.1 Typical stress-strain curves for steel

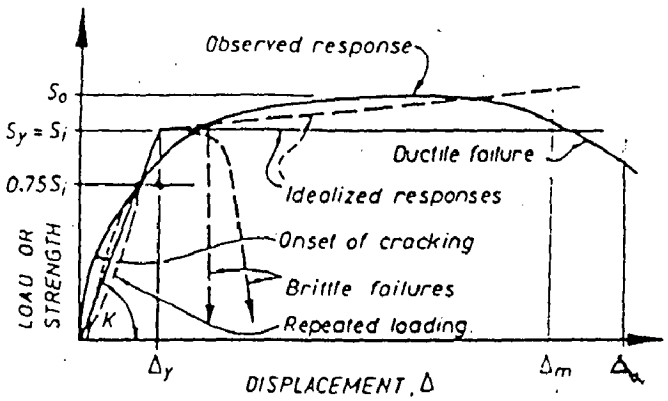

Fig. 3.2 Change in Strength with Displacement

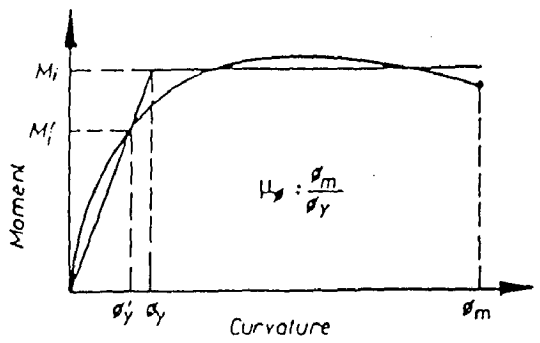

Fig. 3.3 Moment curvature relationship

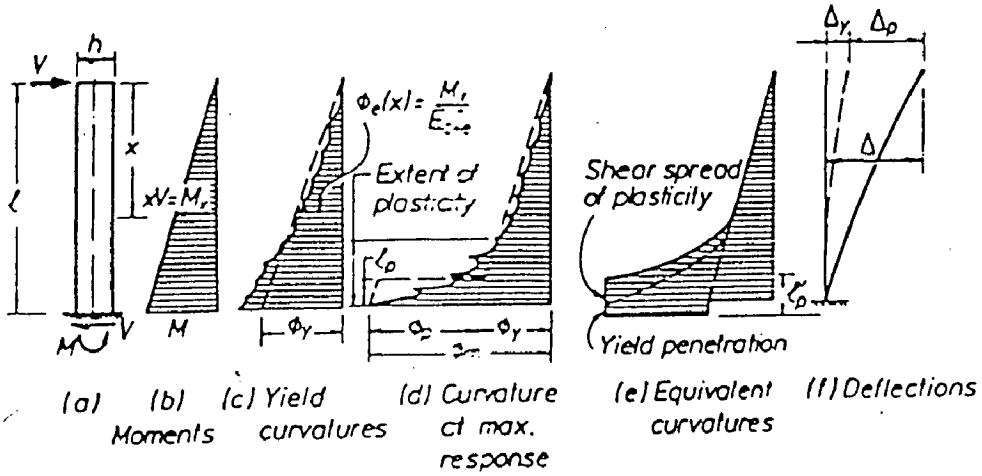

Fig. 3.4 Moment, curvature and deflection relationships for a cantilever

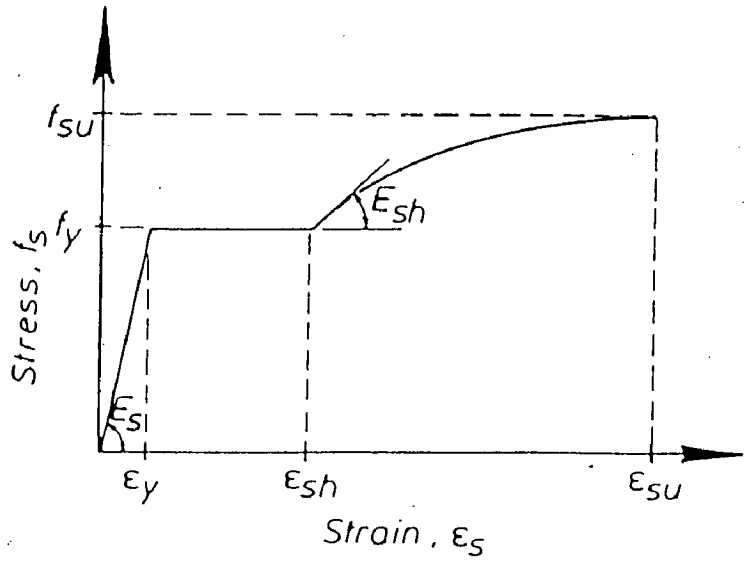

Fig.4.1 Stress-Strain Model for steel used in Moment Curvature Analysis

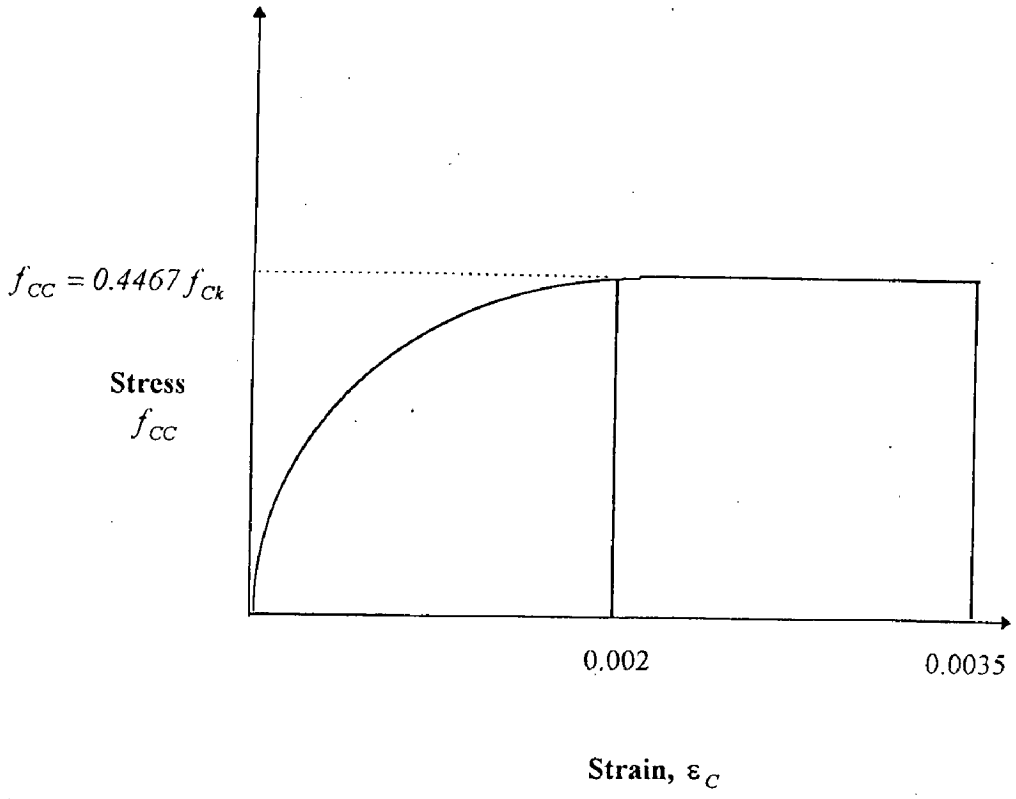

Fig.4.2 **Stress-Strain Model for Unconfined concrete used in the momentCurvature Analysis**

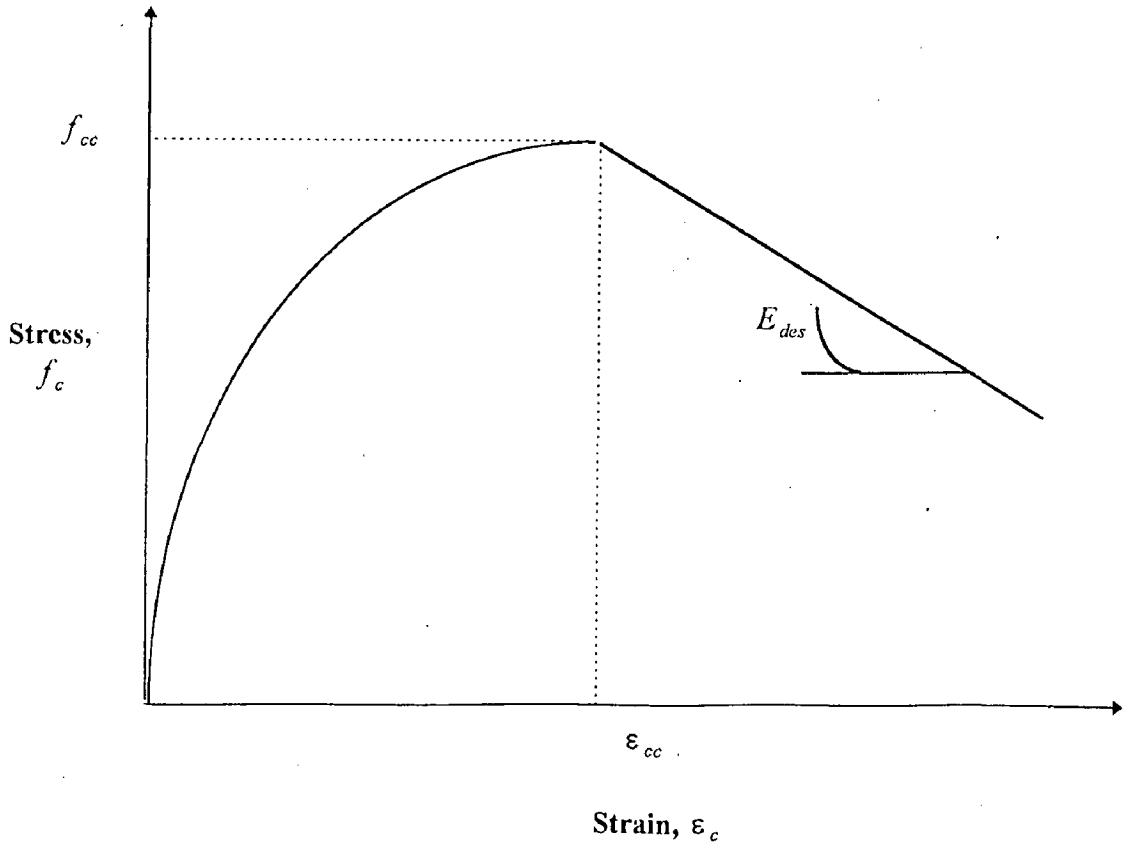

Fig.4.3 **Stress-Strain Model for Confined Concrete used in Moment Curvature Analysis**

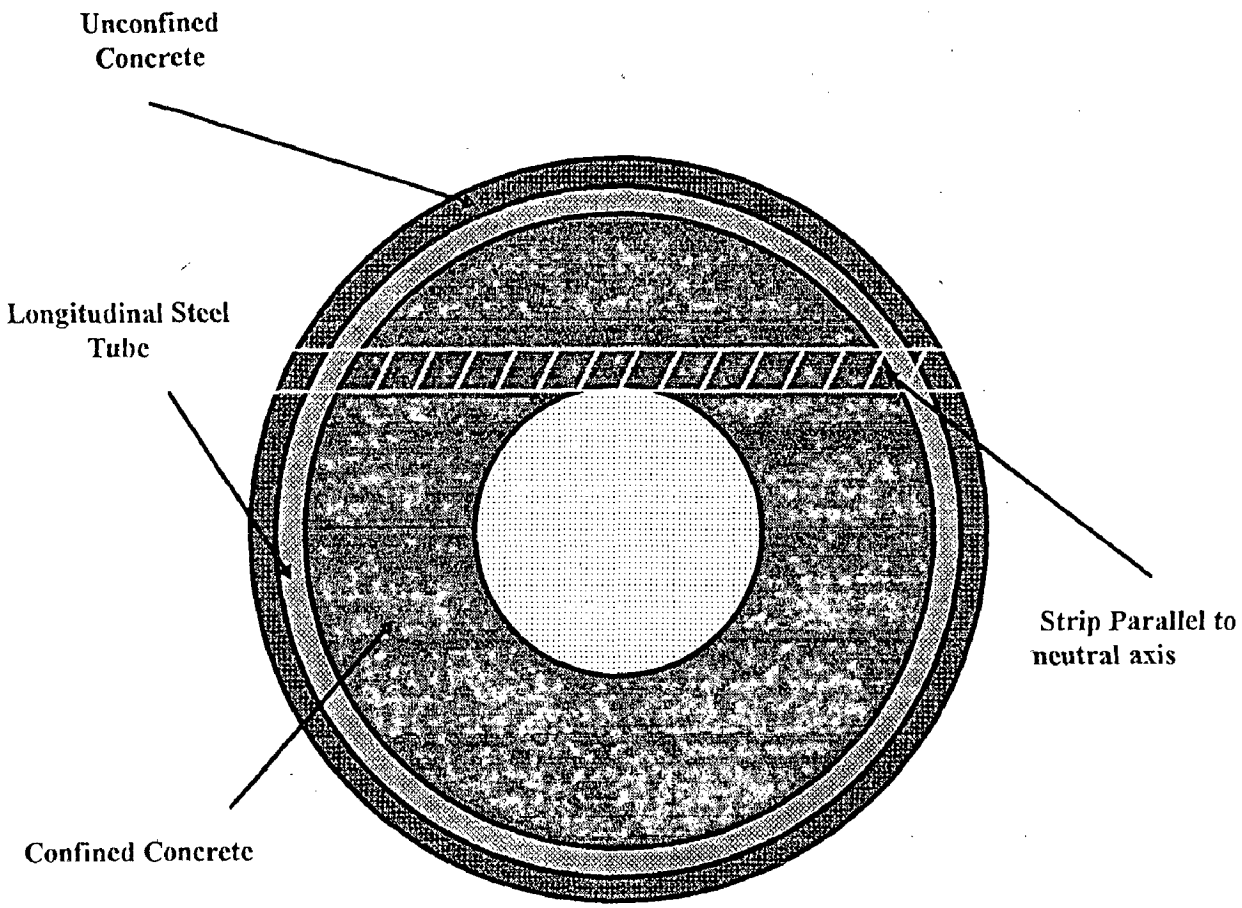

Fig. 4.4 Cross-sectional shape of Hollow Circular Column Section, Longitudinal reinforcement is replaced with a equivalent tube of steel

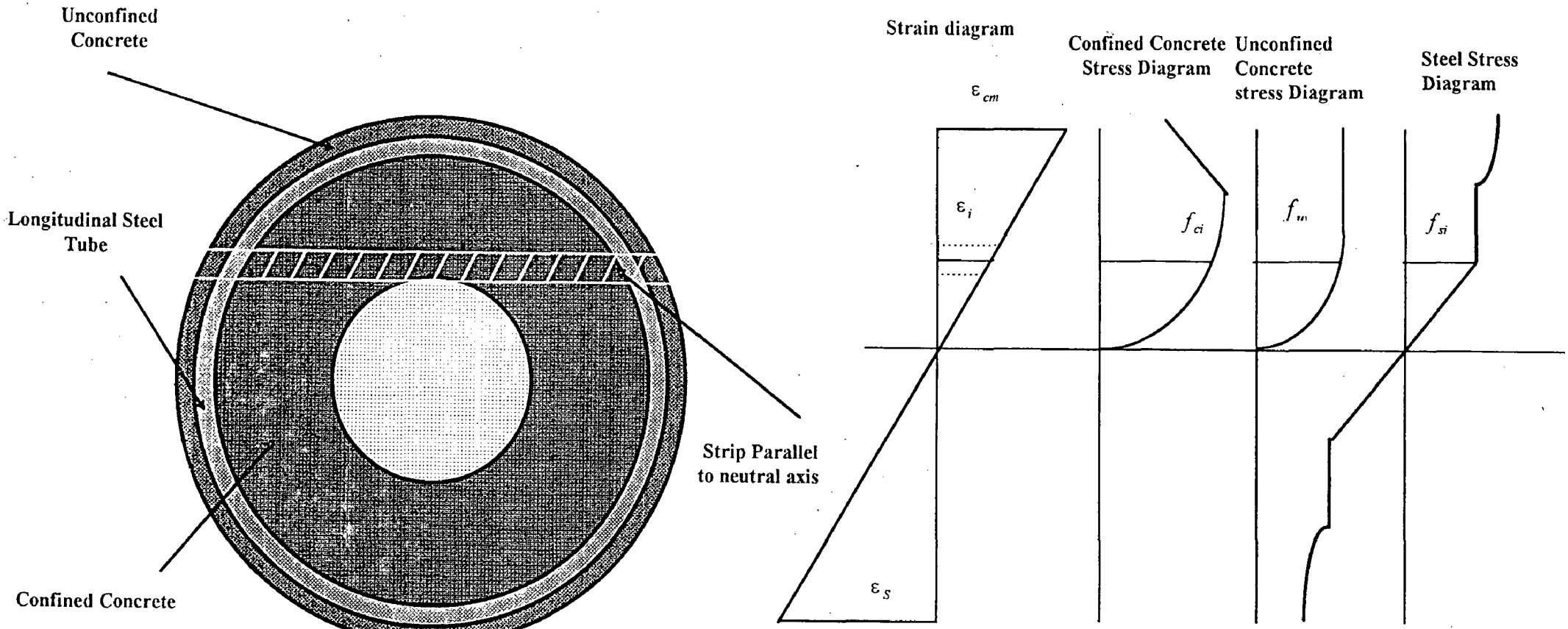

Fig. 4.5 Stresses corresponding to Strain in Unconfined concrete, Confined concrete and Steel

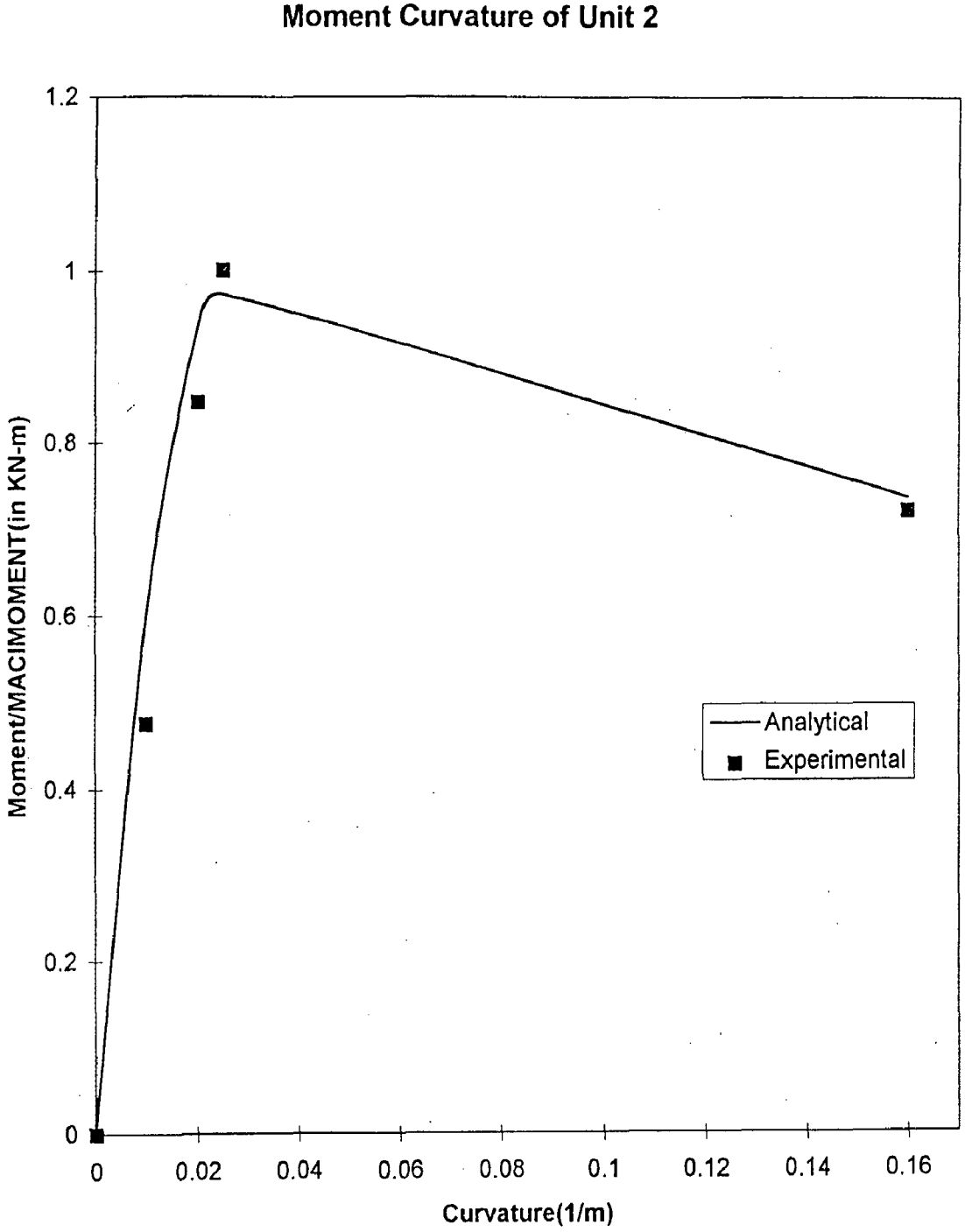

Fig.4.6 Comparision of experimental and analytical results of column unit 2

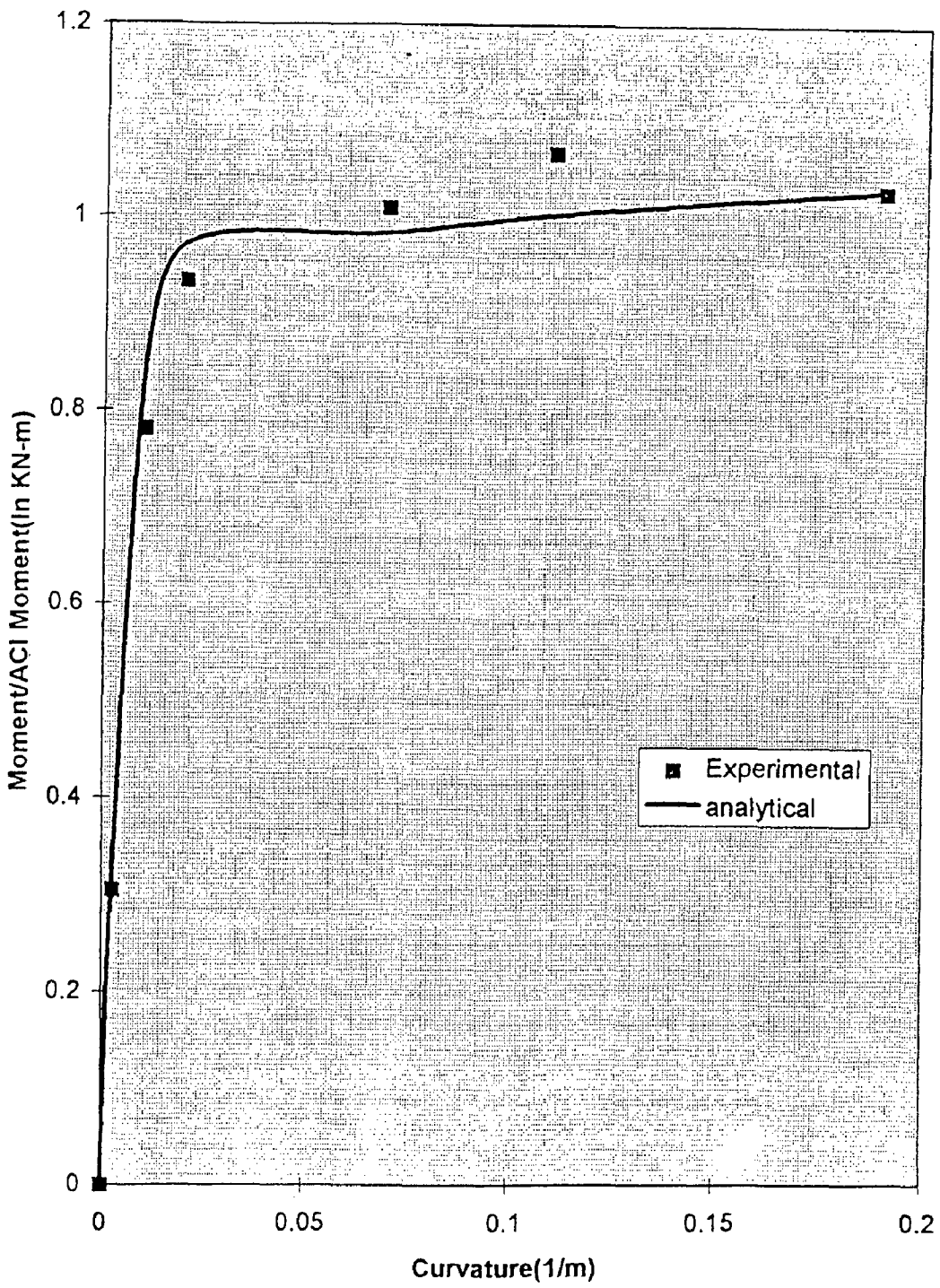

Fig.4.7 Comparision of experimental and analytical results of column unit 3

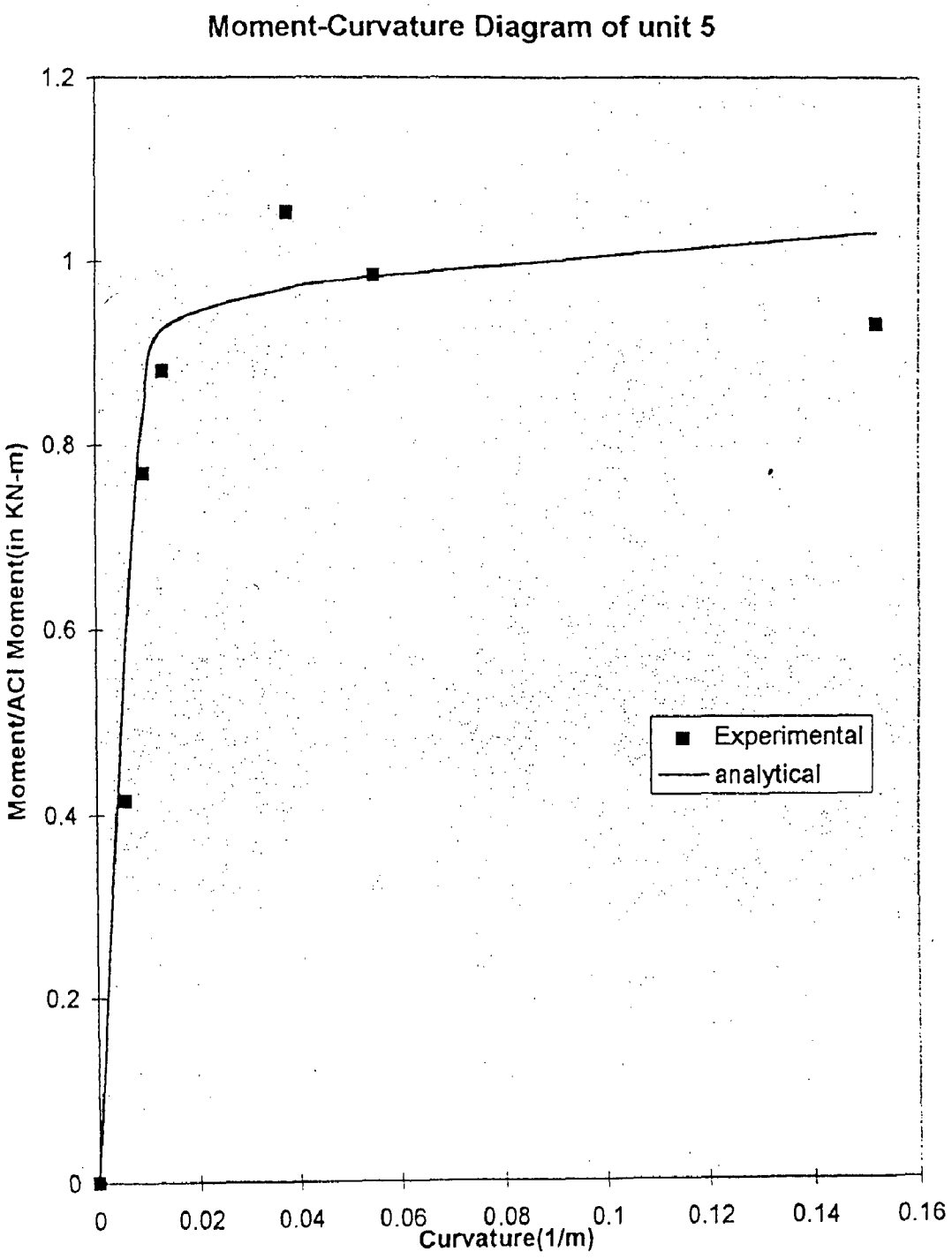

Fig.4.8 **Comparision of experimental and analytical results of column unit 5**

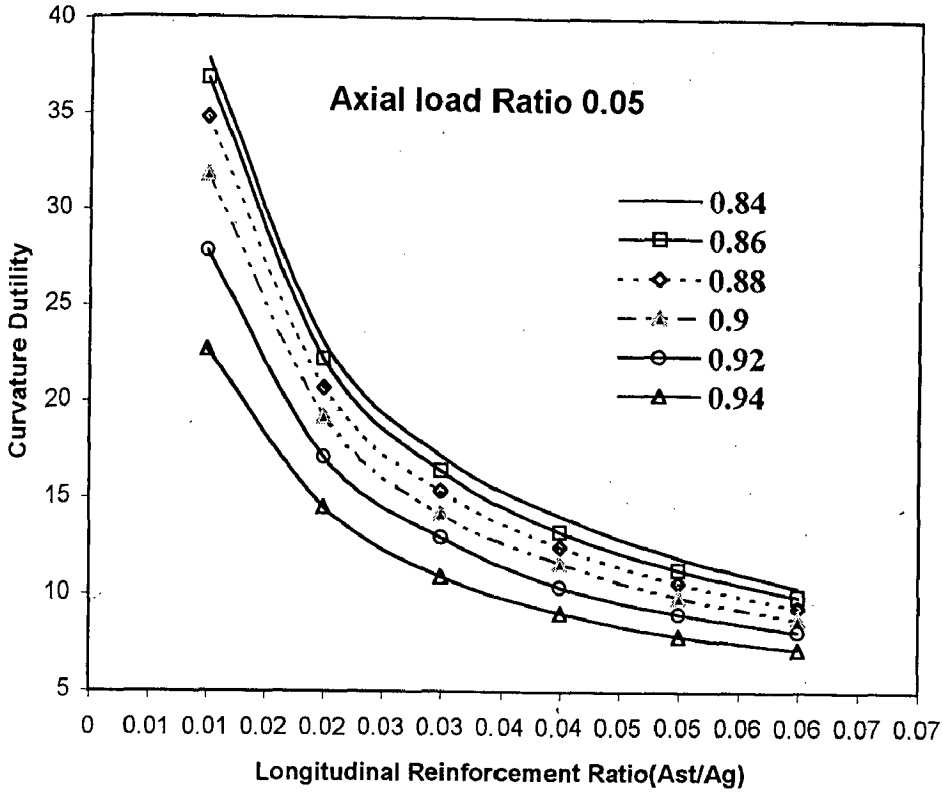

Fig.5.1 Change in Curvature Ductility with Thickness of the section at Axial load Ratio 0.05
(f_c=30.0,f_y=250.0,f_{yh}=415.0,TransverseReinforcement Ratio=0.005)

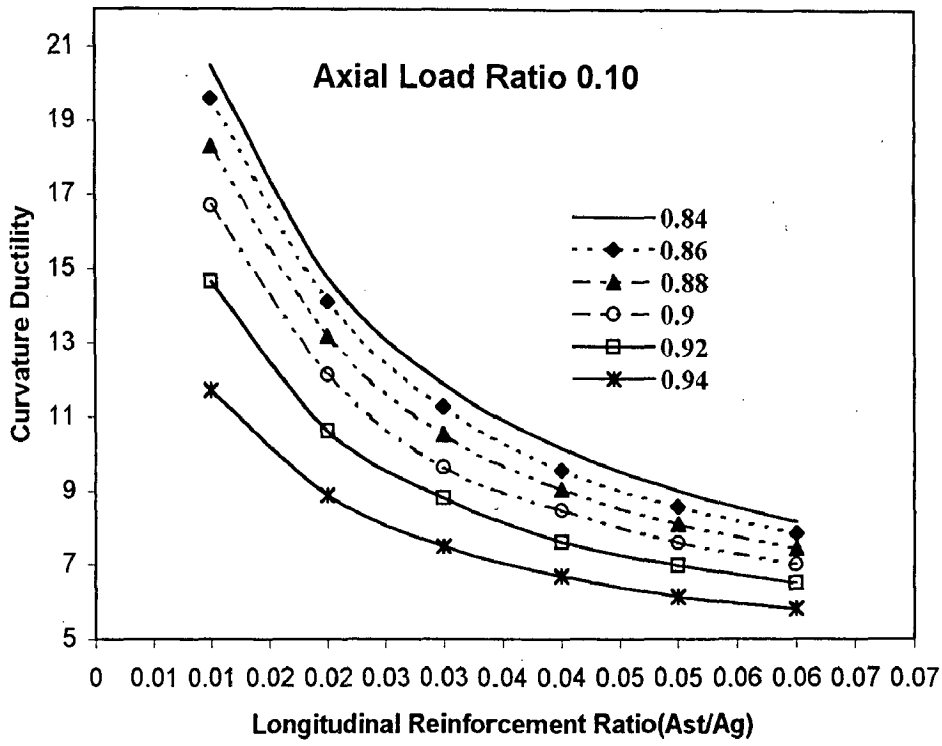

Fig.5.2 Change in Curvature Ductility with Thickness of the section at Axial load Ratio 0.10
(f_c=30.0,f_y=250.0,f_{yh}=415.0,TransverseReinforcement Ratio=0.005)

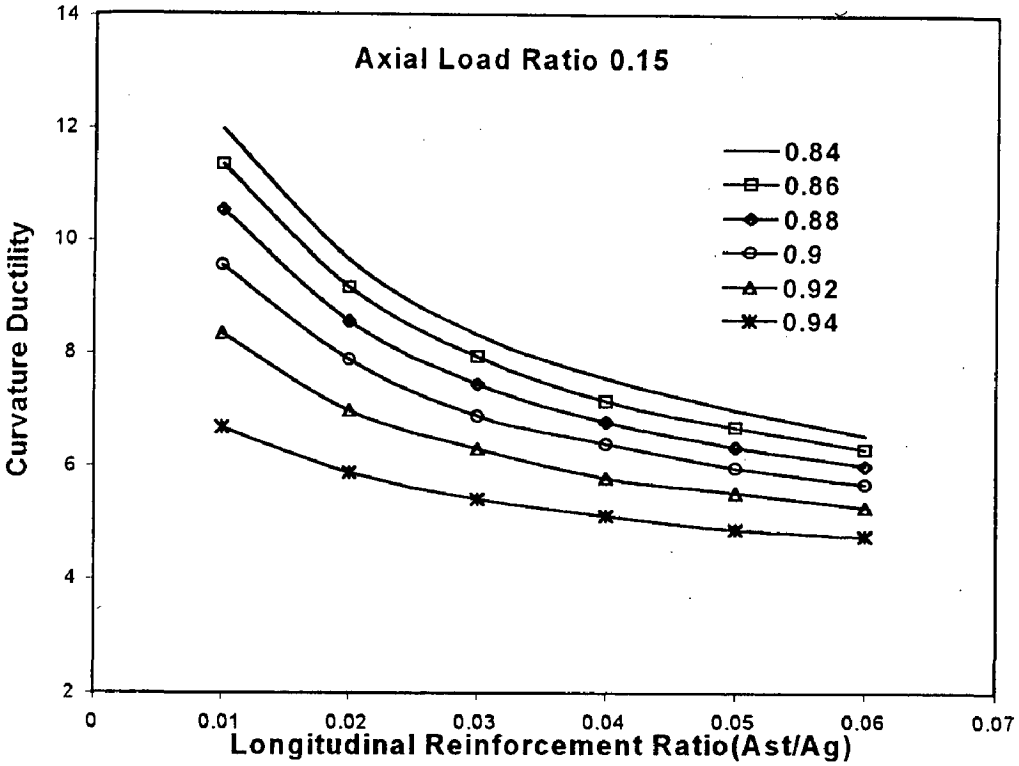

Fig.5.3 Change in Curvature Ductility with Thickness of the section at Axial load Ratio 0.15
(f_c=30.0,f_y=250.0,f_{yh}=415.0,TransverseReinforcement Ratio=0.005)

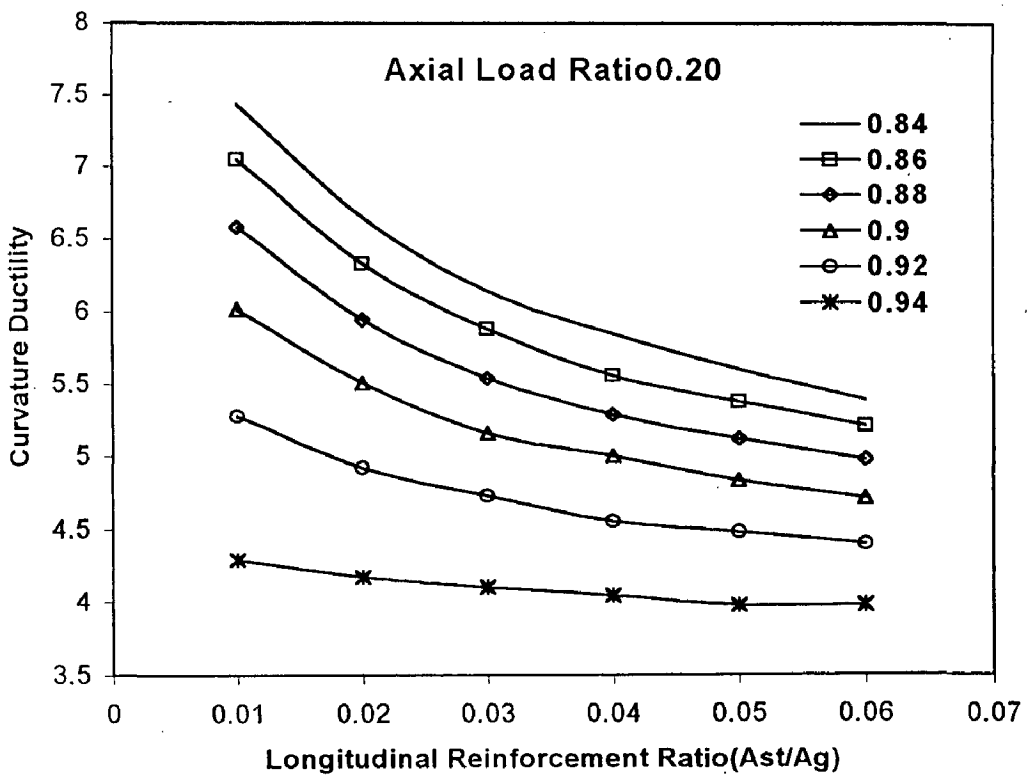

Fig.5.4 Change in Curvature Ductility with Thickness of the section at Axial load Ratio 0.20
(f_c=30.0,f_y=250.0,f_{yh}=415.0,TransverseReinforcement Ratio=0.005)

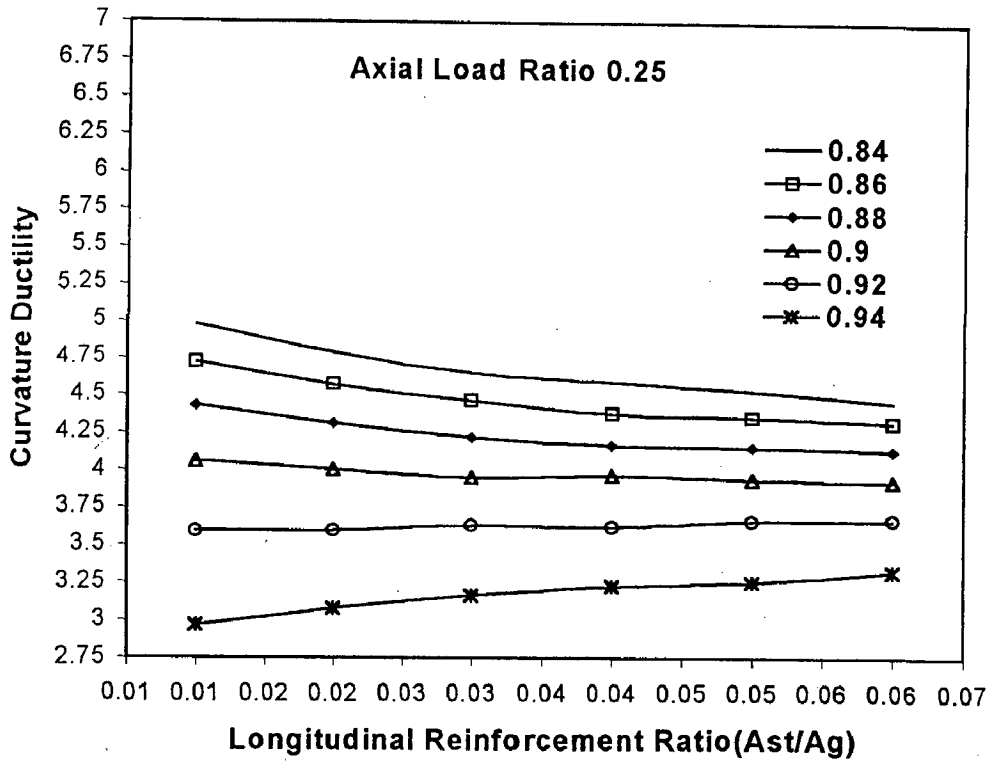

Fig.5.5 Change in Curvature Ductility with Thickness of the section at Axial load Ratio 0.25
(f_c=30.0,f_y=250.0,f_{yh}=415.0,TransverseReinforcement Ratio=0.005)

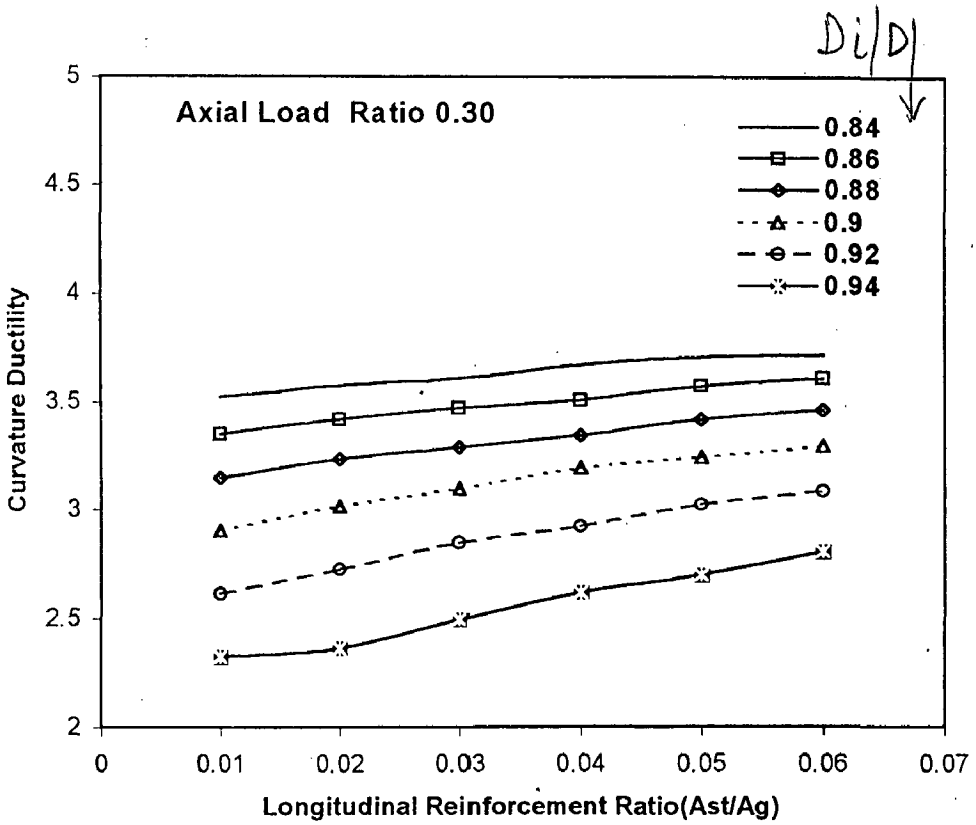

Fig.5.6 Change in Curvature Ductility with Thickness of the section at Axial load Ratio 0.30
(f_c=30.0,f_y=250.0,f_{yh}=415.0,TransverseReinforcement Ratio=0.005)

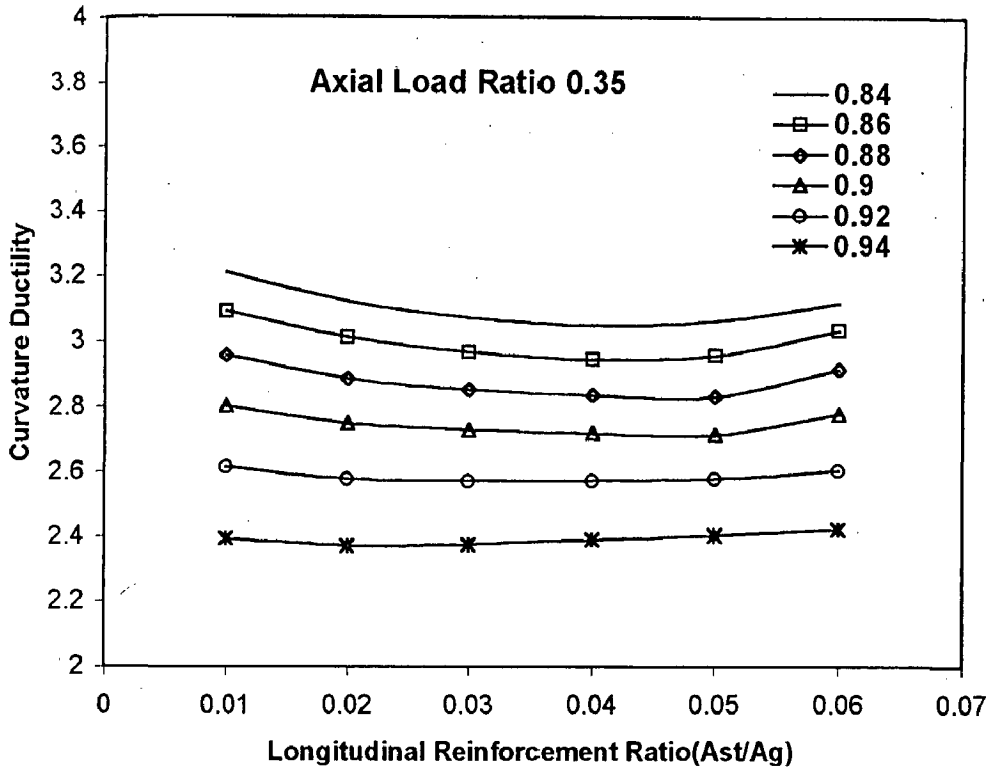

Fig.5.7 Change in Curvature Ductility with Thickness of the section at Axial load Ratio 0.35
(f_c=30.0,f_y=250.0,f_{yh}=415.0,TransverseReinforcement Ratio=0.005)

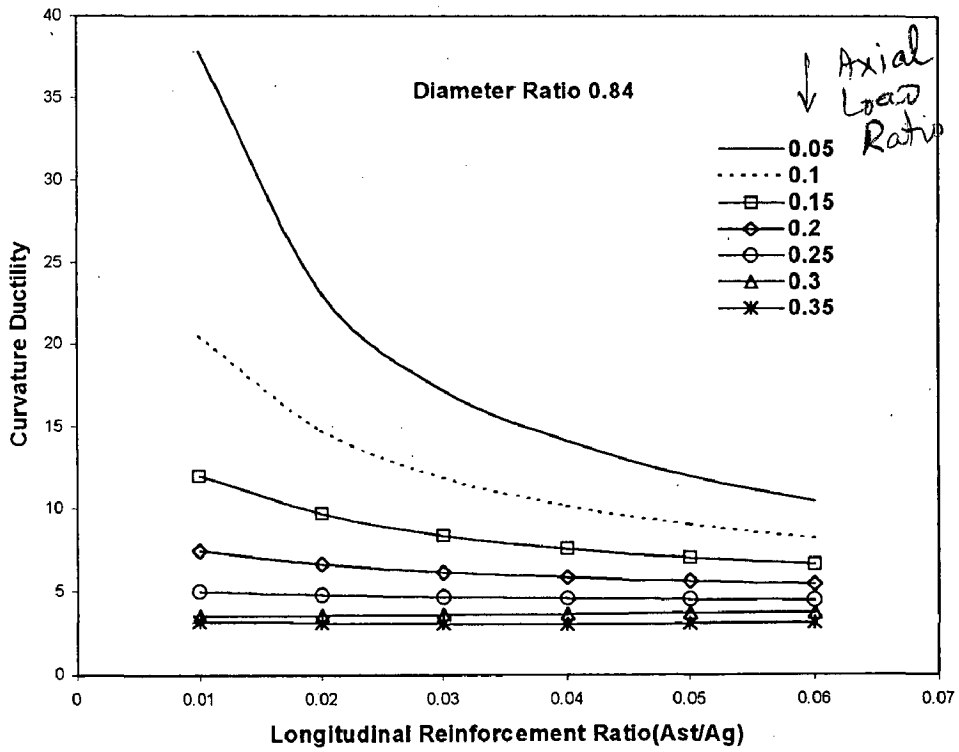

Fig.5.8 Change in Curvature Ductility with Axial load ratio at constant Diameter ratio 0.84
(f_c=30.0,f_y=250.0,f_{yh}=415.0,TransverseReinforcement Ratio=0.005)

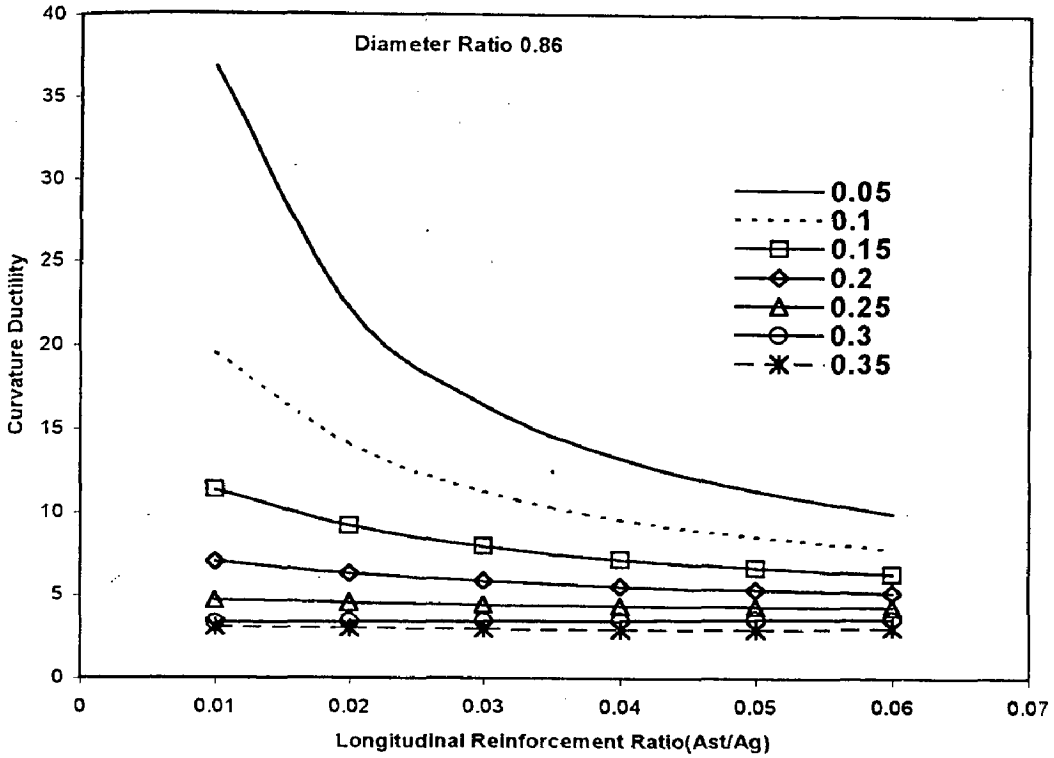

Fig.5.9 Change in Curvature Ductility with Axial load ratio at constant Thickness 0.86
(f_c=30.0,f_y=250.0,f_{yh}=415.0,TransverseReinforcement Ratio=0.005)

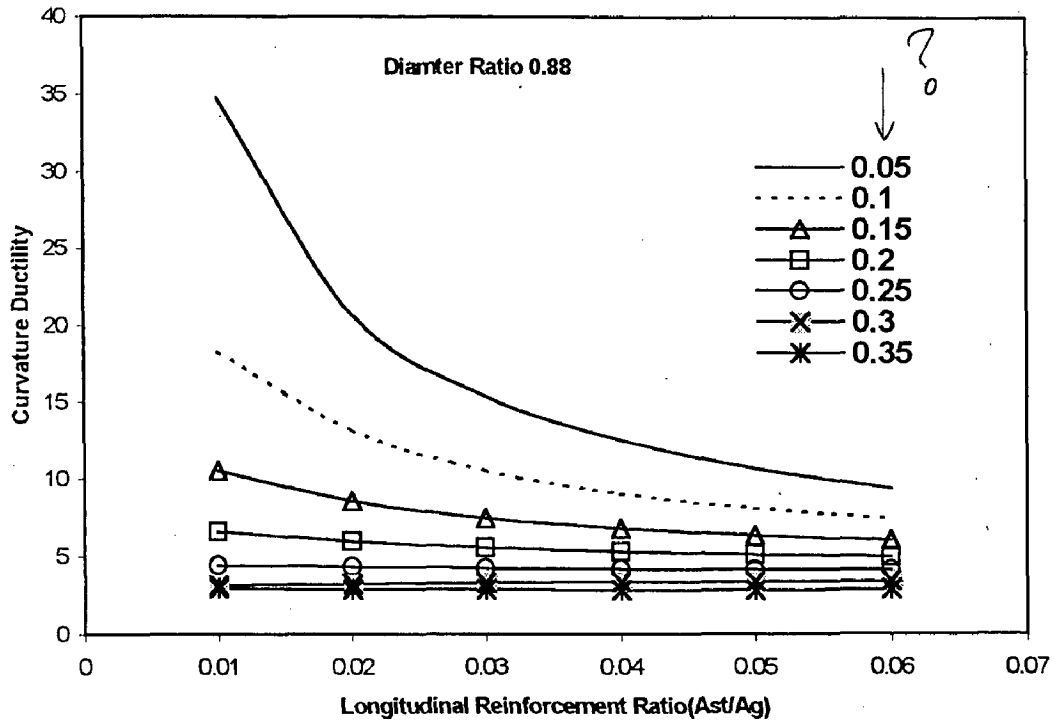

Fig.5.10 Change in Curvature Ductility with Axial load ratio at constant Thickness 0.88
(f_c=30.0,f_y=250.0,f_{yh}=415.0,TransverseReinforcement Ratio=0.005)

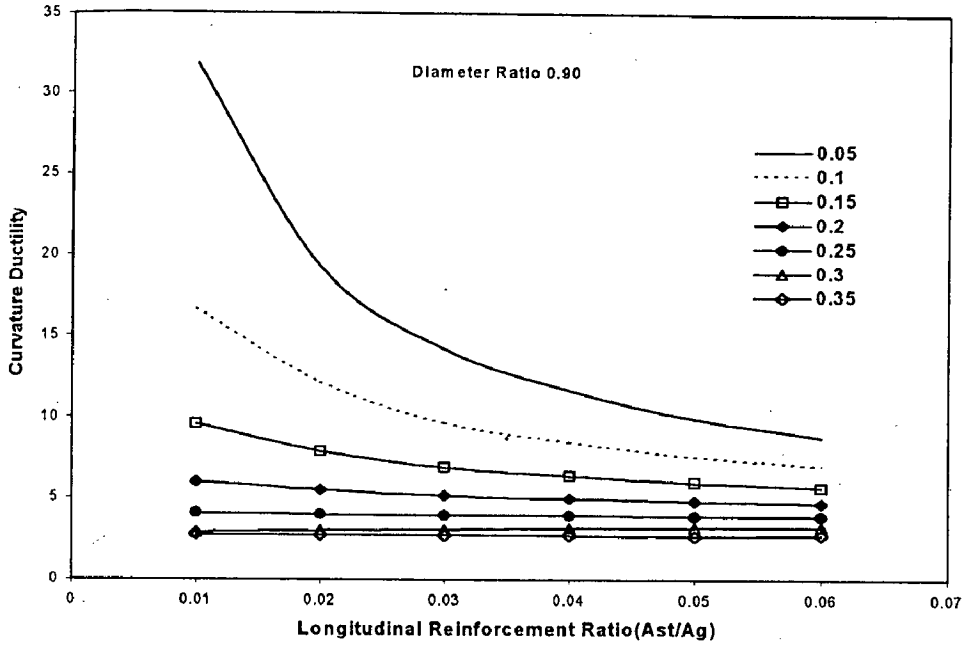

Fig.5.11 Change in Curvature Ductility with Axial load ratio at constant Thickness 0.90
(f_c=30.0,f_y=250.0,f_{yh}=415.0,TransverseReinforcement Ratio=0.005)

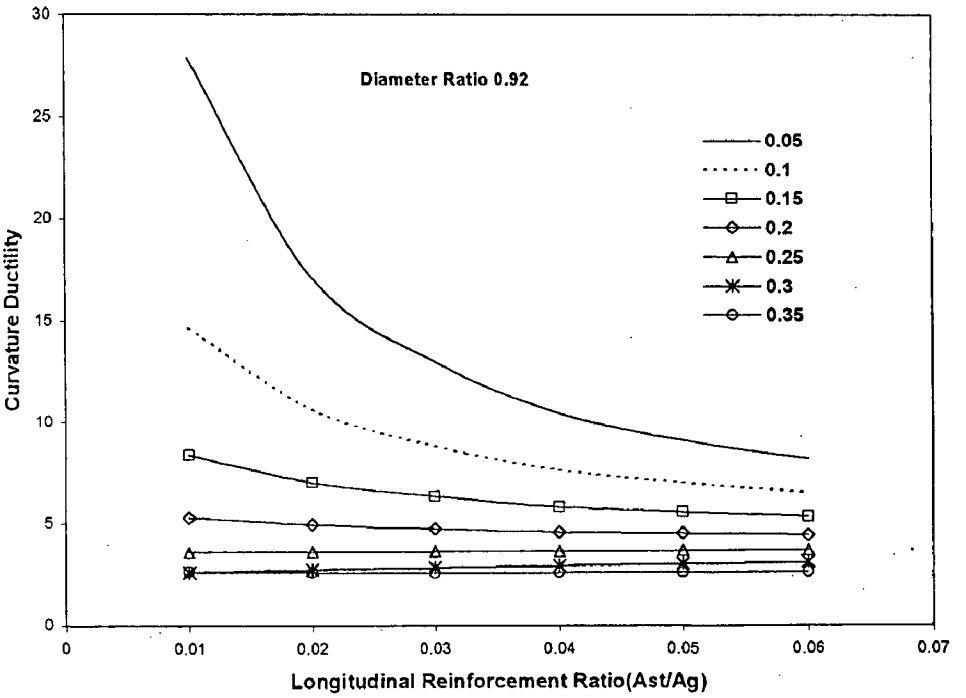

Fig.5.12 Change in Curvature Ductility with Axial load ratio at constant Thickness 0.92
(f_c=30.0,f_y=250.0,f_{yh}=415.0,TransverseReinforcement Ratio=0.005)

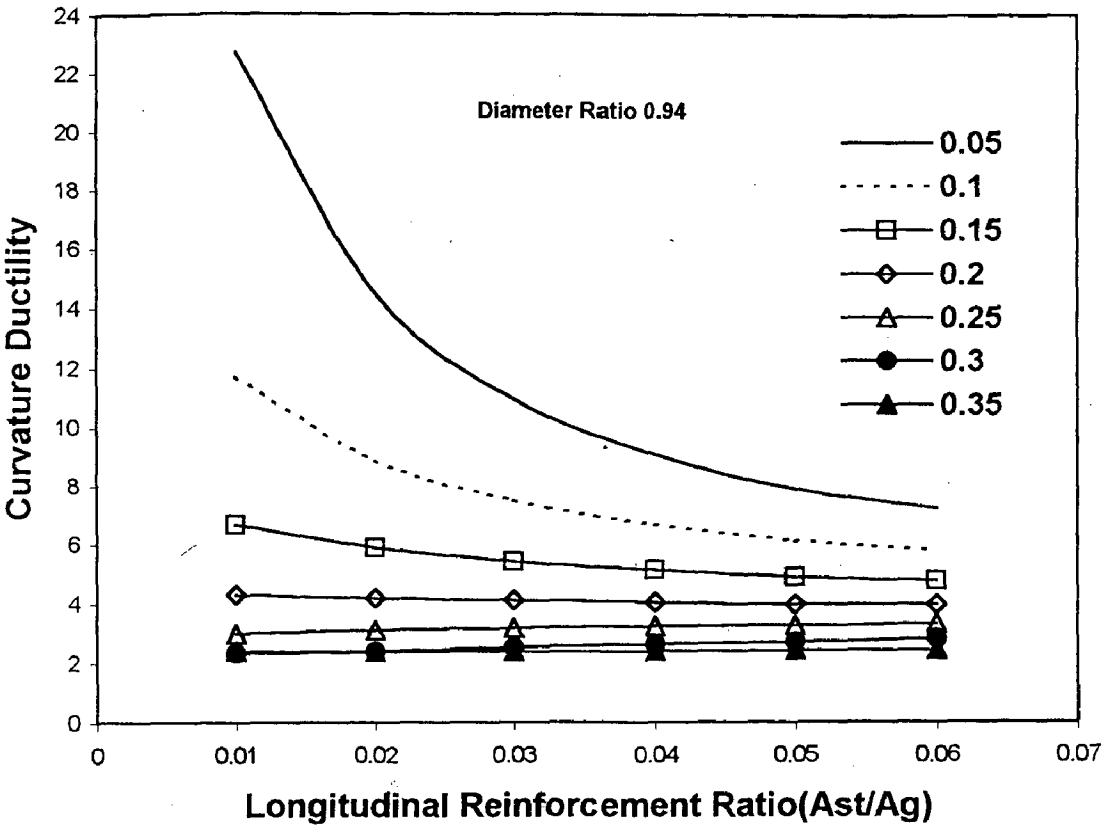

Fig.5.13 Change in Curvature Ductility with Axial load ratio at constant Thickness 0.94
(f_c=30.0,f_y=250.0,f_{yh}=415.0,TransverseReinforcement Ratio=0.005)

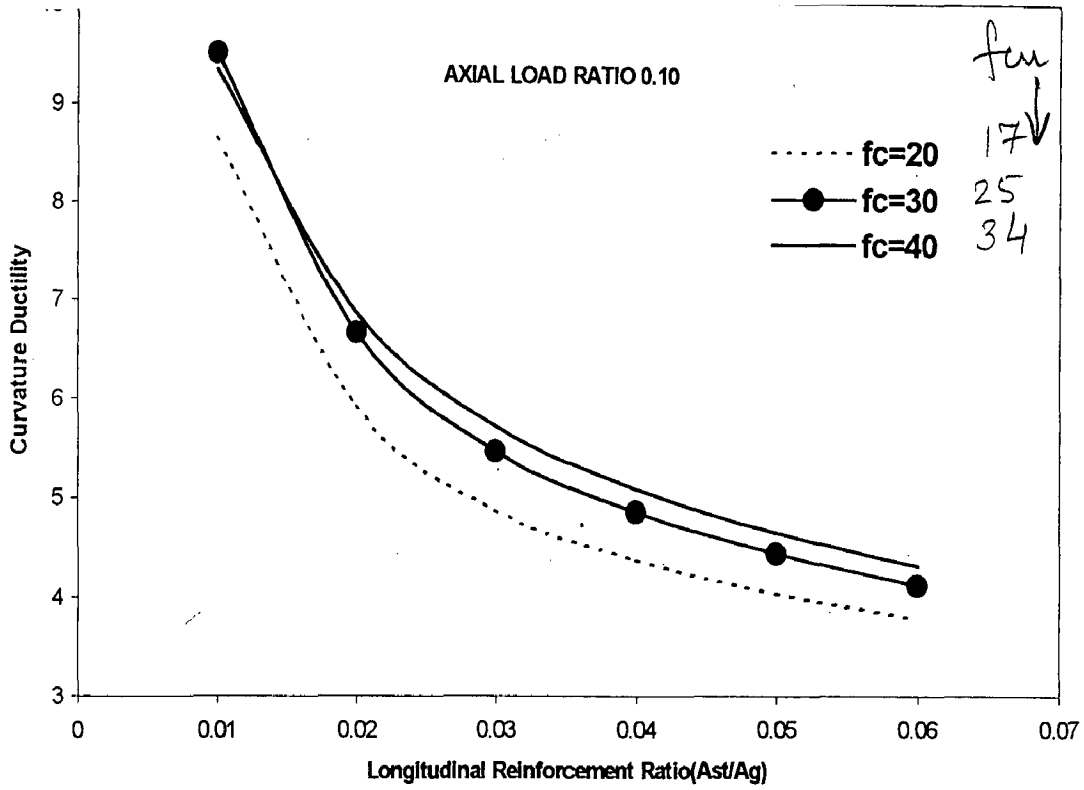

Fig.5.14 Change in Curvature Ductility with Concrete Strength at Axial load ratio 0.10
(f_y=415.0,f_{yh}=415.0,,Transverse Reinforcement Ratio=0.005,Diameter Ratio=0.84)

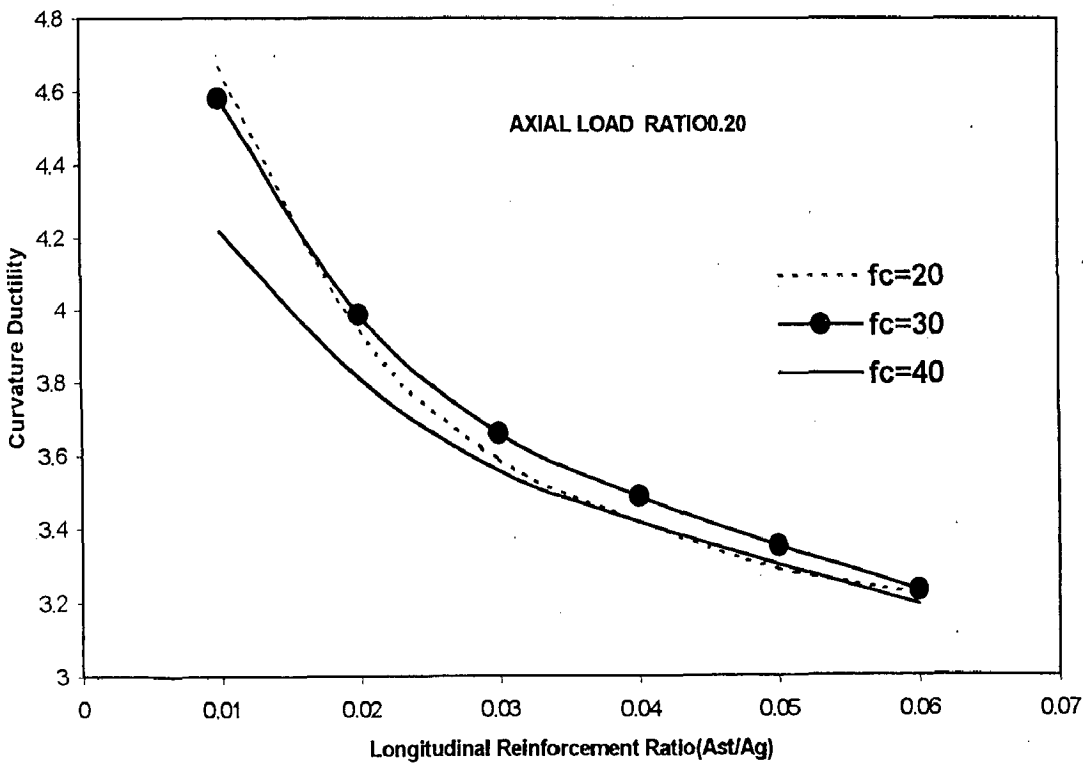

Fig.5.15 Change in Curvature Ductility with Concrete Strength at Axial load ratio 0.20
(f_y=415.0,f_{yh}=415.0,,Transverse Reinforcement Ratio=0.005,Diameter Ratio=0.84

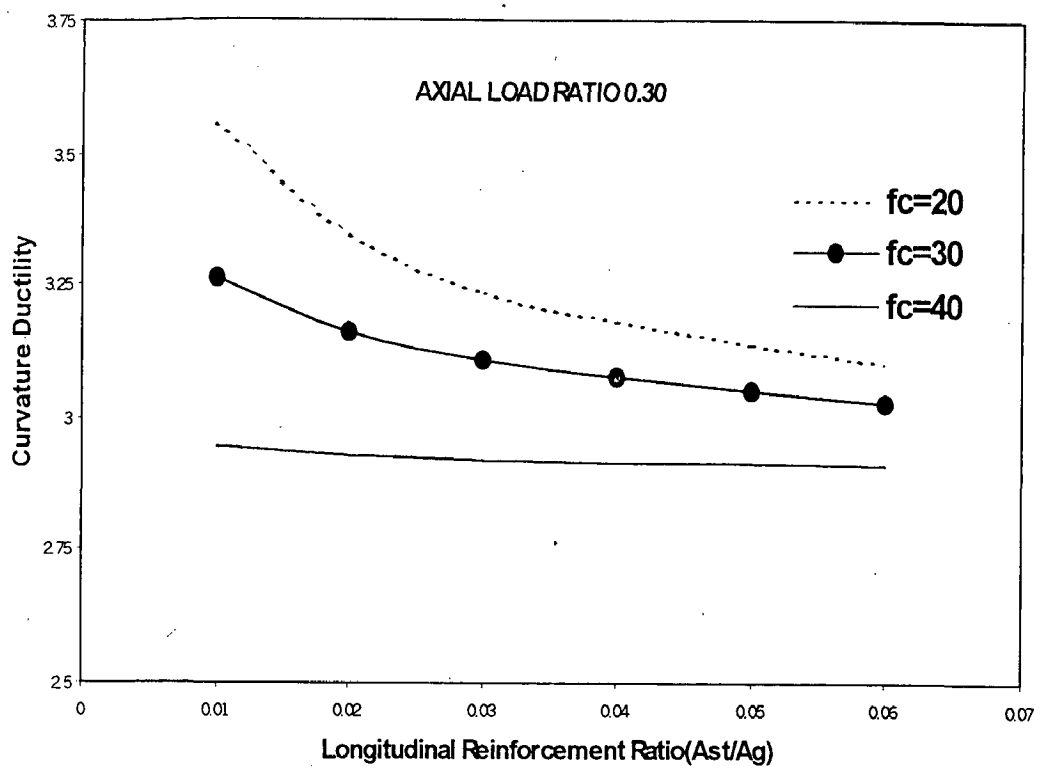

Fig.5.16 Change in Curvature Ductility with Concrete Strength at Axial load ratio 0.30
(f_y=415.0,f_{yh}=415.0,,Transverse Reinforcement Ratio=0.005,Diameter Ratio=0.84

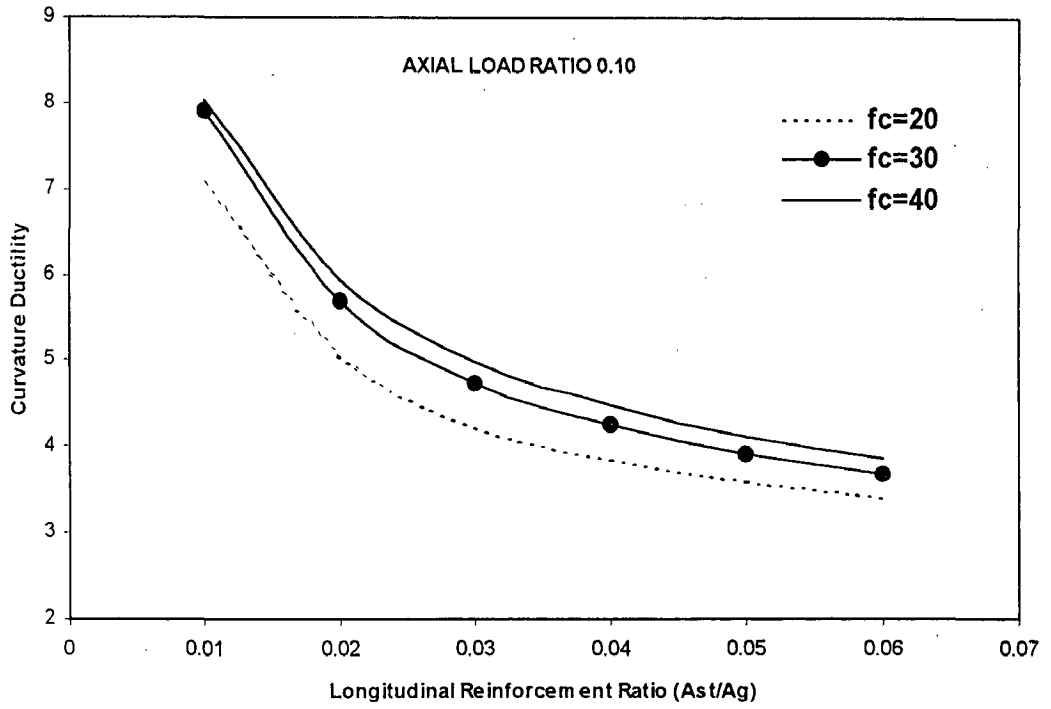

Fig.5.17 Change in Curvature Ductility with Concrete Strength at Axial load ratio 0.10
(f_y=415.0,f_{yh}=415.0,,Transverse Reinforcement Ratio=0.005,Diameter Ratio=0.90

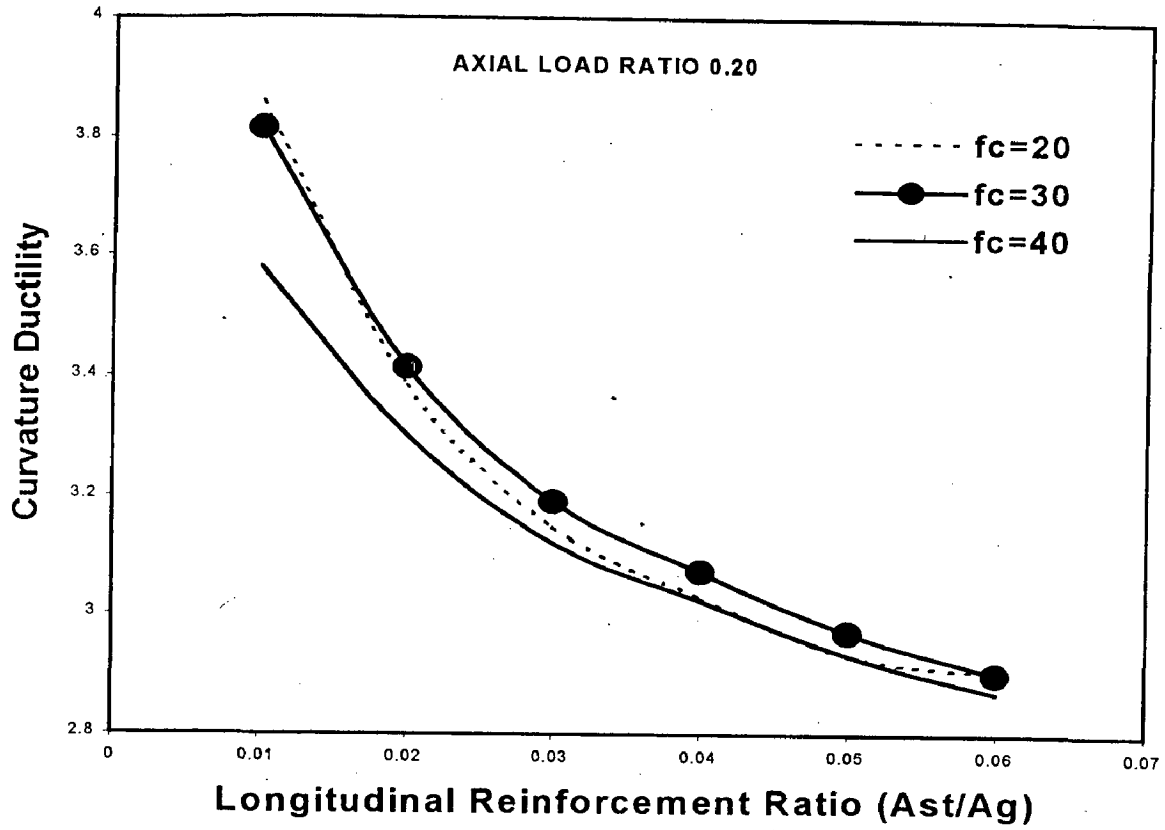

Fig.5.18 Change in Curvature Ductility with Concrete Strength at Axial load ratio 0.20
(f_y=415.0,f_{yh}=415.0,,Transverse Reinforcement Ratio=0.005,Diameter Ratio=0.90

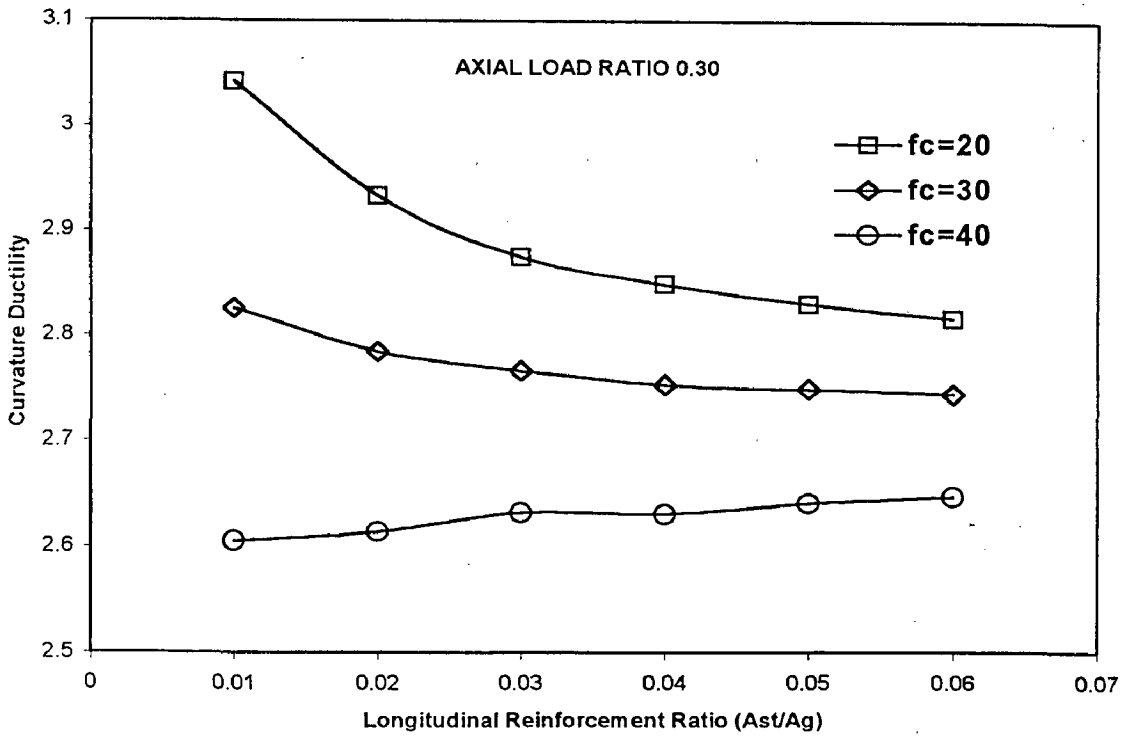

Fig.5.19 Change in Curvature Ductility with Concrete Strength at Axial load ratio 0.30
(f_y=415.0,f_{yh}=415.0,,Transverse Reinforcement Ratio=0.005,Diameter Ratio=0.90

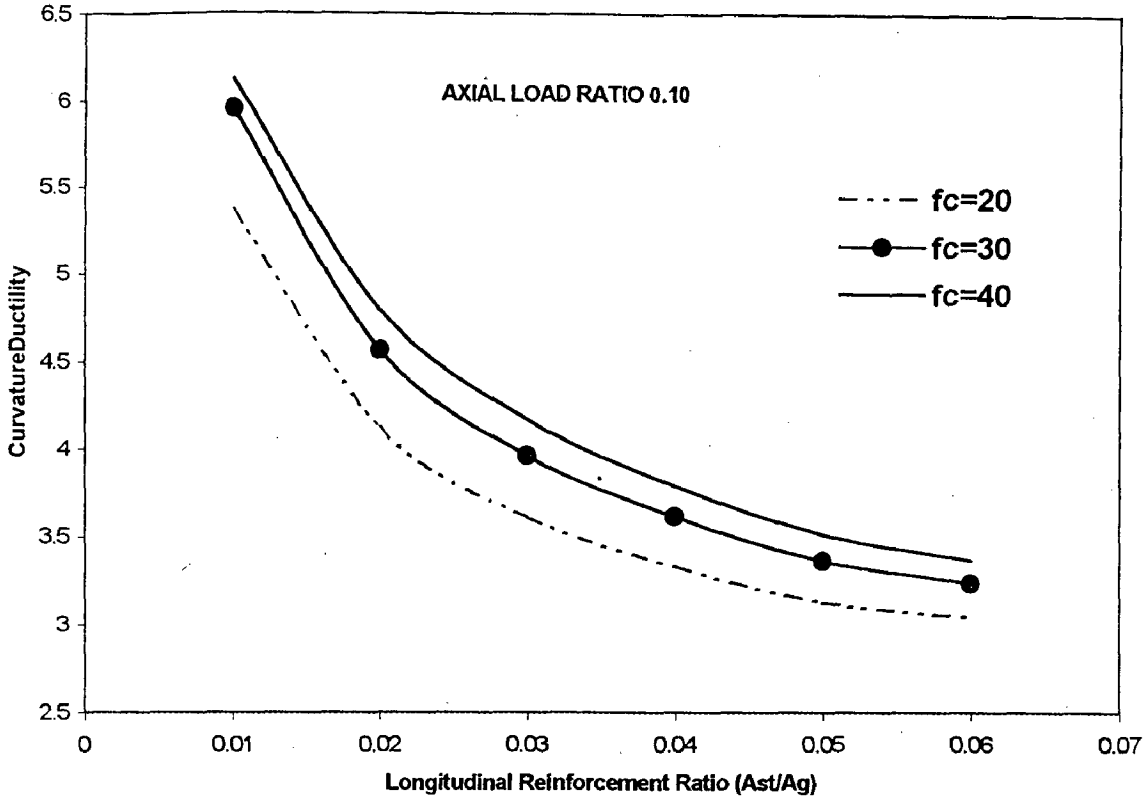

Fig.5.20 Change in Curvature Ductility with Concrete Strength at Axial load ratio 0.10
(f_y=415.0,f_{yh}=415.0,,Transverse Reinforcement Ratio=0.005,Diameter Ratio=0.94

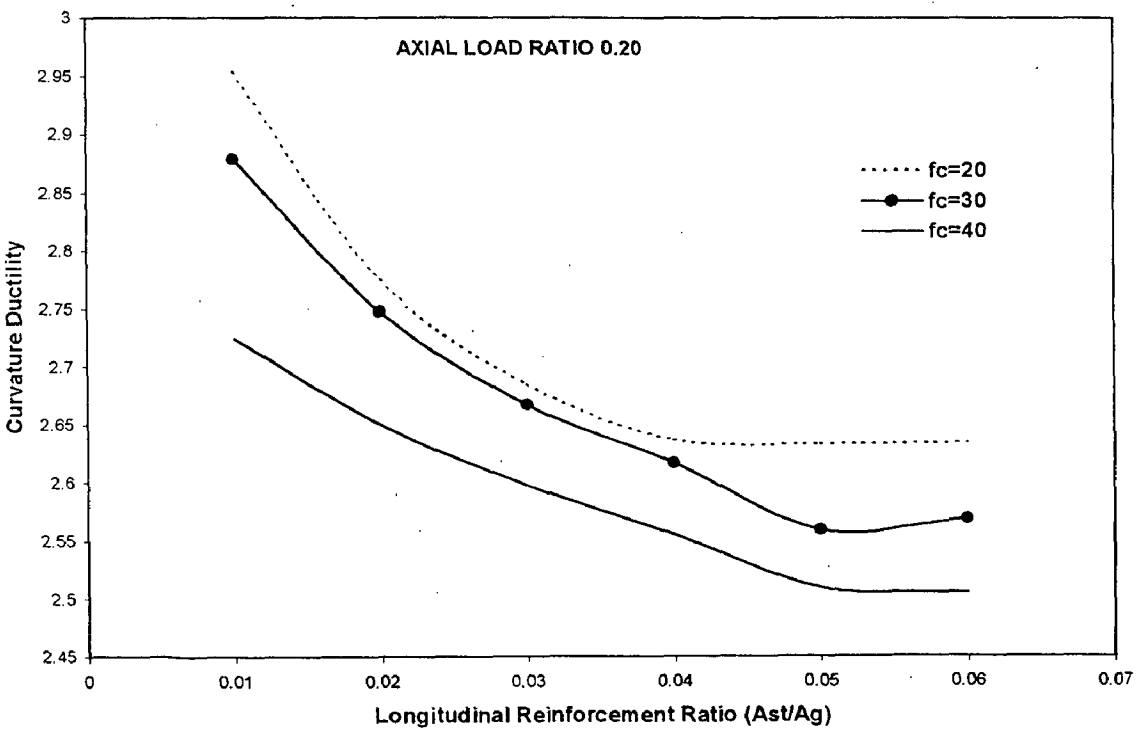

Fig.5.21 Change in Curvature Ductility with Concrete Strength at Axial load ratio 0.20
(f_y=415.0,f_{yh}=415.0,,Transverse Reinforcement Ratio=0.005,Diameter Ratio=0.94

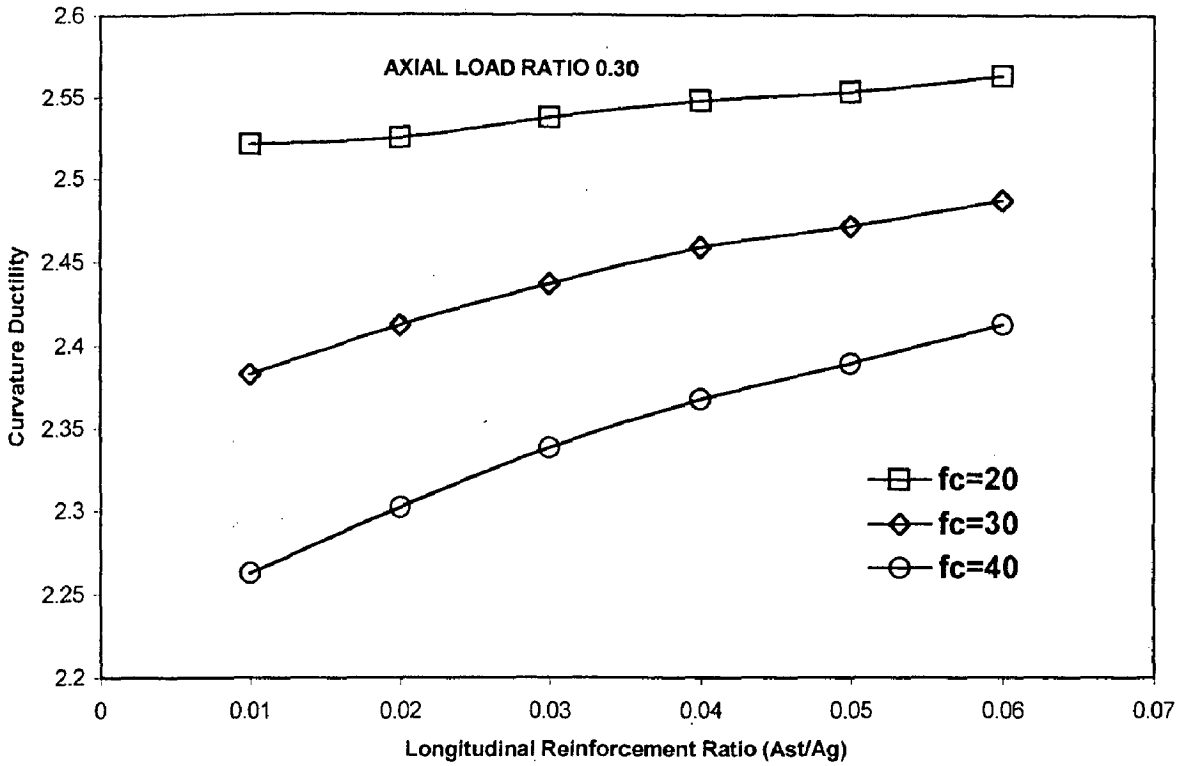

**Fig.5.22 Change in Curvature Ductility with Concrete Strength at Axial load ratio 0.30 (f_y=415.0,f_{yh}=415.0,,*Transverse Reinforcement Ratio=0.005,Diameter Ratio=0.94*

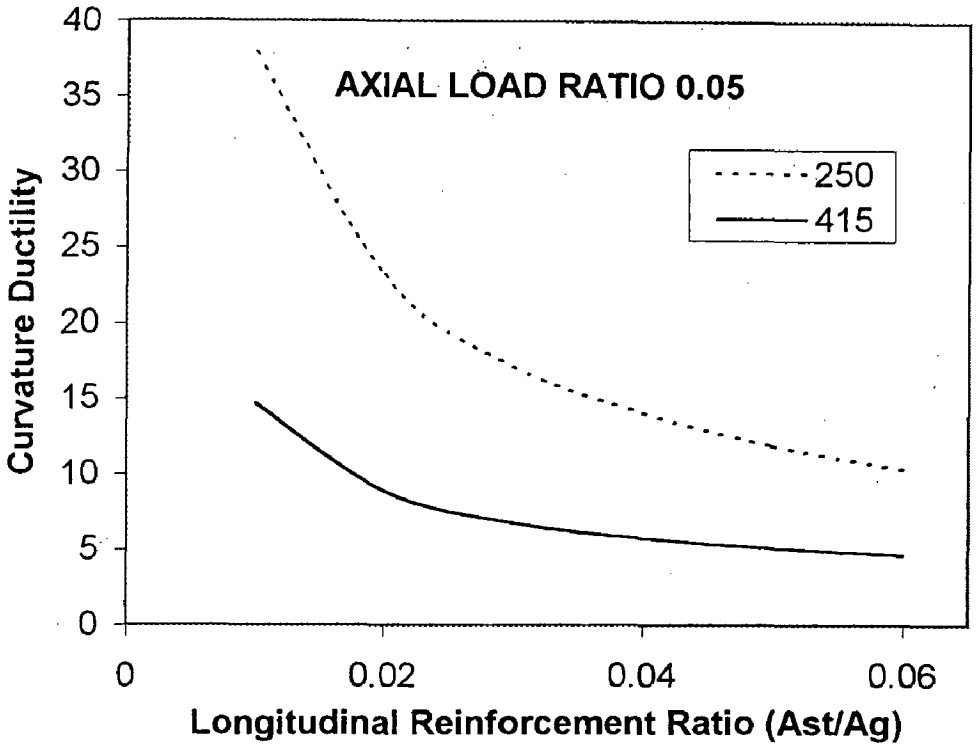

Fig.5.23 Change in Curvature Ductility with Yield strength of Longitudinal steel (fc=30.0,fyh=415.0,Transverse Reinforcement Ratio=0.005,Diameter Ratio=0.84)

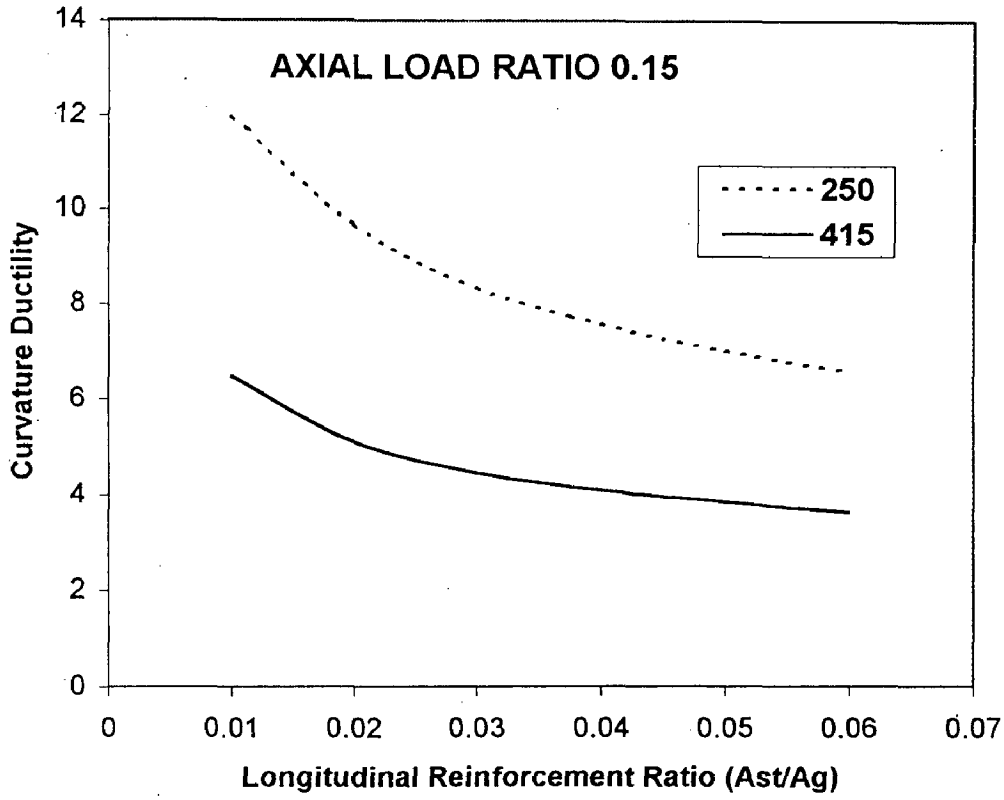

Fig.5.24 Change in Curvature Ductility with Yield strength of Longitudinal steel (fc=30.0,fyh=415.0,Transverse Reinforcement Ratio=0.005,Diameter Ratio=0.84)

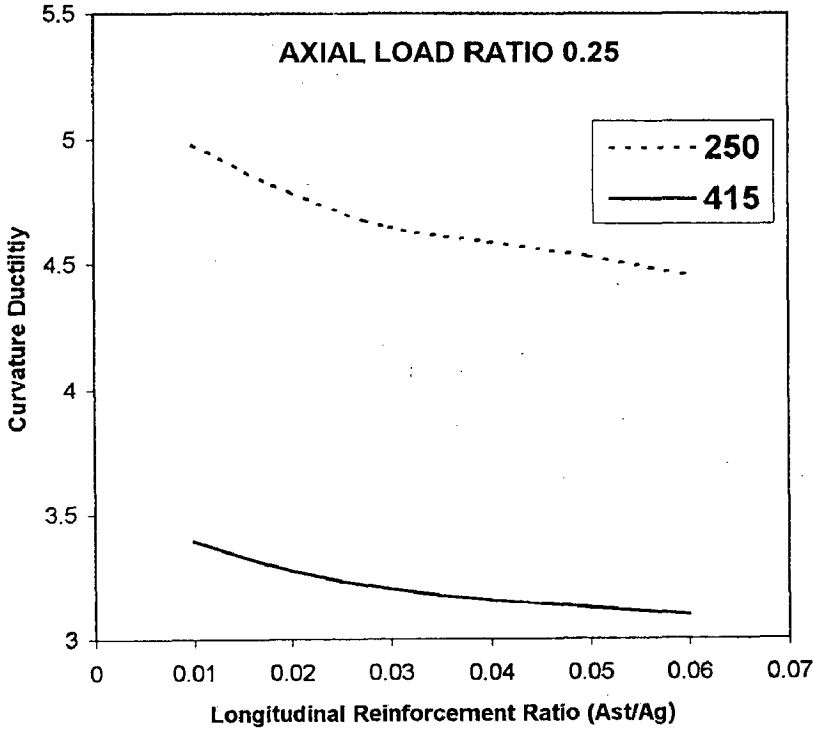

Fig.5.25 Change in Curvature Ductility with Yield strength of Longitudinal steel (fc=30.0,fyh=415.0,Transverse Reinforcement Ratio=0.005,Diameter Ratio=0.84)

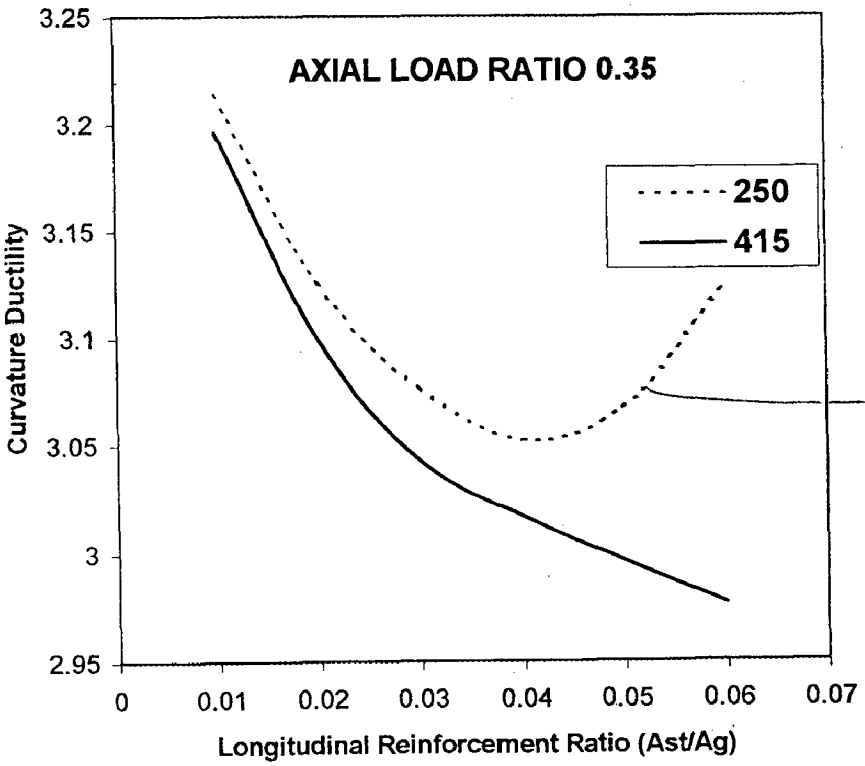

why does it increase?

Fig.5.26 Change in Curvature Ductility with Yield strength of Longitudinal steel (fc=30.0,fyh=415.0,Transverse Reinforcement Ratio=0.005,Diameter Ratio=0.84)

$\frac{Di}{D}$

$D_i = 0.84D$

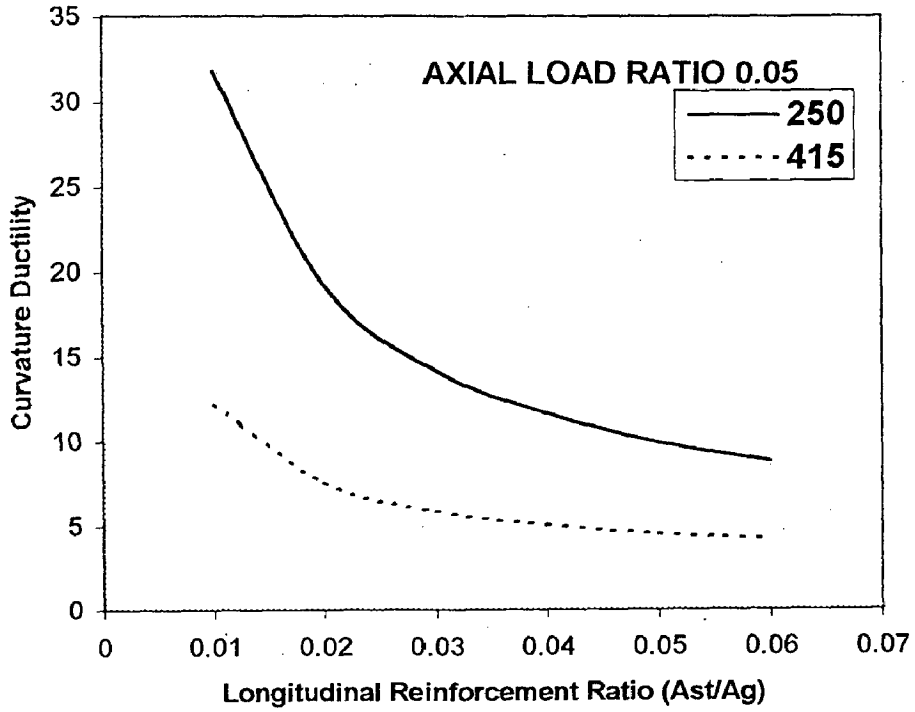

Fig.5.27 Change in Curvature Ductility with Yield strength of Longitudinal steel (fc=30.0,fyh=415.0,Transverse Reinforcement Ratio=0.005,Diameter Ratio=0.90)

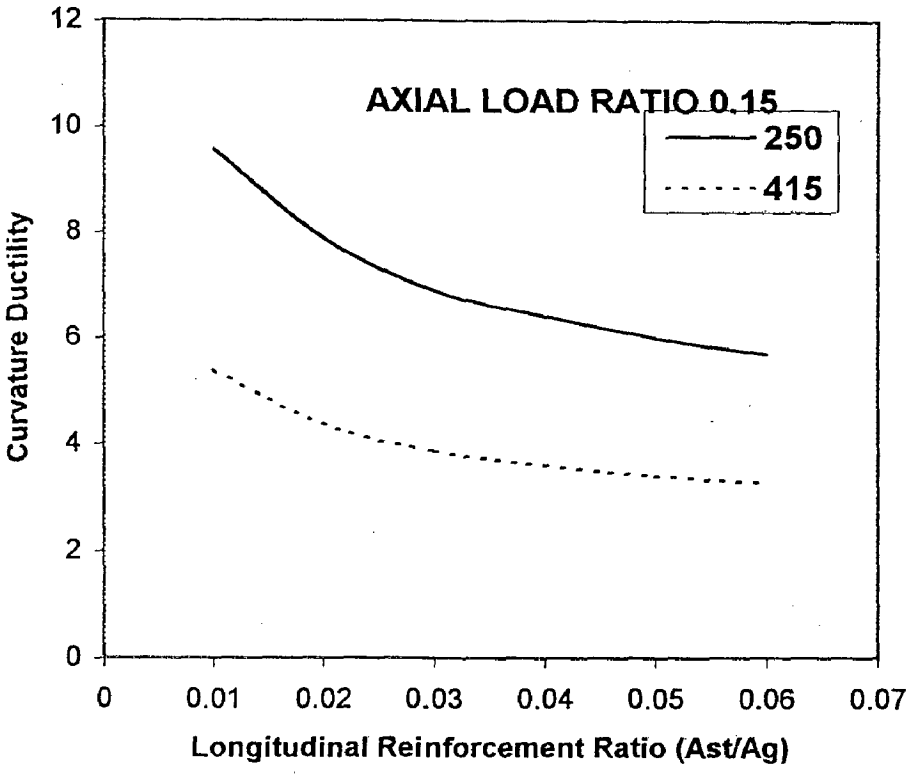

Fig.5.28 Change in Curvature Ductility with Yield strength of Longitudinal steel (fc=30.0,fyh=415.0,Transverse Reinforcement Ratio=0.005,Diameter Ratio=0.90)

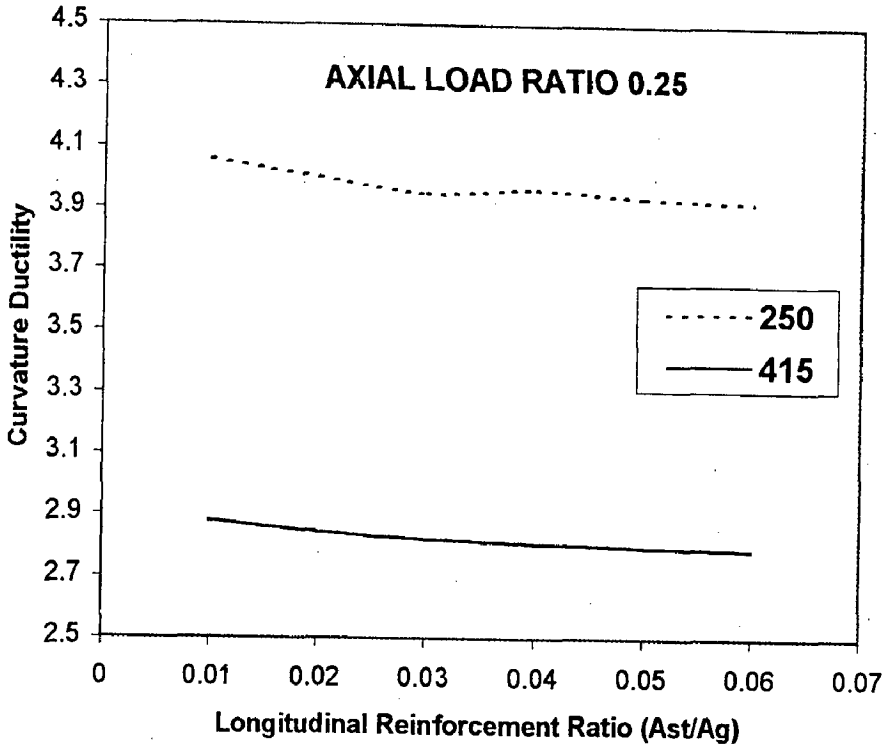

Fig.5.29 Change in Curvature Ductility with Yield strength of Longitudinal steel (fc=30.0,fyh=415.0,Transverse Reinforcement Ratio=0.005,Diameter Ratio=0.90)

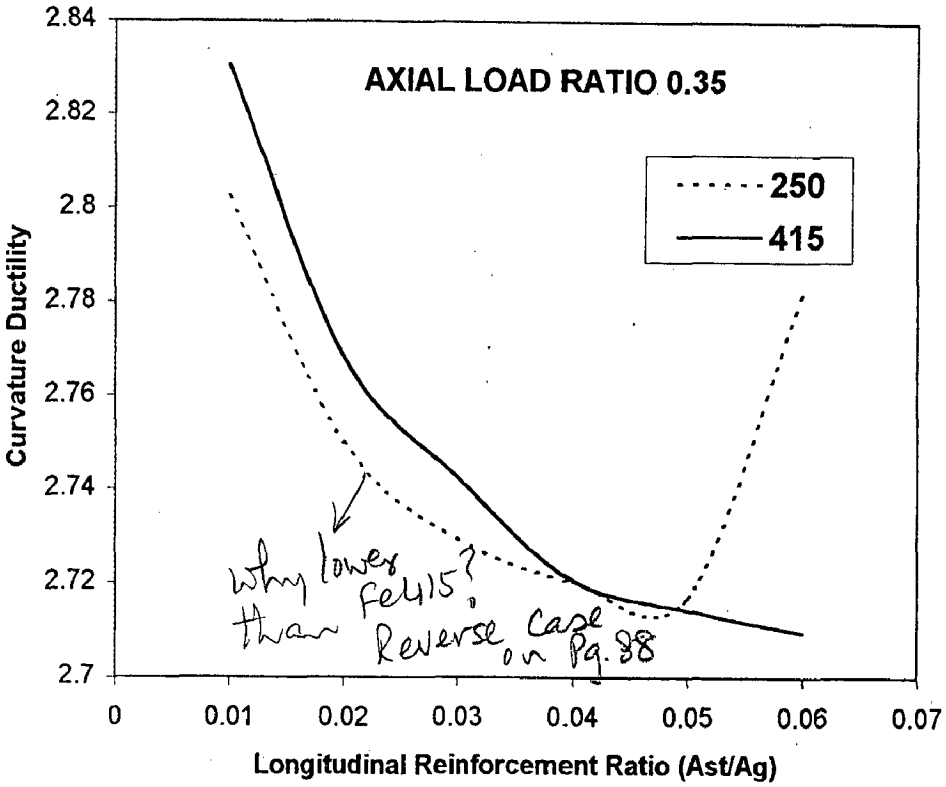

Fig.5.30 Change in Curvature Ductility with Yield strength of Longitudinal steel (fc=30.0,fyh=415.0,Transverse Reinforcement Ratio=0.005,Diameter Ratio=0.90)

$D_i = 0.90\,D$

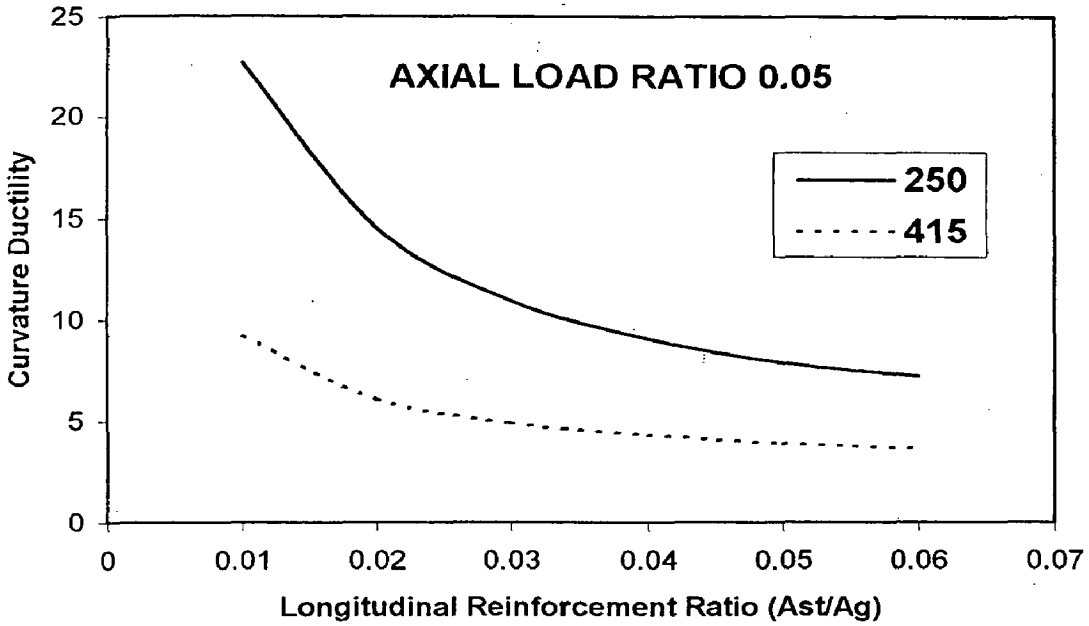

Fig.5.31 Change in Curvature Ductility with Yield strength of Longitudinal steel (fc=30.0,fyh=415.0,Transverse Reinforcement Ratio=0.005,Diameter Ratio=0.94)

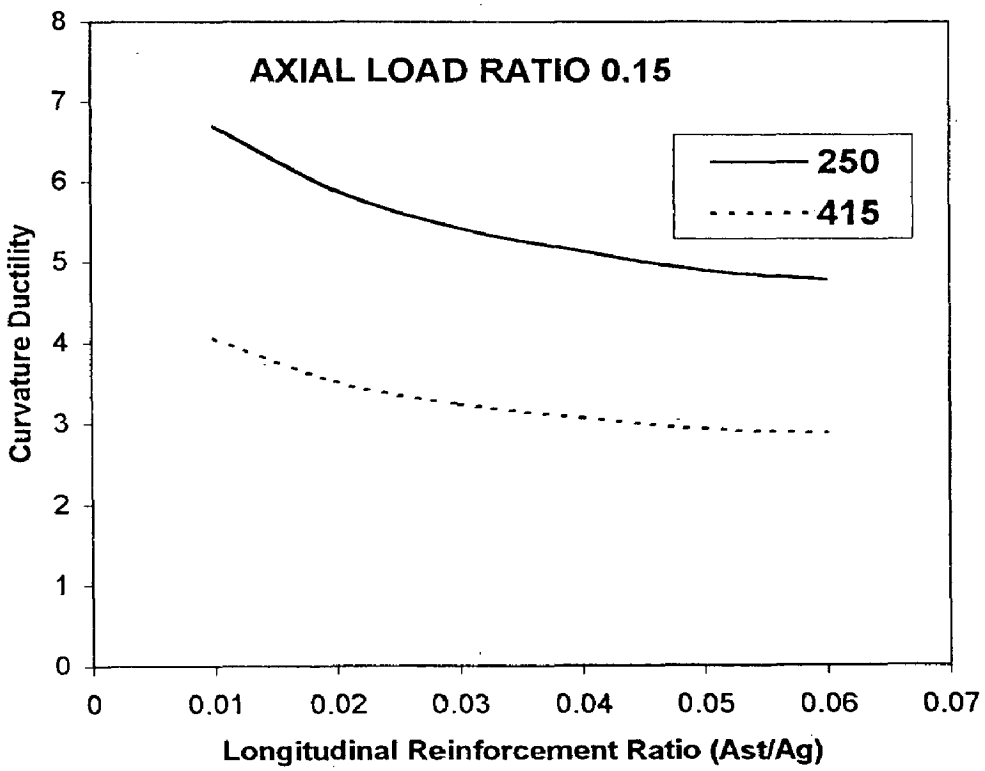

Fig.5.32 Change in Curvature Ductility with Yield strength of Longitudinal steel (fc=30.0,fyh=415.0,Transverse Reinforcement Ratio=0.005,Diameter Ratio=0.94)

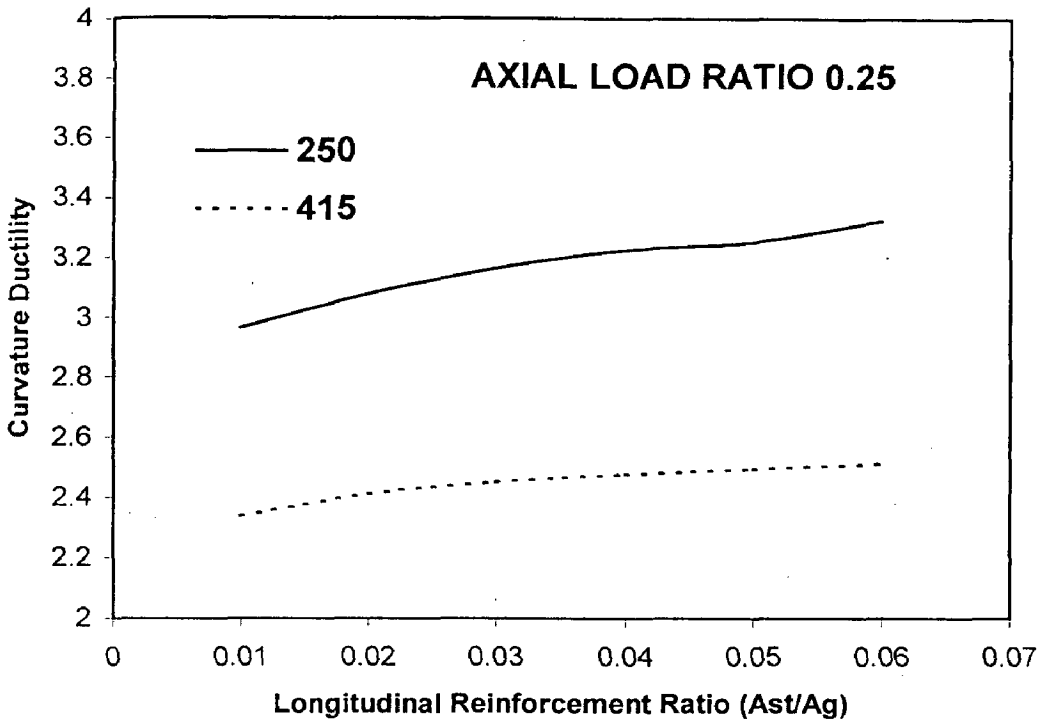

Fig.5.33 Change in Curvature Ductility with Yield strength of Longitudinal steel (fc=30.0,fyh=415.0,Transverse Reinforcement Ratio=0.005,Diameter Ratio=0.94)

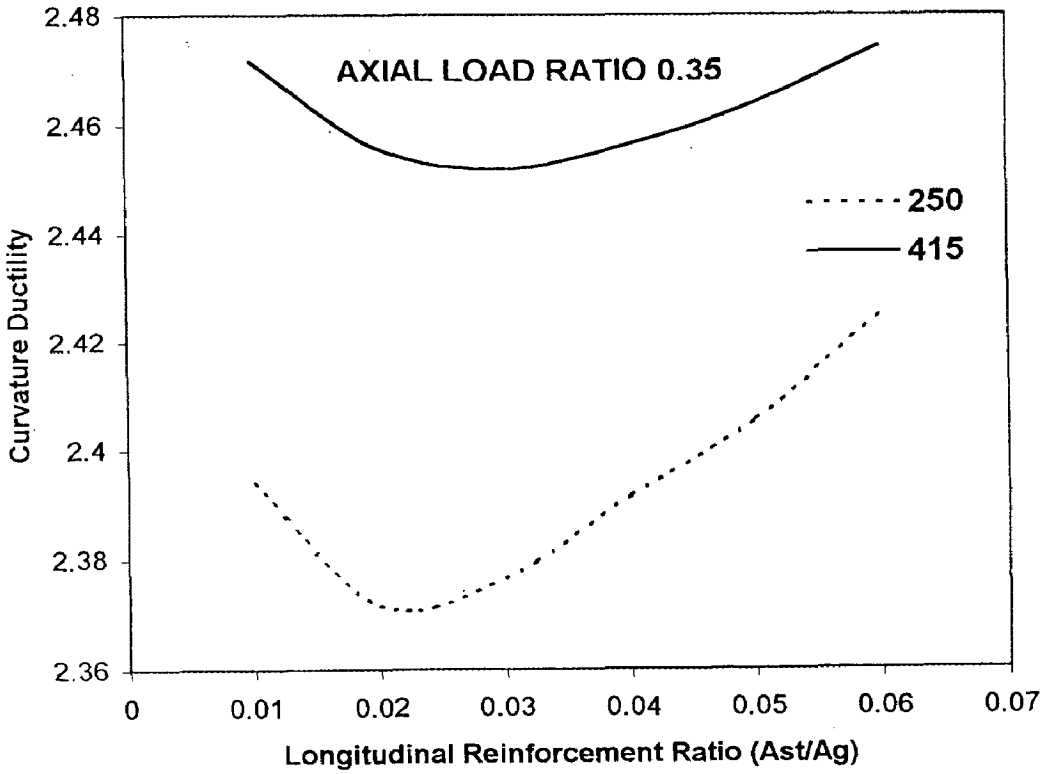

Fig.5.34 Change in Curvature Ductility with Yield strength of Longitudinal steel (fc=30.0,fyh=415.0,Transverse Reinforcement Ratio=0.005,Diameter Ratio=0.94)

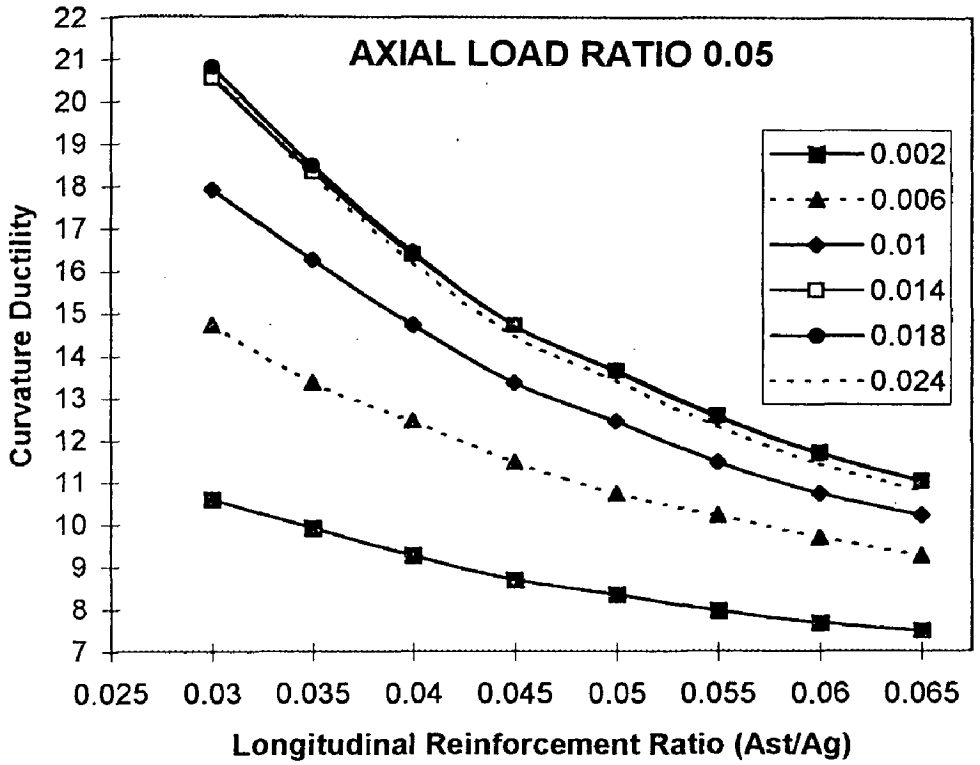

Fig.5.35 Change in Curvature Ductility With Transverse Reinforcement Ratio
(fc=30.0,fy=250.0,Diameter Ratio=0.84)

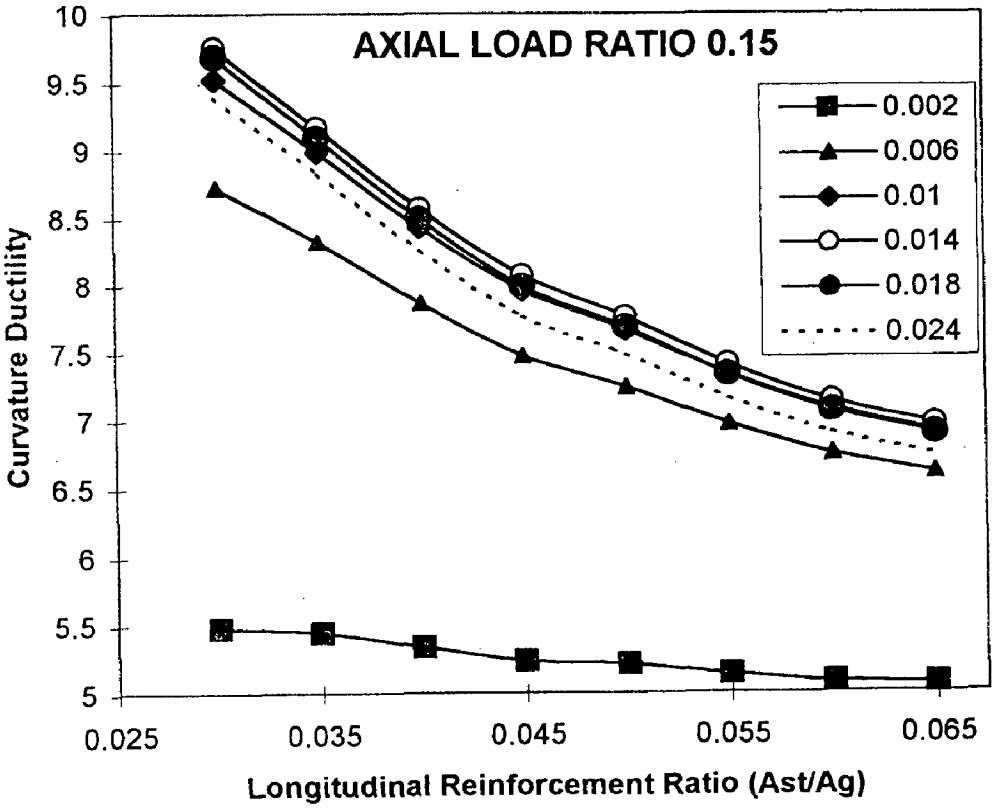

Fig.5.36 Change in Curvature Ductility With Transverse Reinforcement Ratio
(fc=30.0,fy=250.0,Diameter Ratio=0.84)

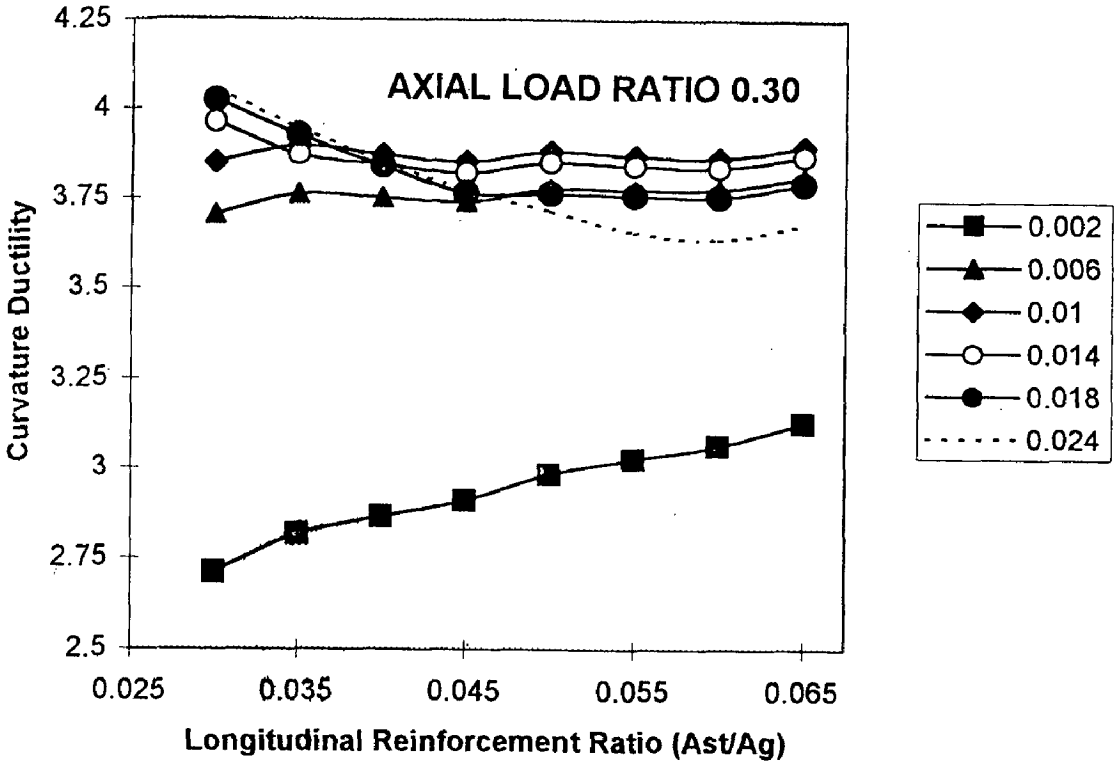

Fig.5.37 Change in Curvature Ductility With Transverse Reinforcement Ratio
(fc=30.0,fy=250.0,Diameter Ratio=0.84)

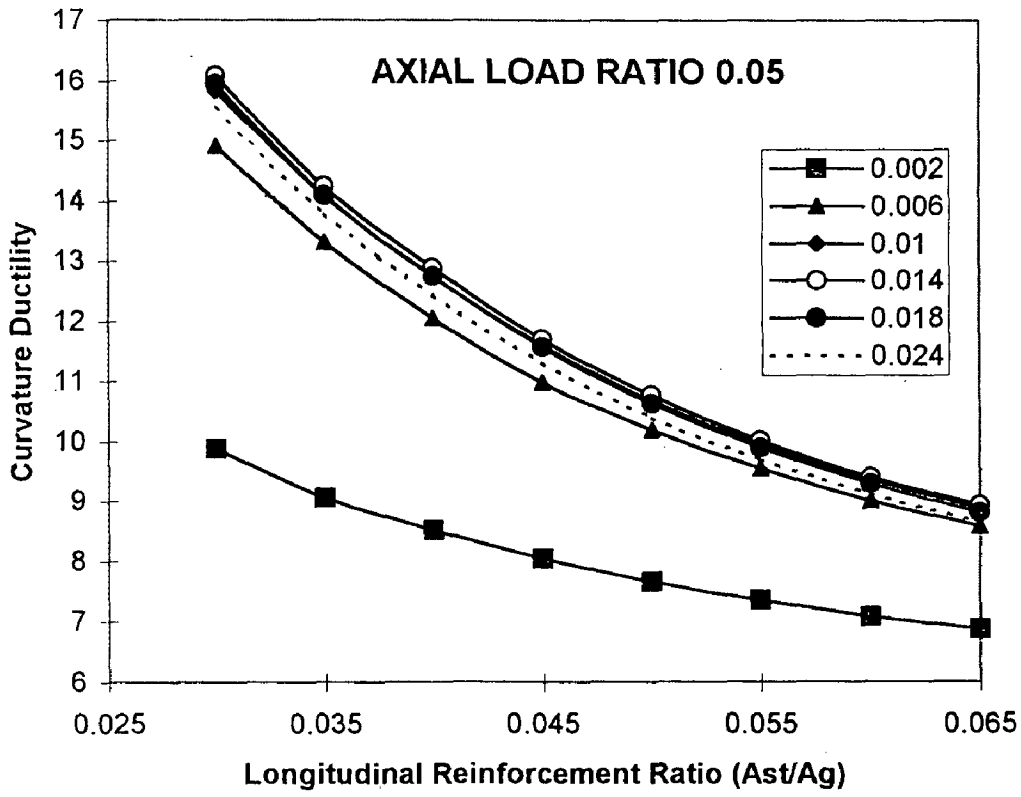

Fig.5.38 Change in Curvature Ductility With Transverse Reinforcement Ratio
(fc=30.0,fy=250.0,Diameter Ratio=0.90)

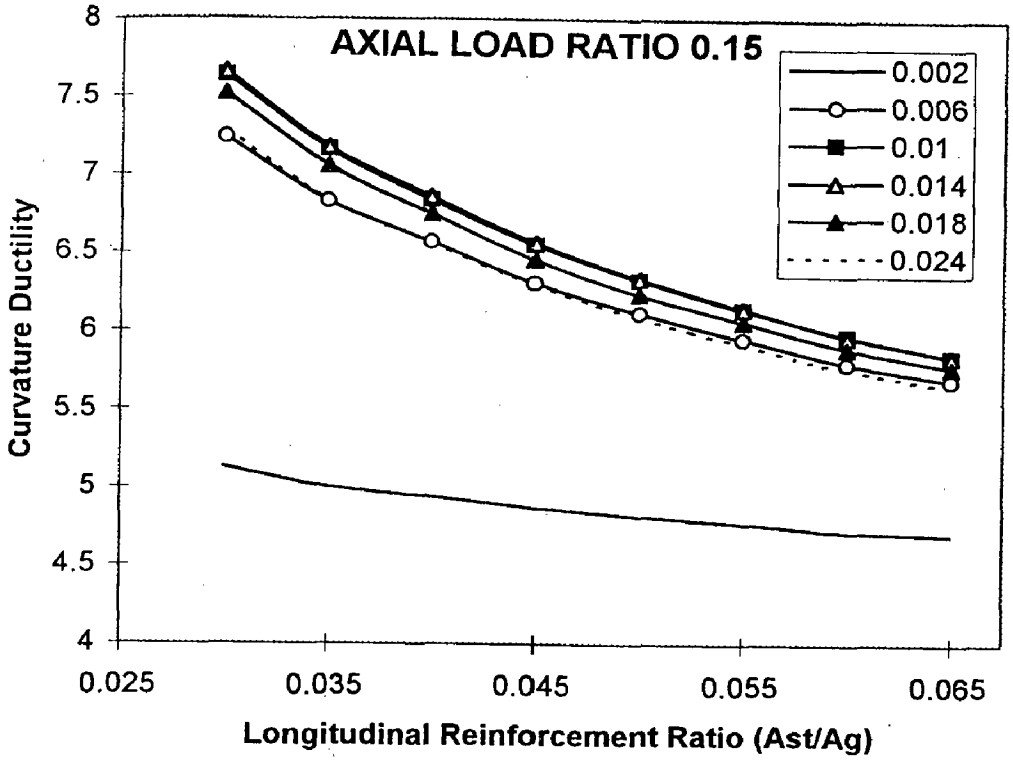

Fig.5.39 Change in Curvature Ductility With Transverse Reinforcement Ratio (fc=30.0,fy=250.0,Diameter Ratio=0.90)

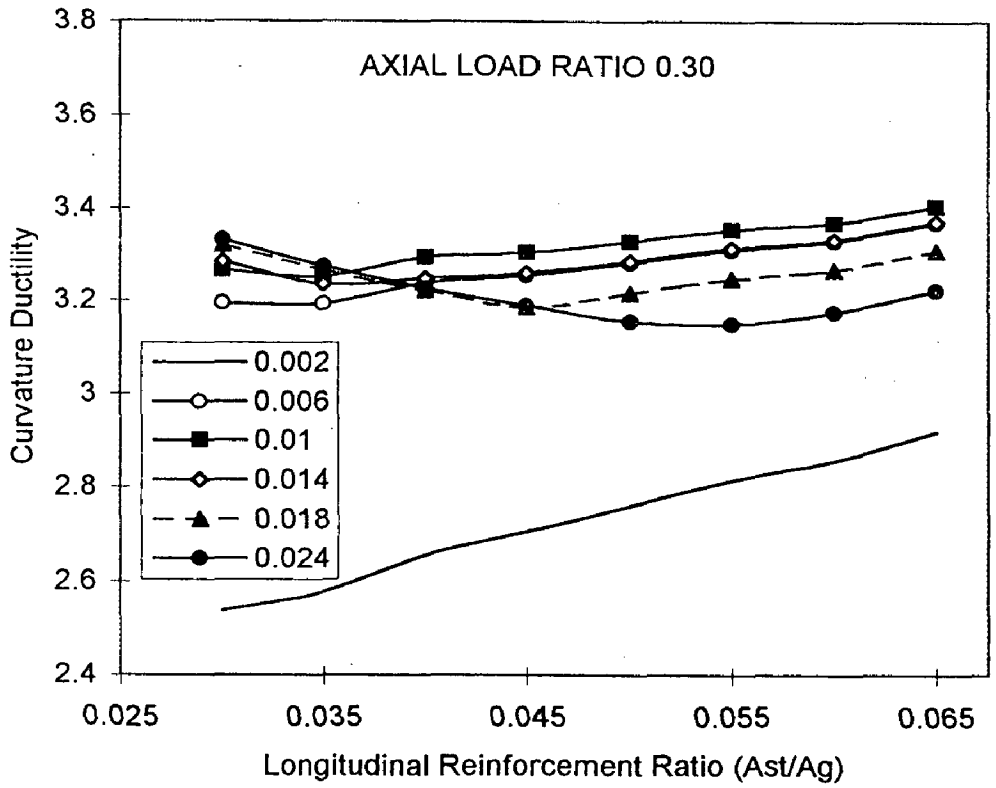

Fig.5.40 Change in Curvature Ductility With Transverse Reinforcement Ratio (fc=30.0,fy=250.0,Diameter Ratio=0.90)

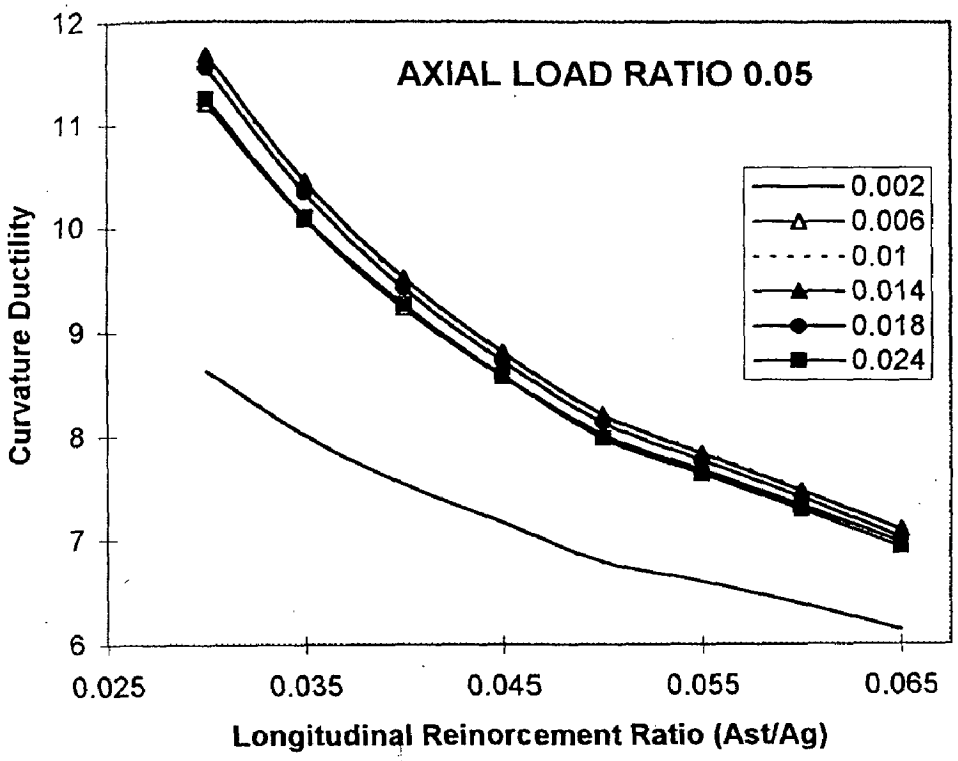

Fig.5.41 Change in Curvature Ductility With Transverse Reinforcement Ratio
(fc=30.0,fy=250.0,Diameter Ratio=0.94)

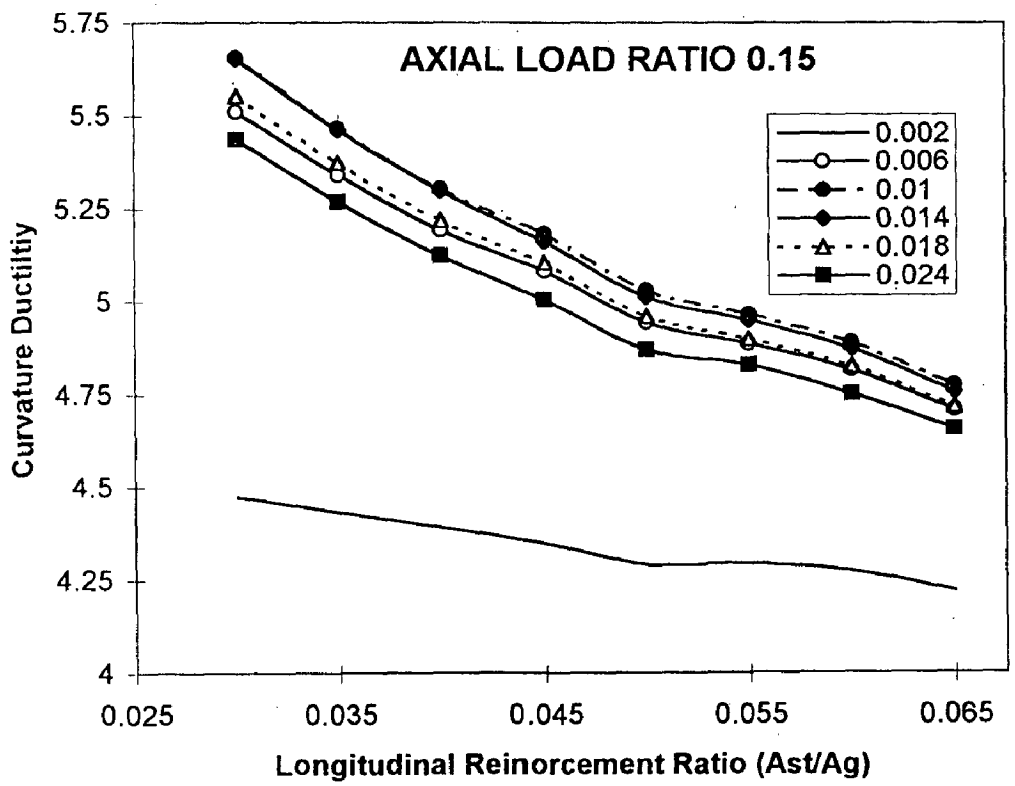

Fig.5.42 Change in Curvature Ductility With Transverse Reinforcement Ratio
(fc=30.0,fy=250.0,Diameter Ratio=0.94)

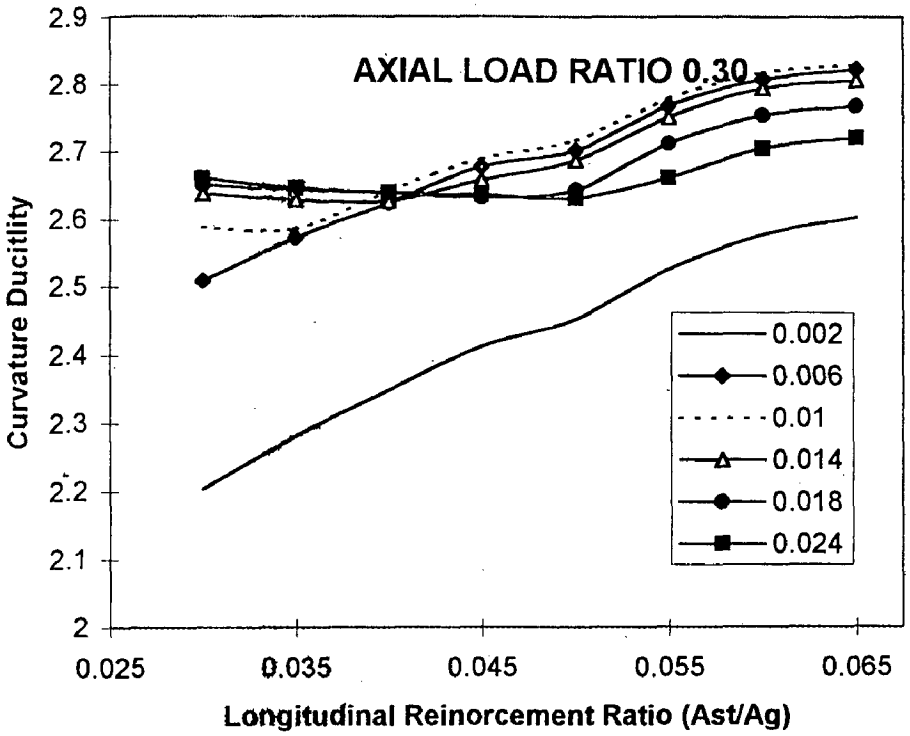

Fig.5.43 Change in Curvature Ductility With Transverse Reinforcement Ratio (fc=30.0,fy=250.0,Diameter Ratio=0.94)

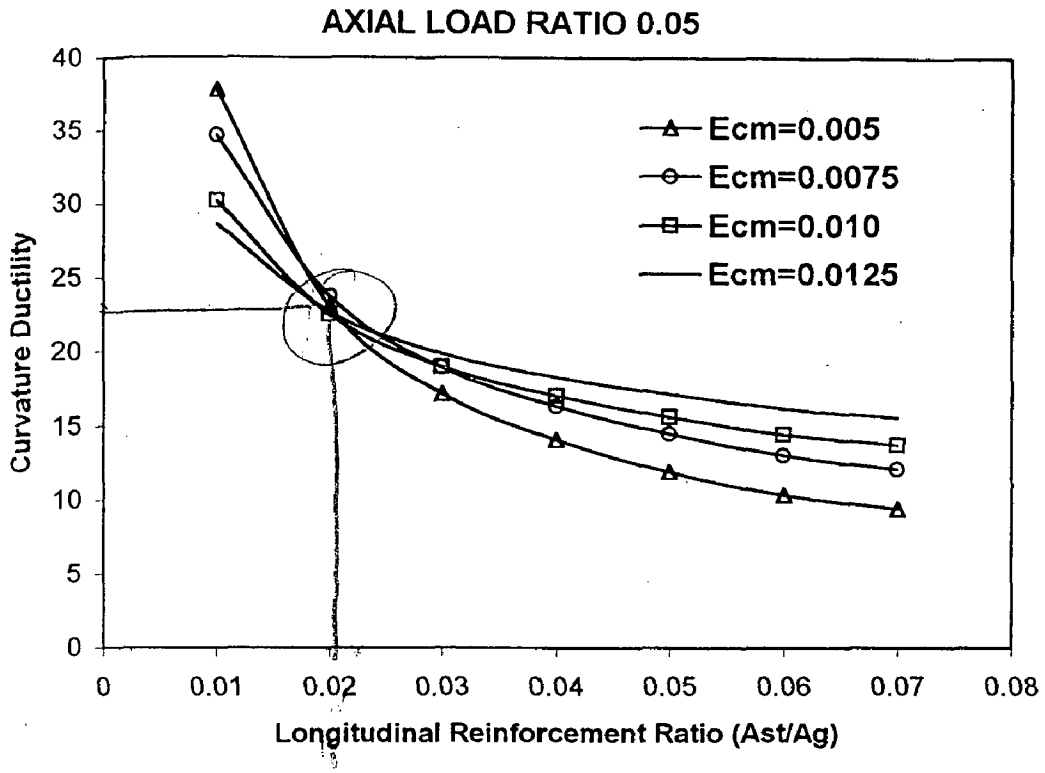

Fig.5.44 Change in Curvature Ductilitywith criticalinside facestrain
(fc=30.0,fy=415.0,Transverse Reinforcement Ratio=0.005,Diameter ratio=0.84)

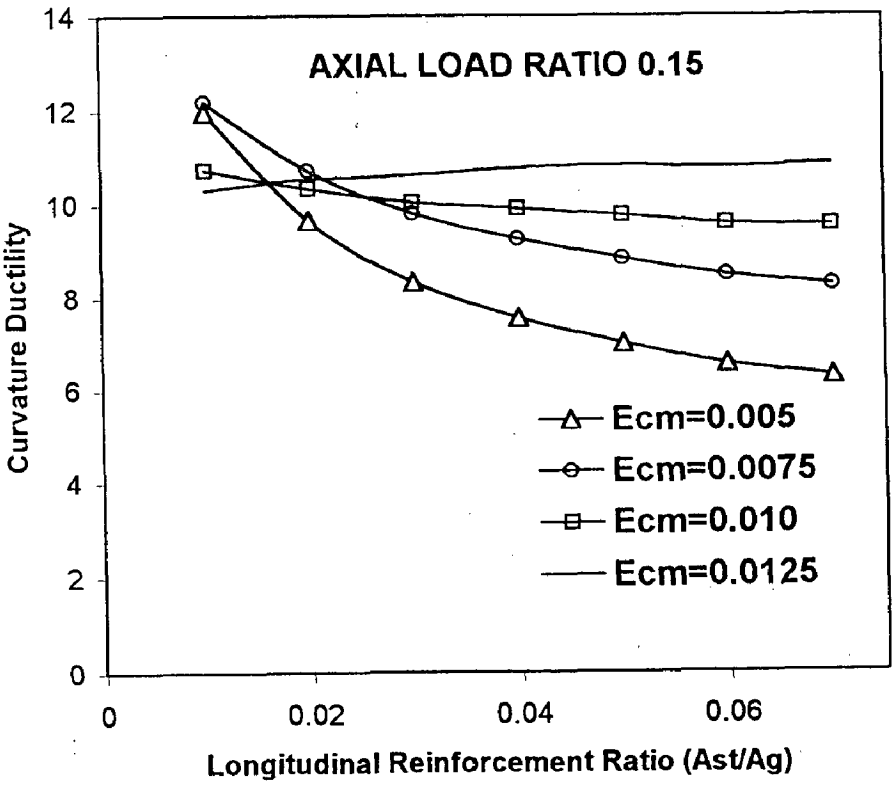

Fig.5.45 Change in Curvature Ductilitywith criticalinside facestrain
(fc=30.0,fy=415.0,Transverse Reinforcement Ratio=0.005,Diameter ratio=0.84)

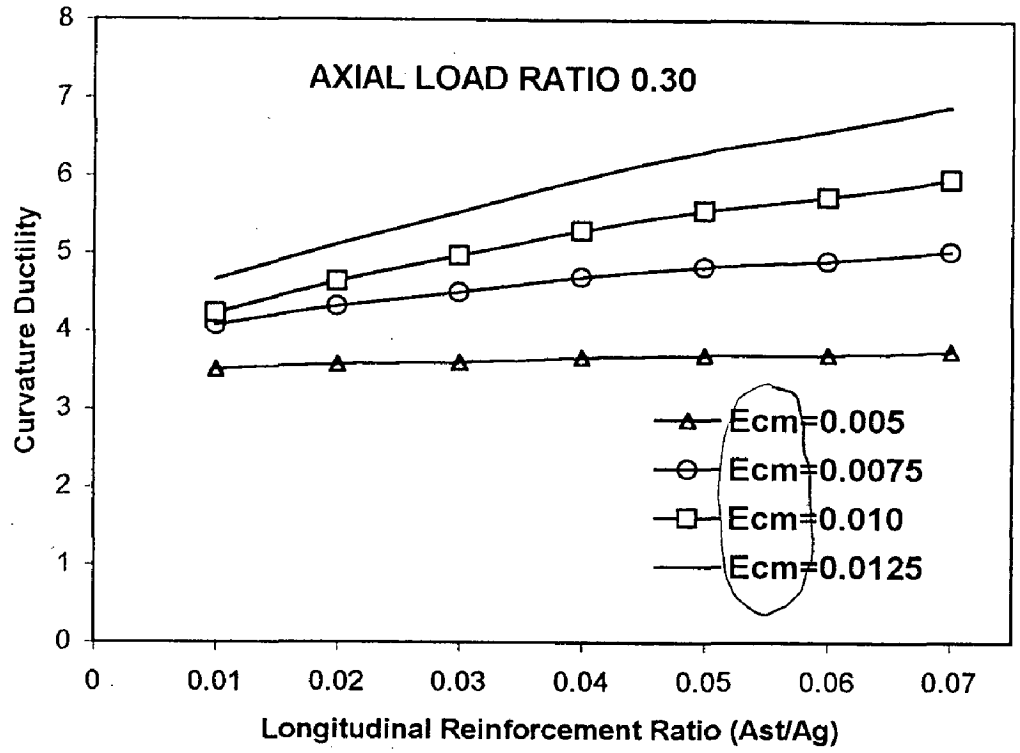

Fig.5.46 Change in Curvature Ductilitywith criticalinside facestrain
(fc=30.0,fy=415.0,Transverse Reinforcement Ratio=0.005,Diameter ratio=0.84)

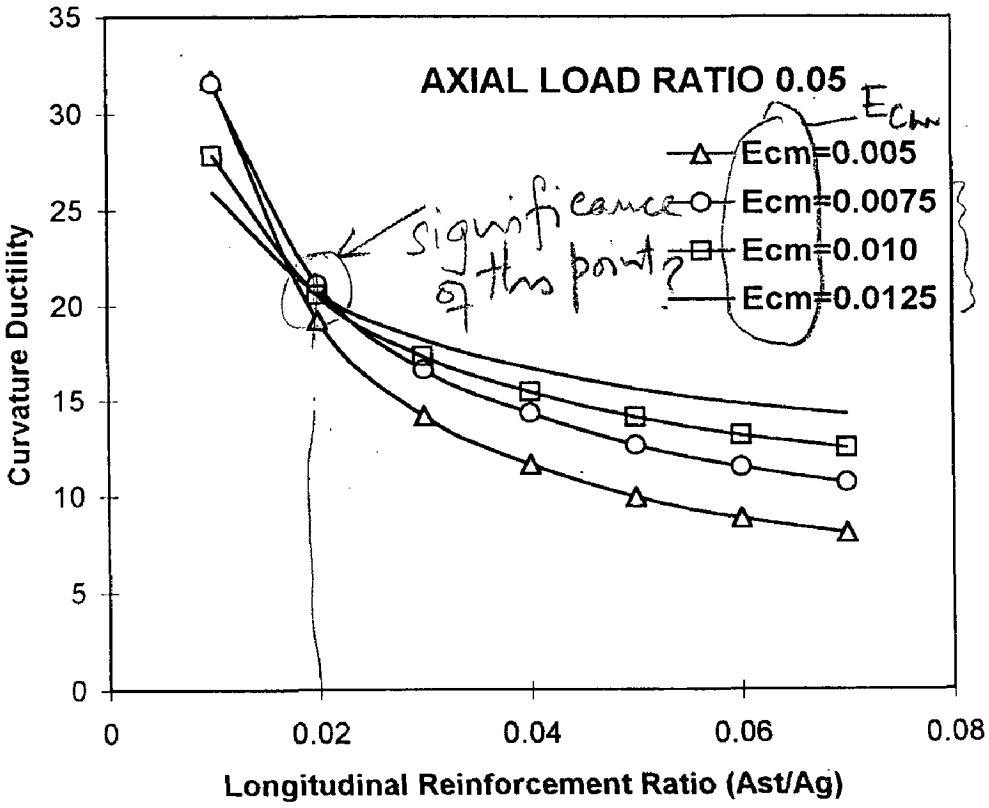

Fig.5.47 Change of Curvature Ductility with Critical Inside-face Strain
(fc=30.0,fy=415.0,Transverse Reinforcement Ratio=0.005,Diameter Ratio=0.90)

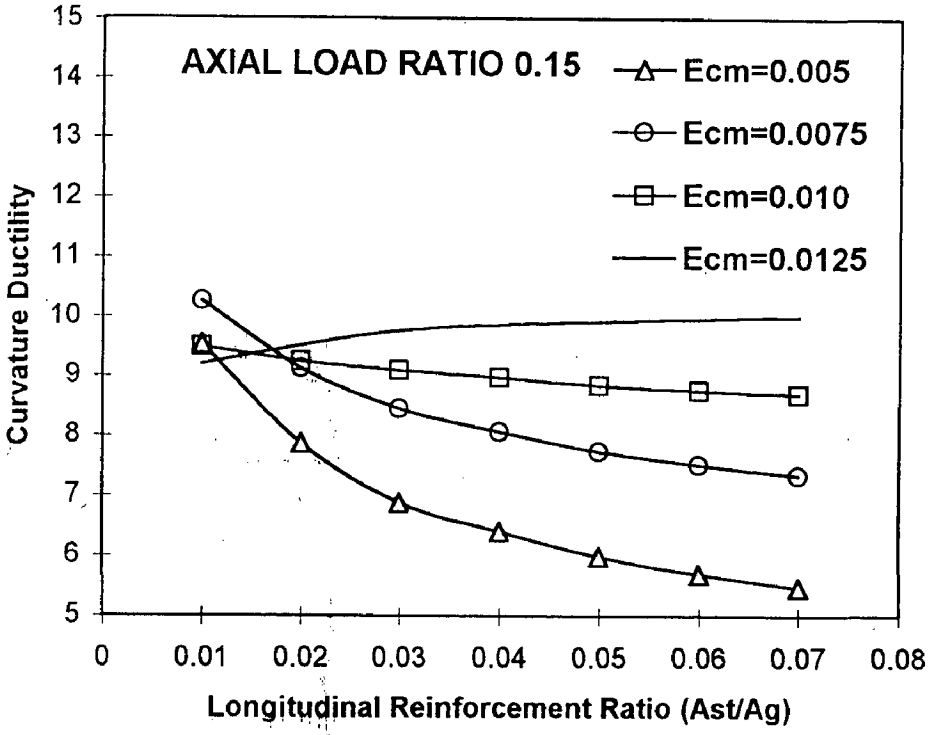

Fig.5.48 Change of Curvature Ductility with Critical Inside-face Strain
(fc=30.0,fy=415.0,Transverse Reinforcement Ratio=0.005,Diameter Ratio=0.90)

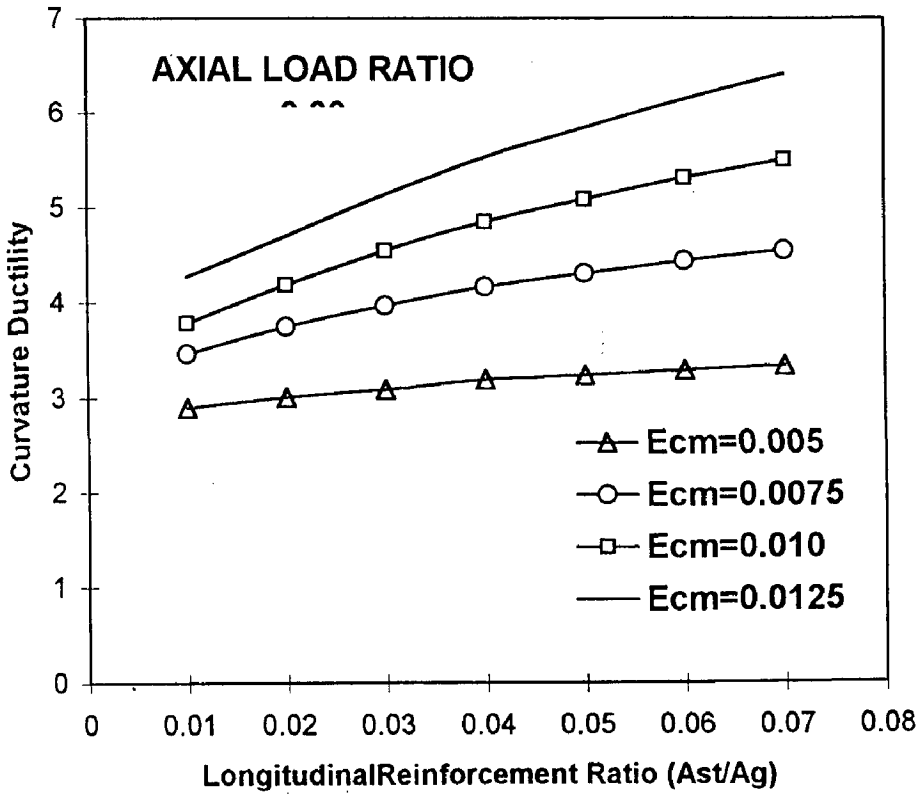

Fig.5.49 Change of Curvature Ductility with Critical Inside-face Strain
(fc=30.0,fy=415.0,Transverse Reinforcement Ratio=0.005,Diameter Ratio=0.90)

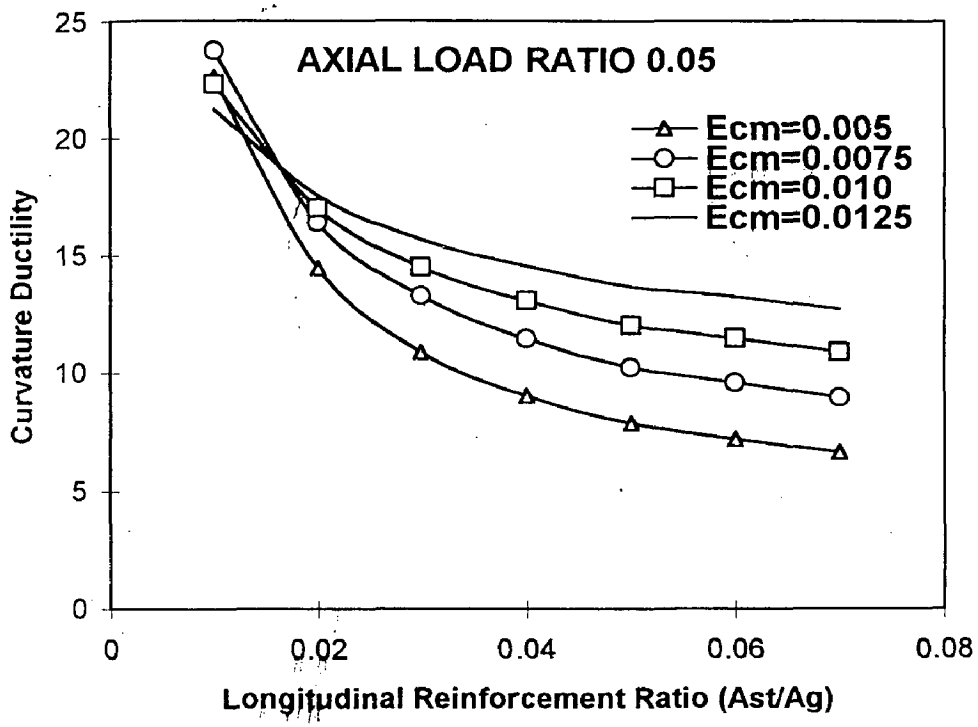

Fig.5.50 Change of Curvature Ductility with Critical Inside-face Strain
(fc=30.0,fy=415.0,Transverse Reinforcement Ratio=0.005,Diameter Ratio=0.94)

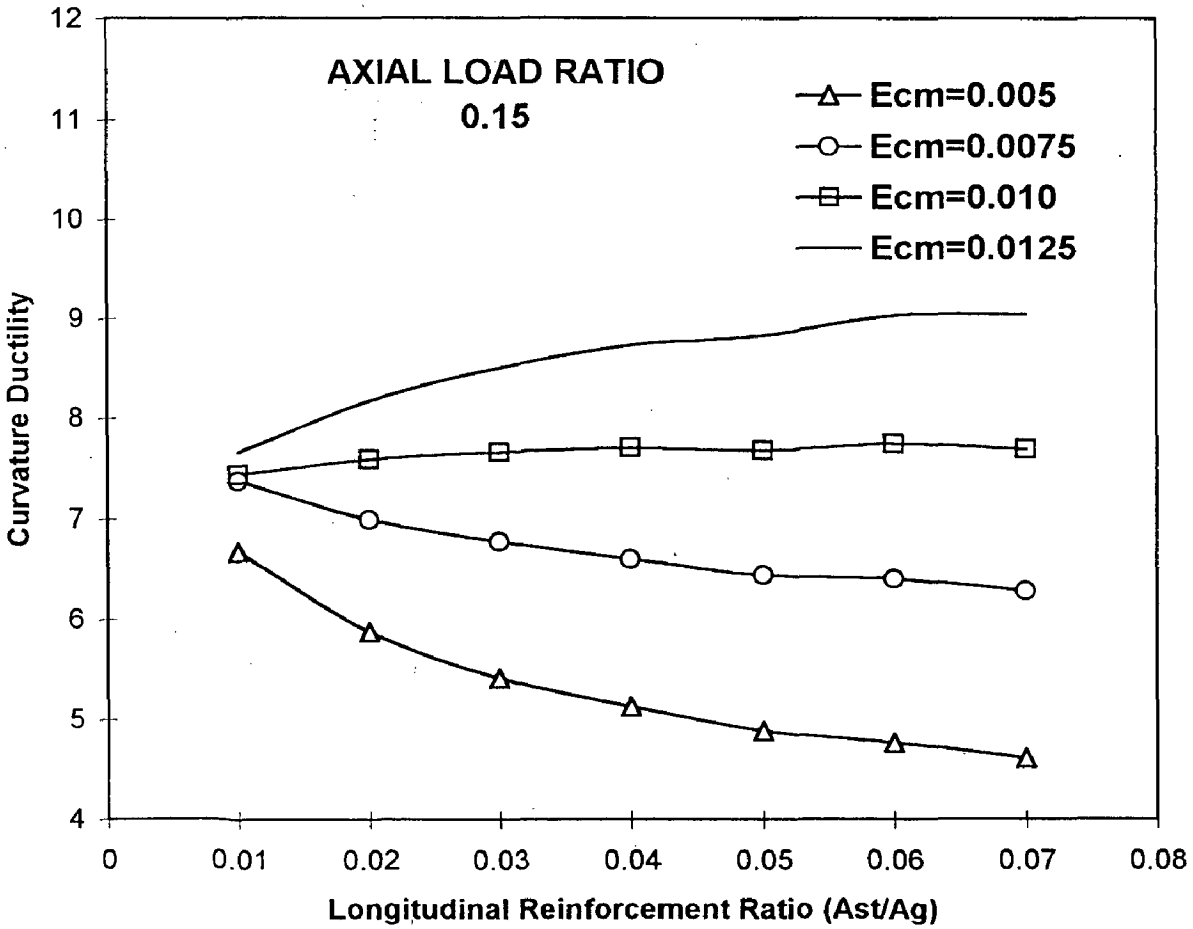

Fig.5.51 Change of Curvature Ductility with Critical Inside-face Strain
(fc=30.0,fy=415.0,Transverse Reinforcement Ratio=0.005,Diameter Ratio=0.94)

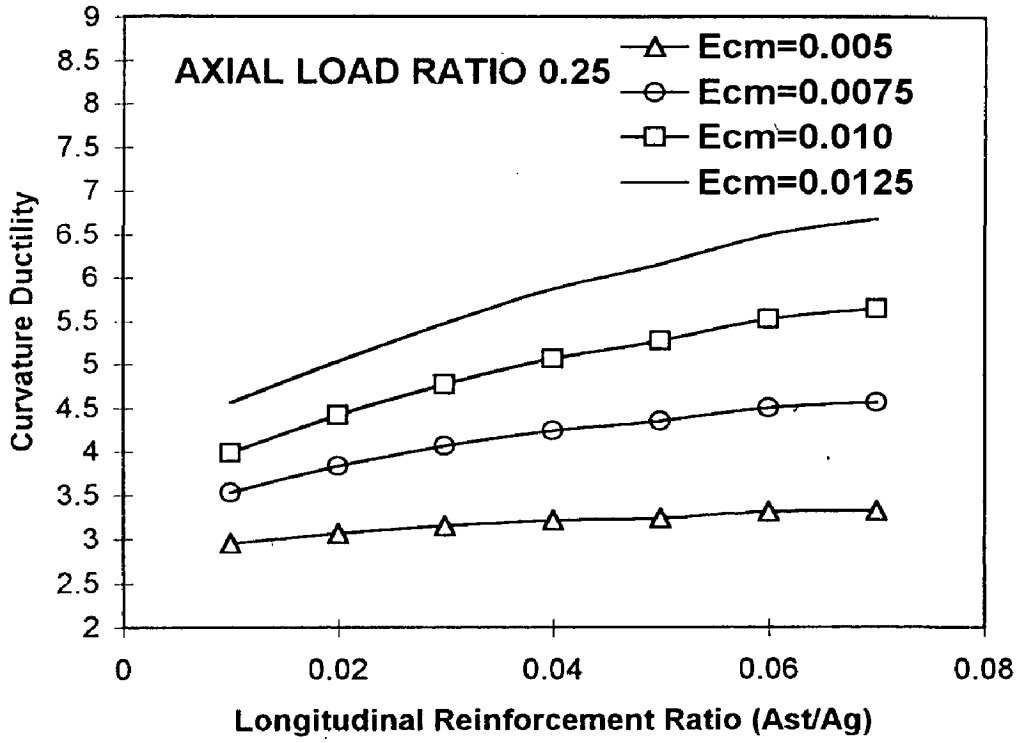

Fig.5.52 Change of Curvature Ductility with Critical Inside-face Strain
(fc=30.0,fy=415.0,Transverse Reinforcement Ratio=0.005,Diameter Ratio=0.94)

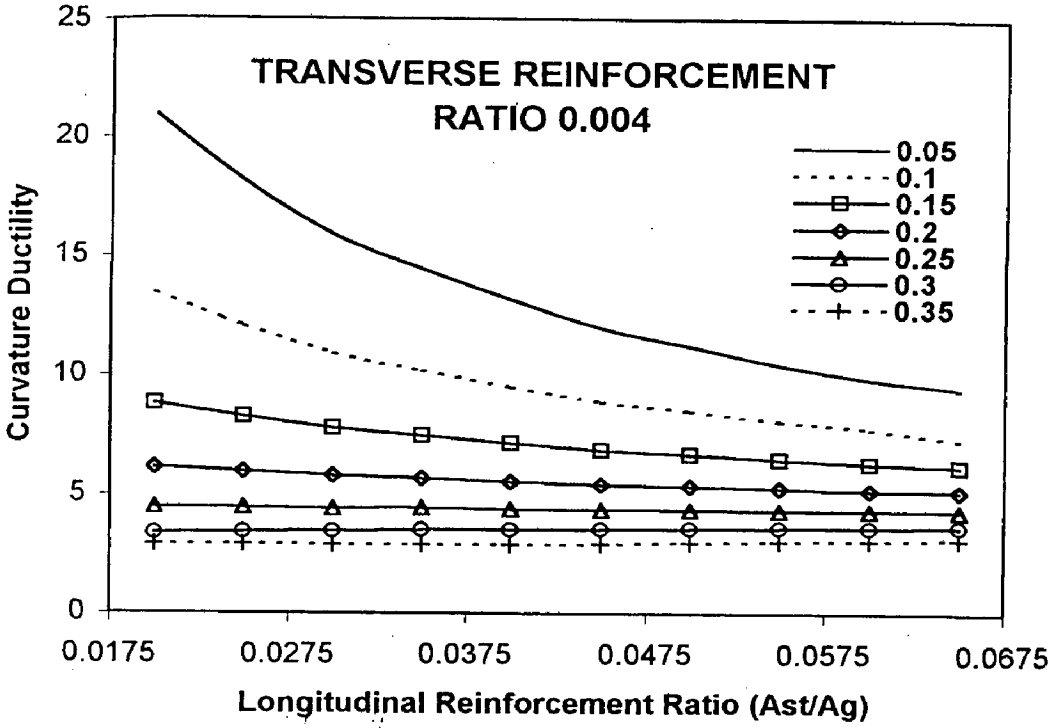

Fig.5.53 Design Chart for 0.84 Diameter Ratio hollow circular section
(fc=30.0,fy=250.0,fyh=415.0)

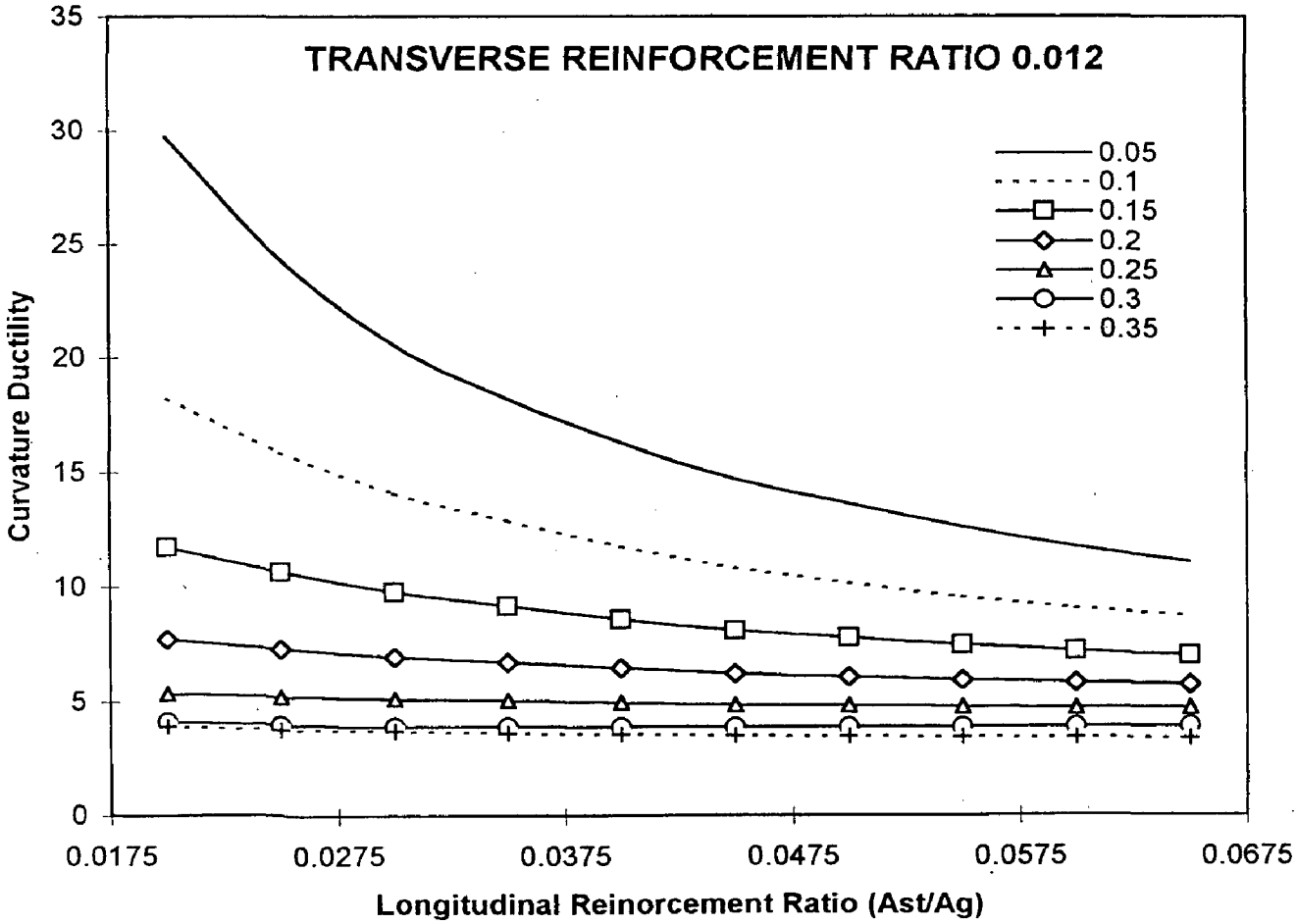

Fig.5.54 Design Chart for 0.84 Diameter Ratio hollow circular section
(fc=30.0,fy=250.0,fyh=415.0)

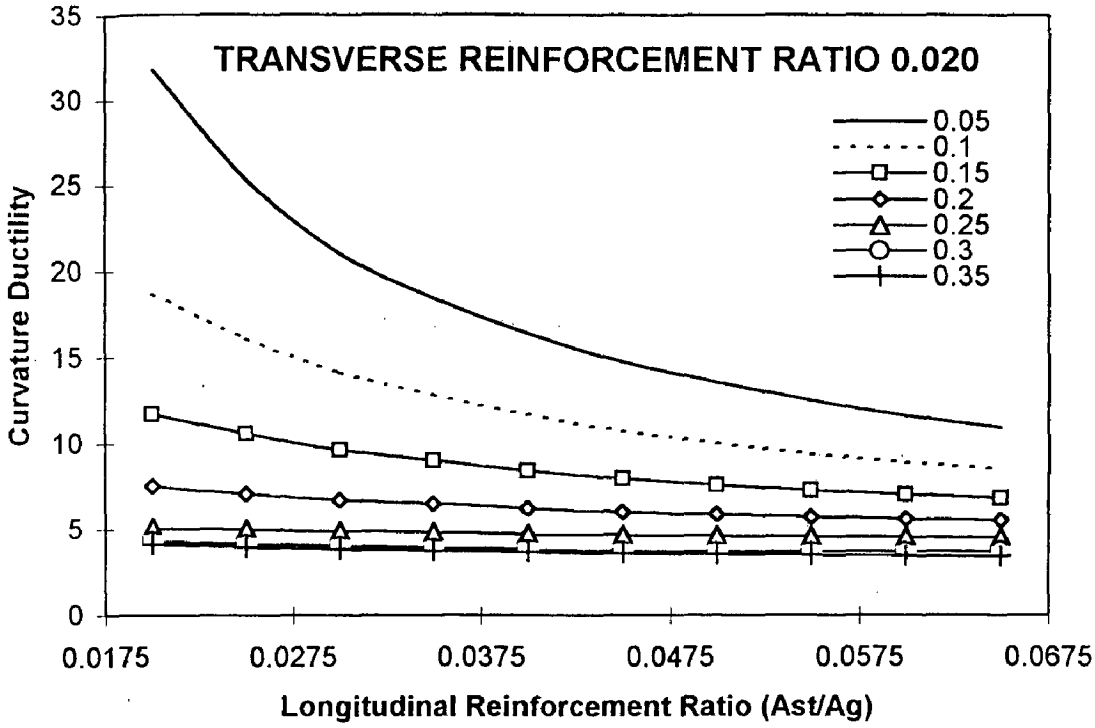

Fig.5.55 Design Chart for 0.84 Diameter Ratio hollow circular section
(fc=30.0,fy=250.0,fyh=415.0)

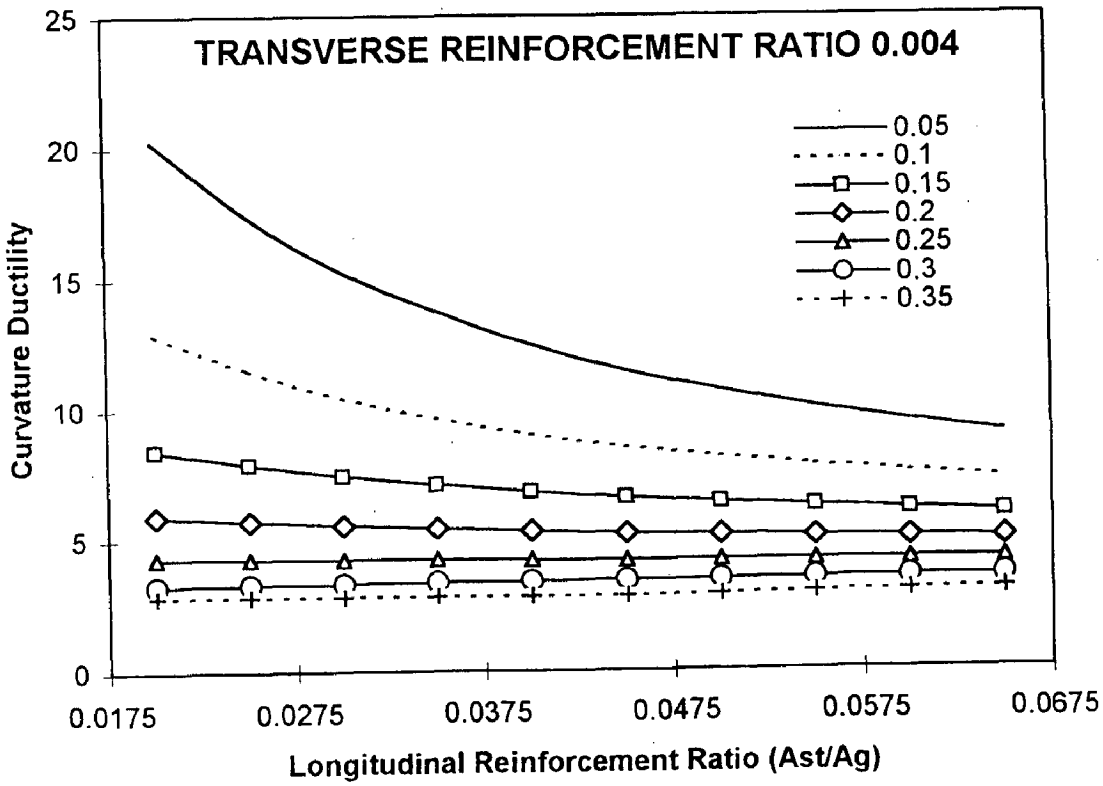

Fig.5.56 Design Chart for 0.86 Diameter Ratio hollow circular section
(fc=30.0,fy=250.0,fyh=415.0)

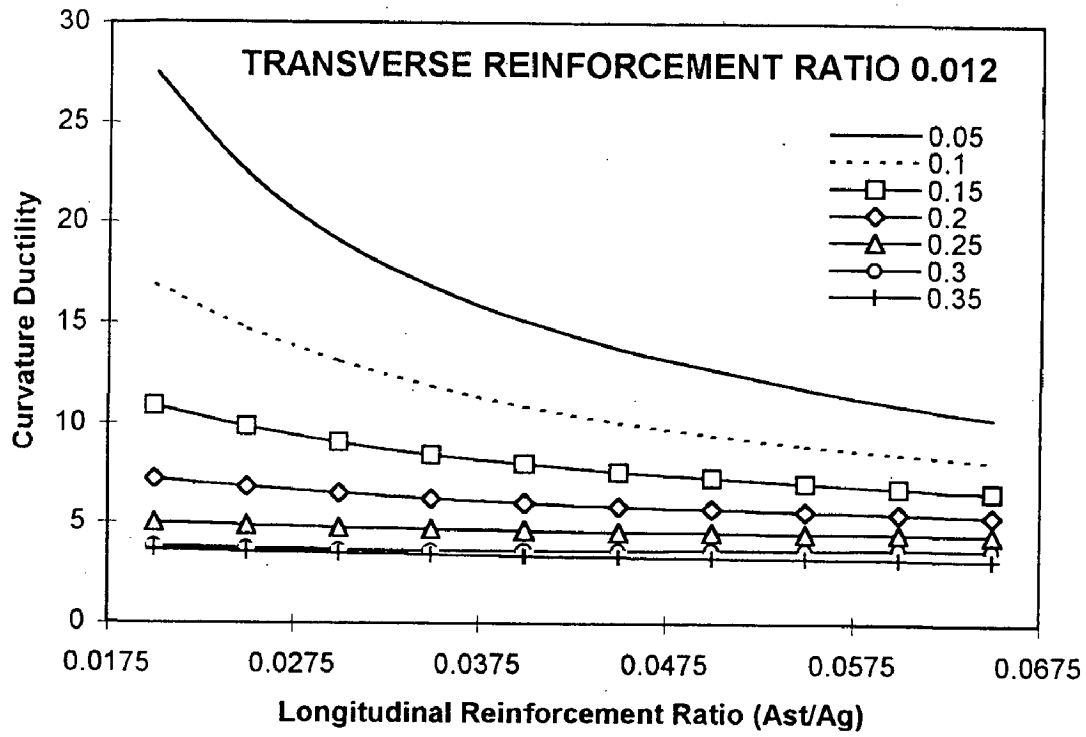

Fig.5.57 Design Chart for 0.86 Diameter Ratio hollow circular section
(fc=30.0,fy=250.0,fyh=415.0)

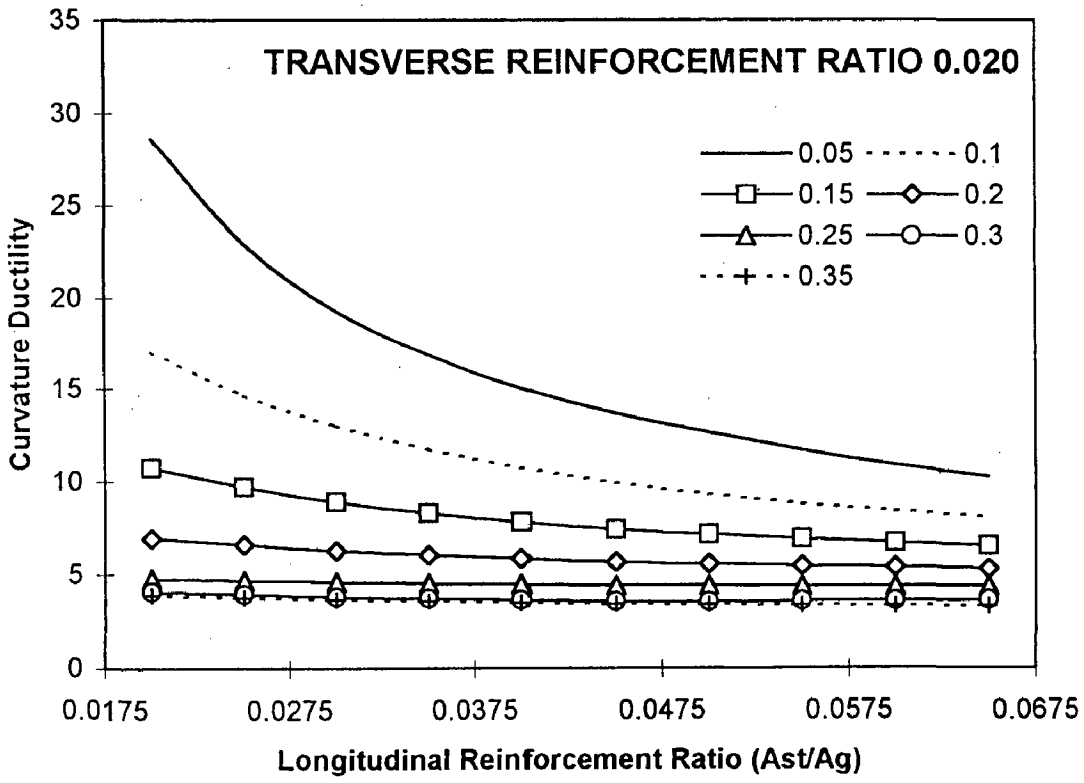

Fig.5.58 Design Chart for 0.86 Diameter Ratio hollow circular section
(fc=30.0,fy=250.0,fyh=415.0)

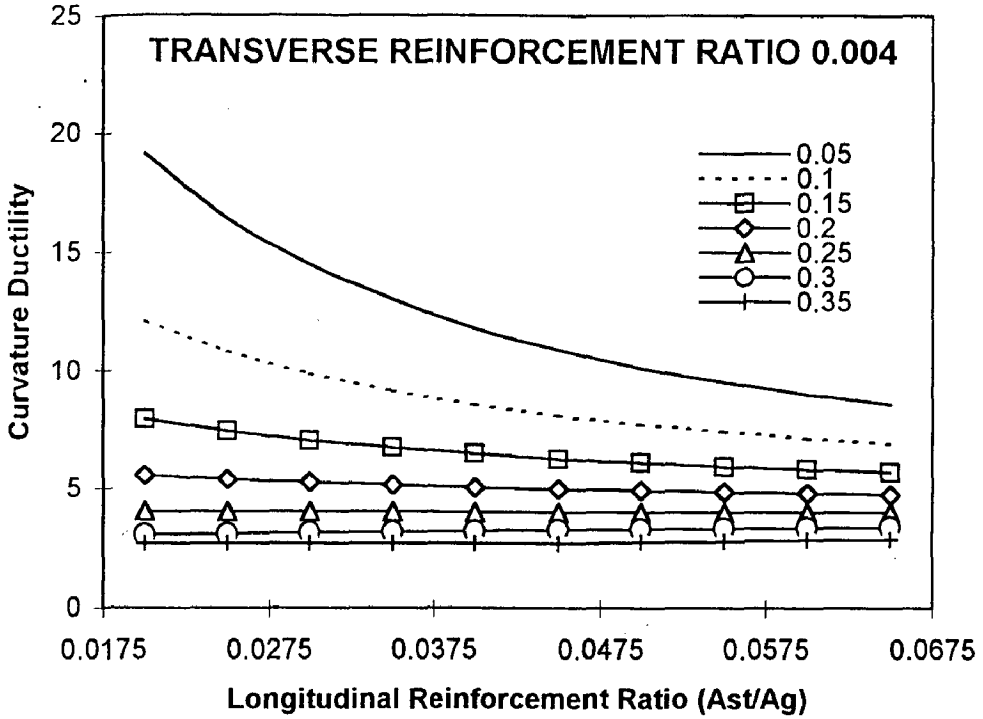

Fig.5.59 Design Chart for 0.88 Diameter Ratio hollow circular section (fc=30.0,fy=250.0,fyh=415.0)

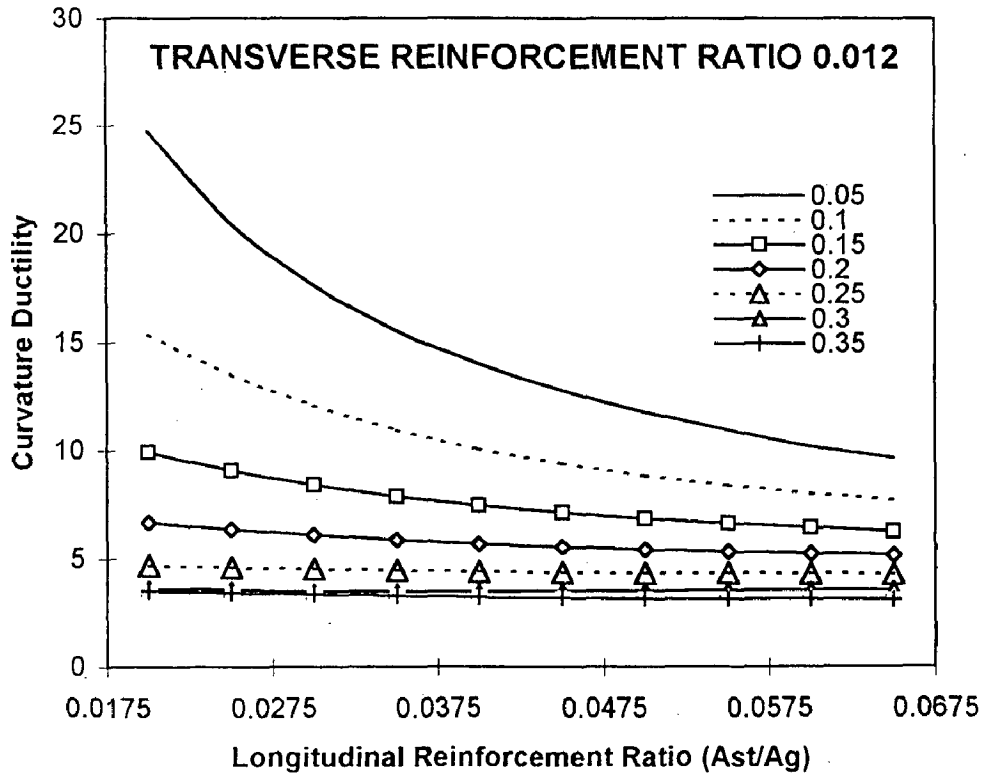

Fig.5.60Design Chart for 0.88 Diameter Ratio hollow circular section (fc=30.0,fy=250.0,fyh=415.0)

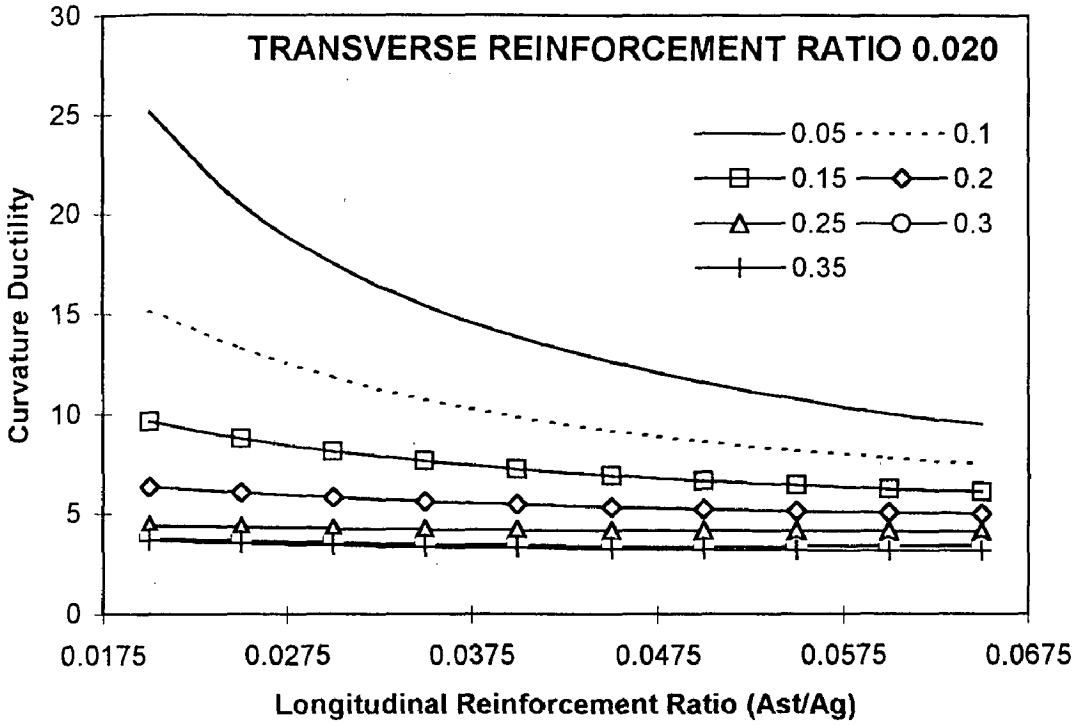

Fig.5.61 Design Chart for 0.88 Diameter Ratio hollow circular section
(fc=30.0,fy=250.0,fyh=415.0)

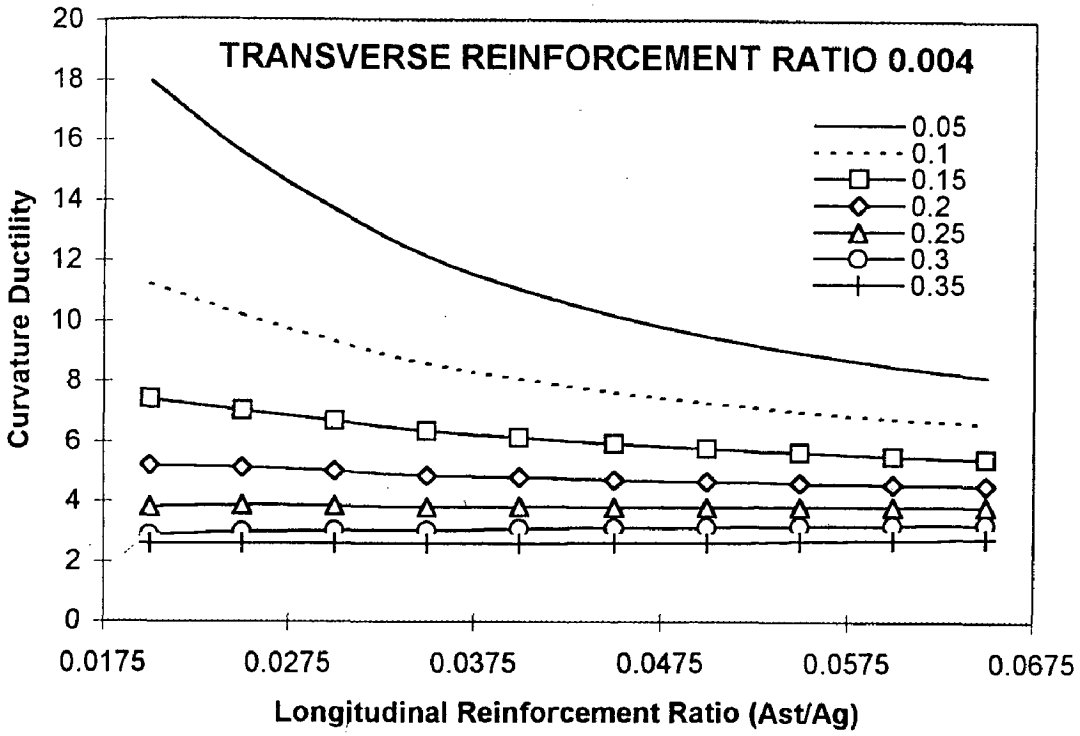

Fig.5.62 Design Chart for 0.90 Diameter Ratio hollow circular section
(fc=30.0,fy=250.0,fyh=415.0)

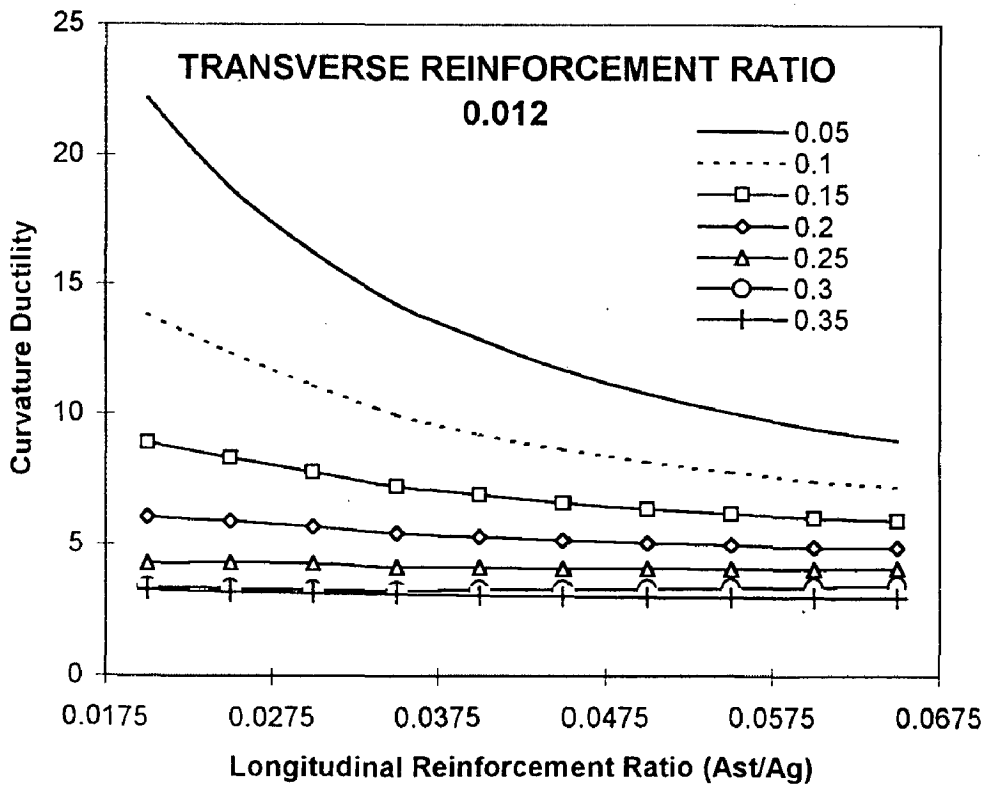

Fig.5.63 Design Chart for 0.90 Diameter Ratio hollow circular section
(fc=30.0,fy=250.0,fyh=415.0)

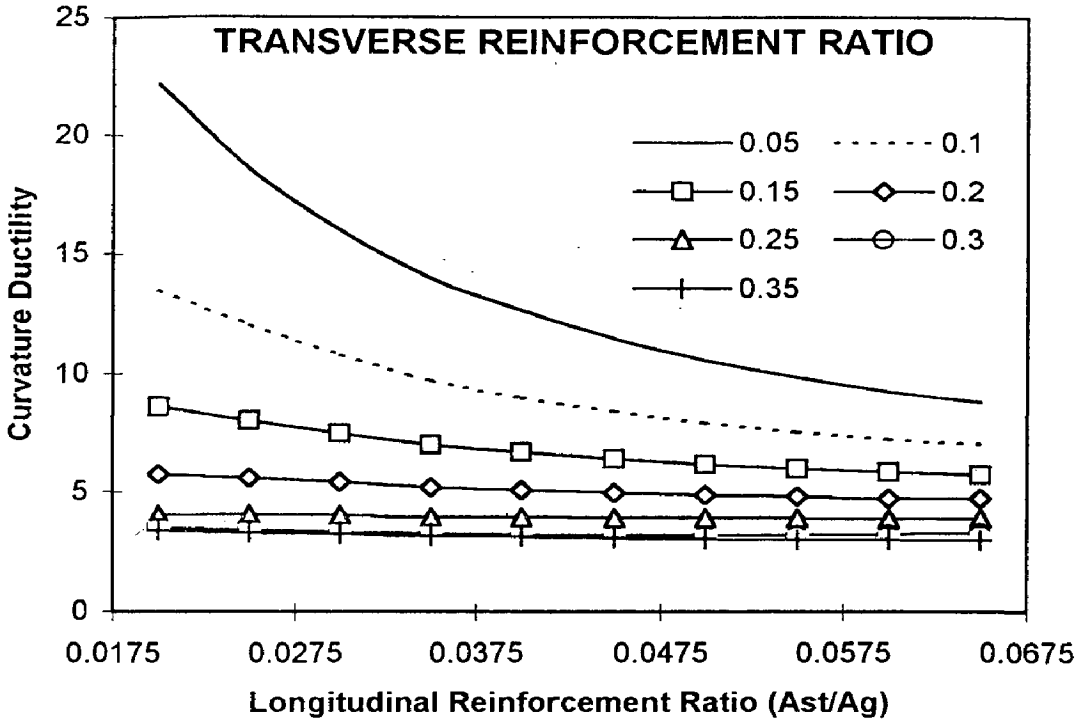

Fig.5.64Design Chart for 0.90 Diameter Ratio hollow circular section (fc=30.0,fy=250.0,fyh=415.0)

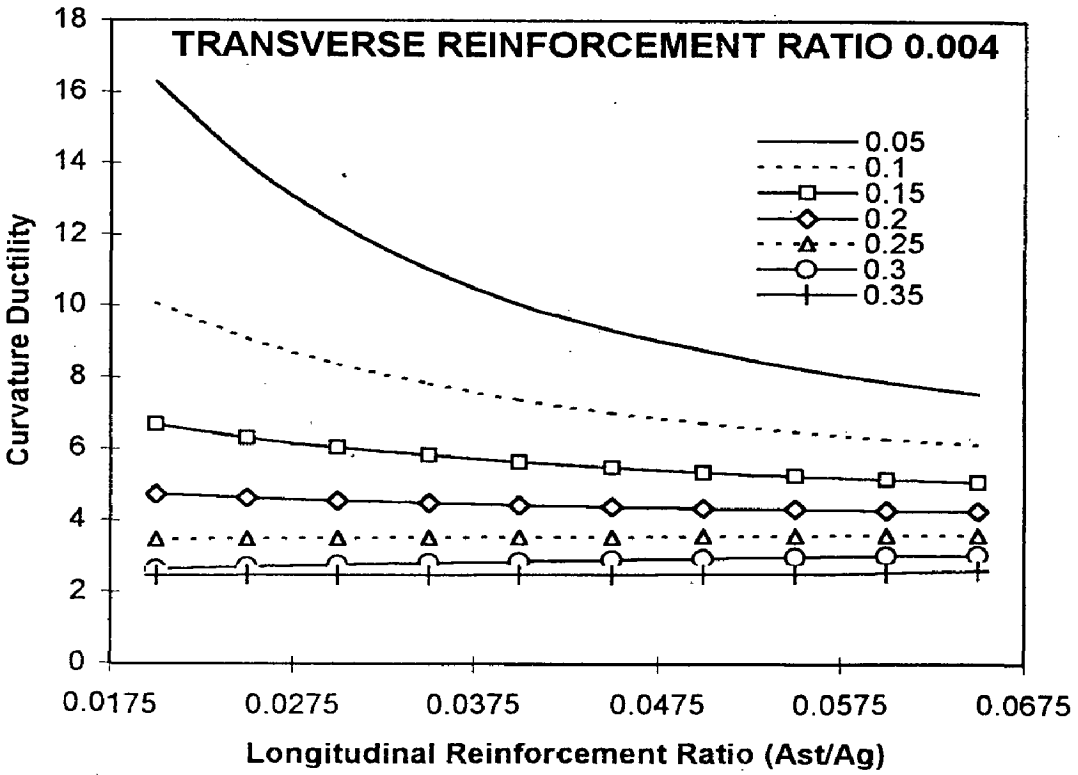

Fig.5.65 Design Chart for 0.92 Diameter Ratio hollow circular section (fc=30.0,fy=250.0,fyh=415.0)

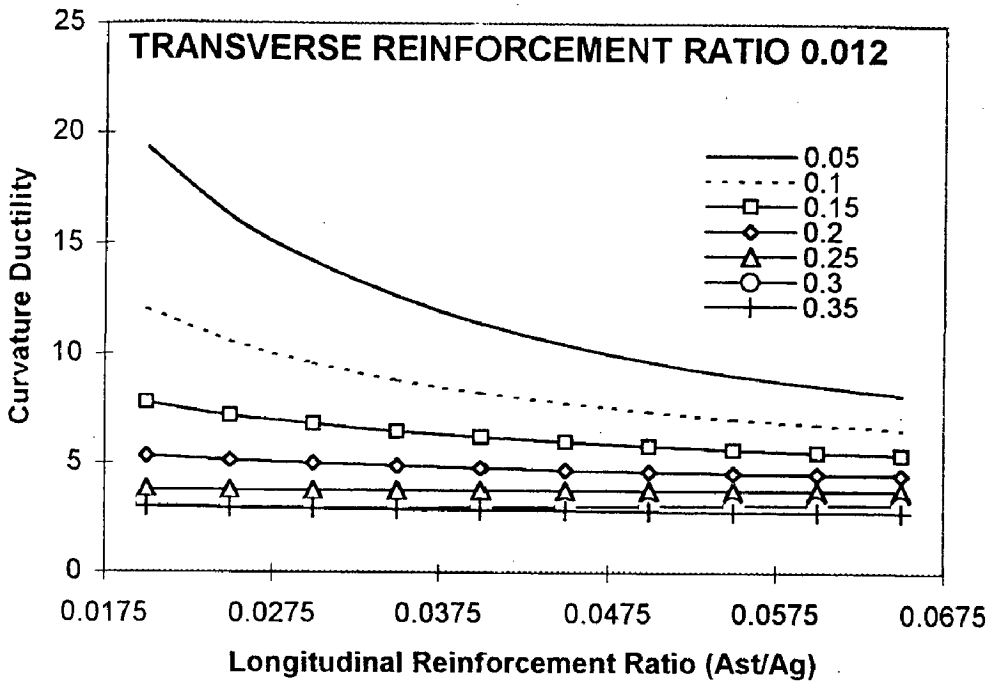

Fig.5.66 Design Chart for 0.92 Diameter Ratio hollow circular section (fc=30.0,fy=250.0,fyh=415.0)

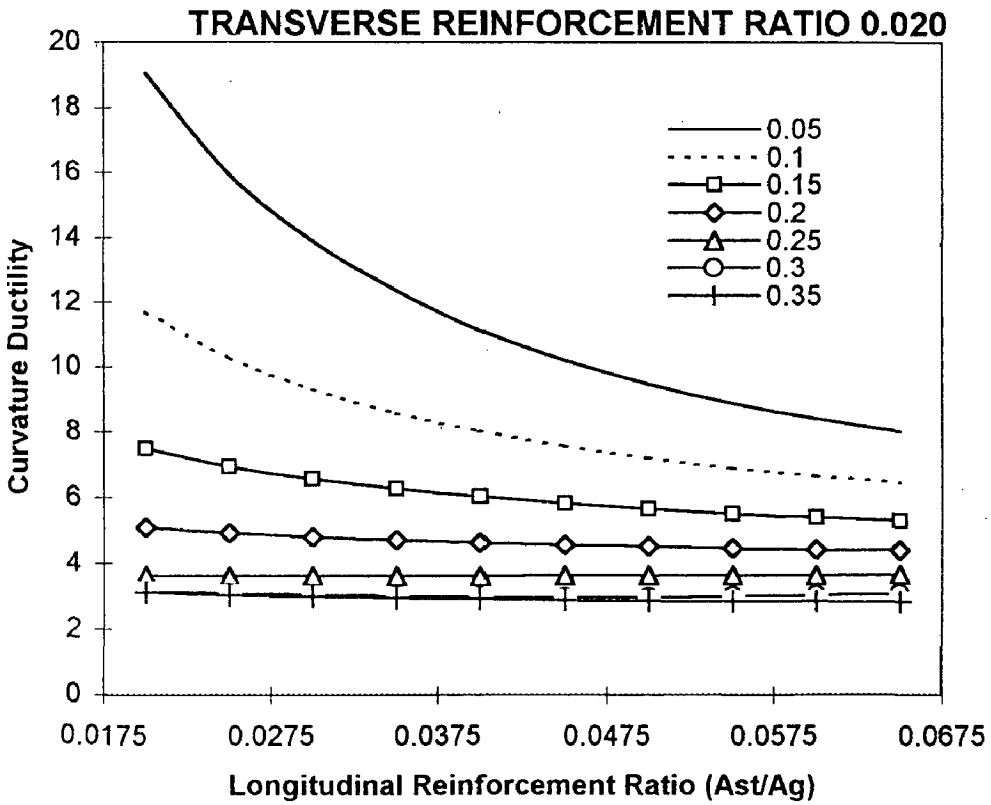

Fig 5.67 Design Chart for 0.92 Diameter Ratio hollow circular section (fc=30.0,fy=250.0,fyh=415.0)

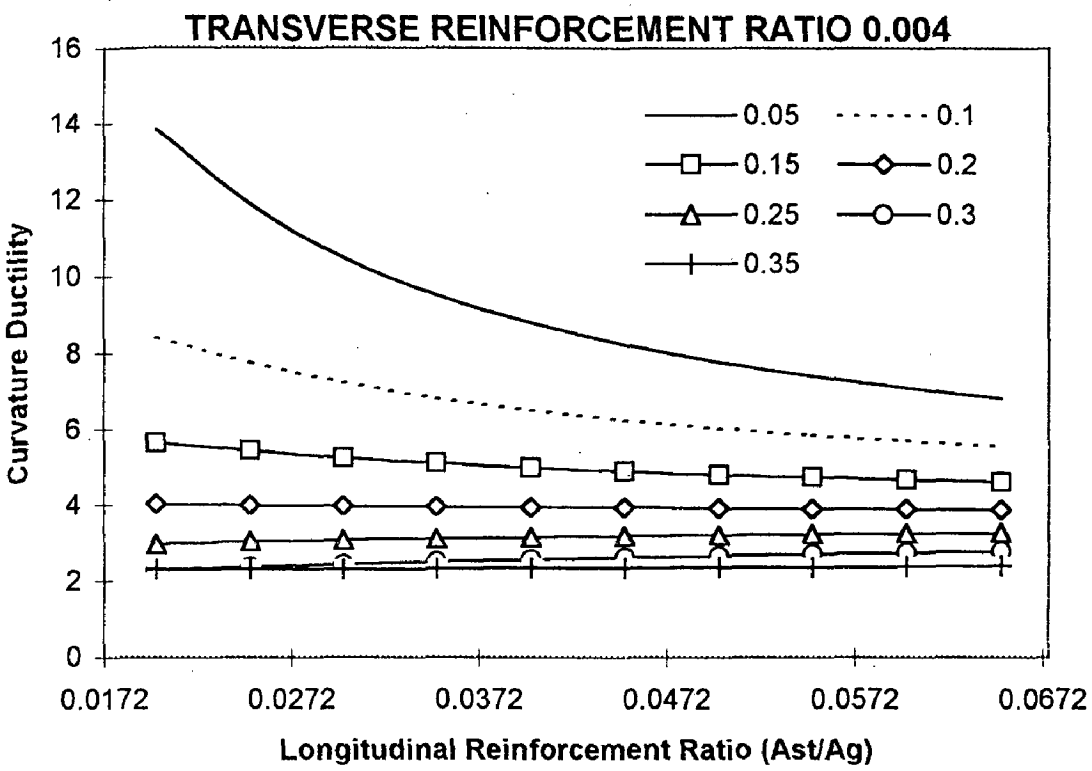

Fig.5.68 Design Chart for 0.94 Diameter Ratio hollow circular section (fc=30.0,fy=250.0,fyh=415.0)

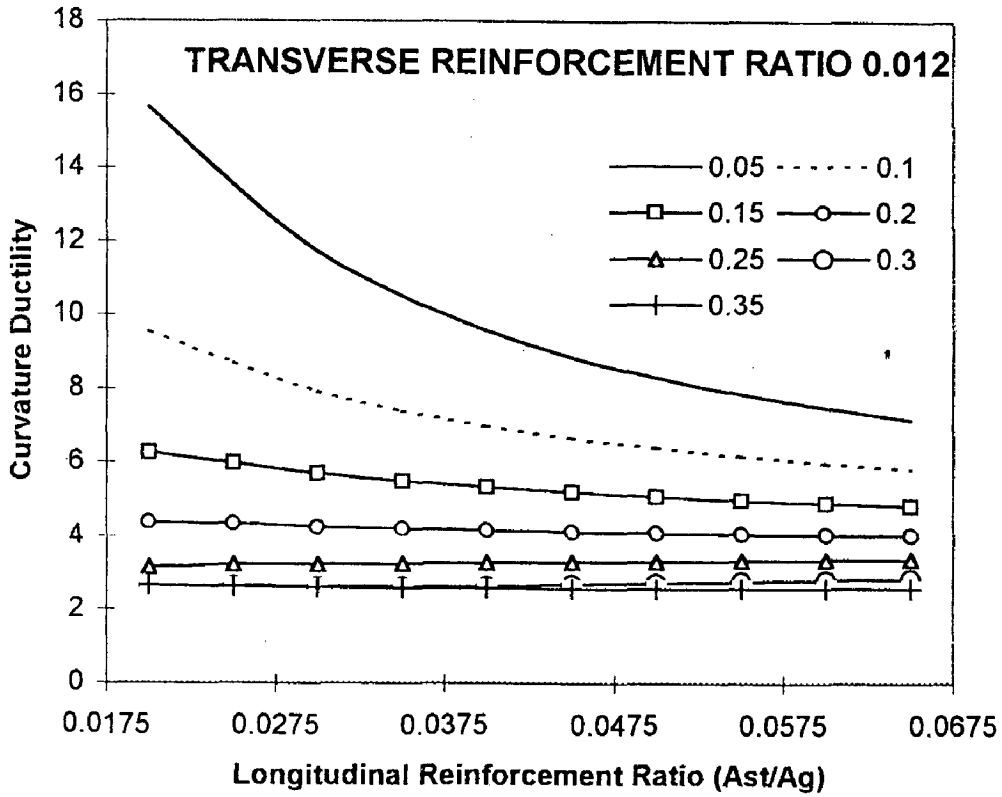

Fig.5.69Design Chart for 0.94 Diameter Ratio hollow circular section (fc=30.0,fy=250.0,fyh=415.0)

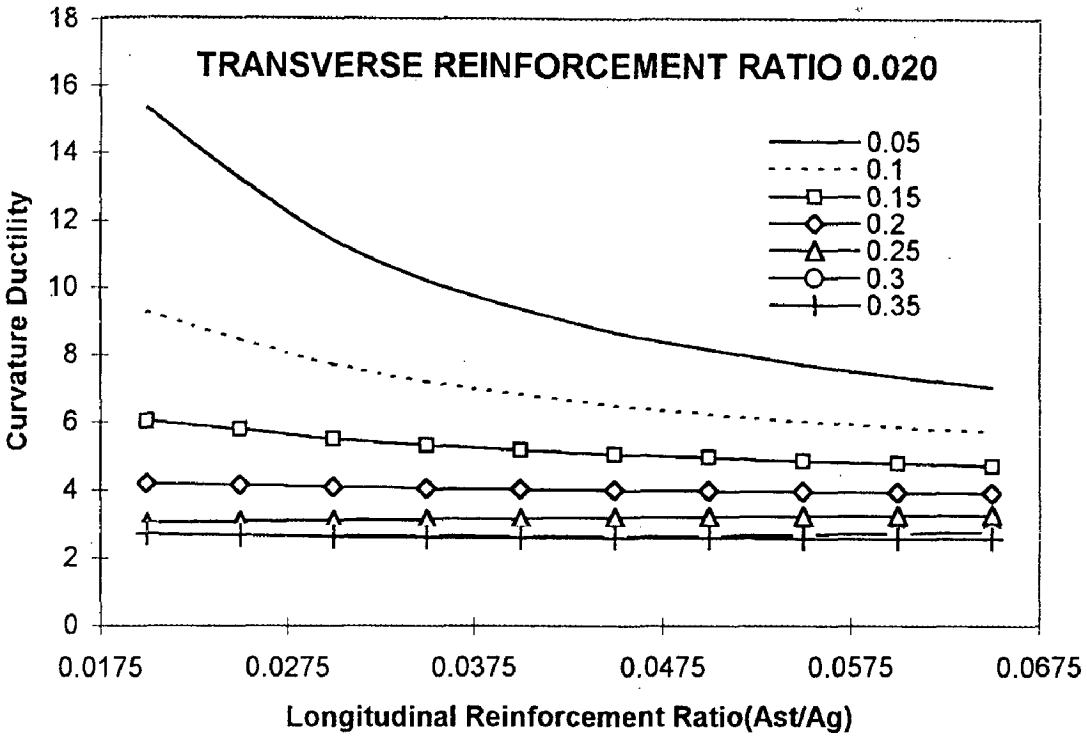

Fig.5.70 Design Chart for 0.94 Diameter Ratio hollow circular section
(fc=30.0,fy=250.0,fyh=415.0)

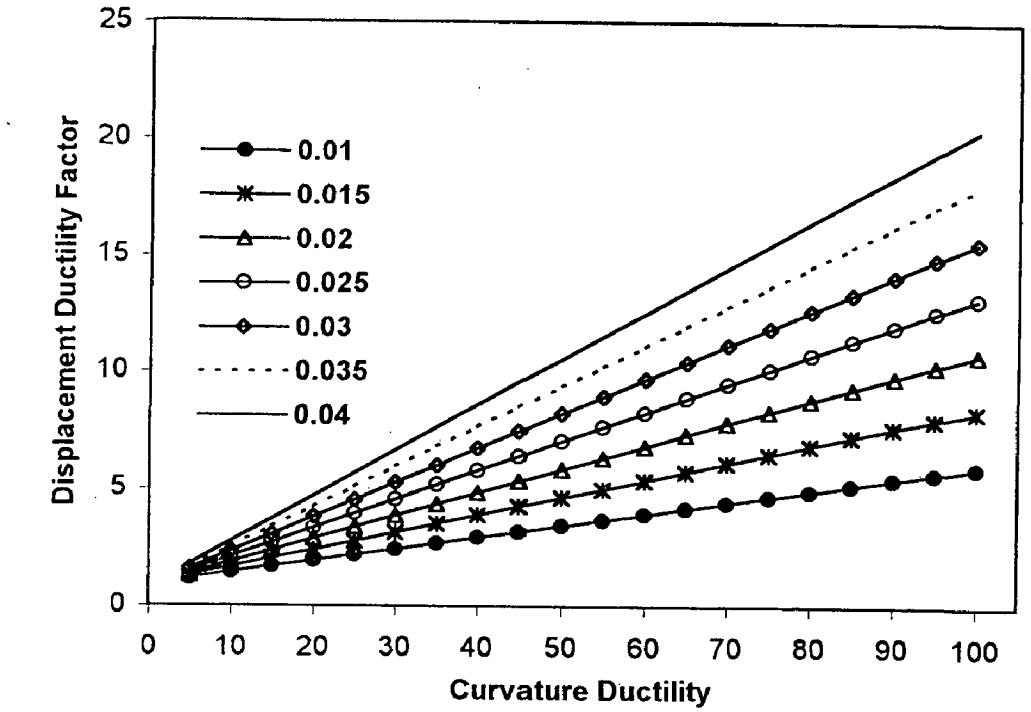

Fig.5.71 Change in Displacement Ductility factor with Curvature Ductility factor (Coefficient C=0.6)

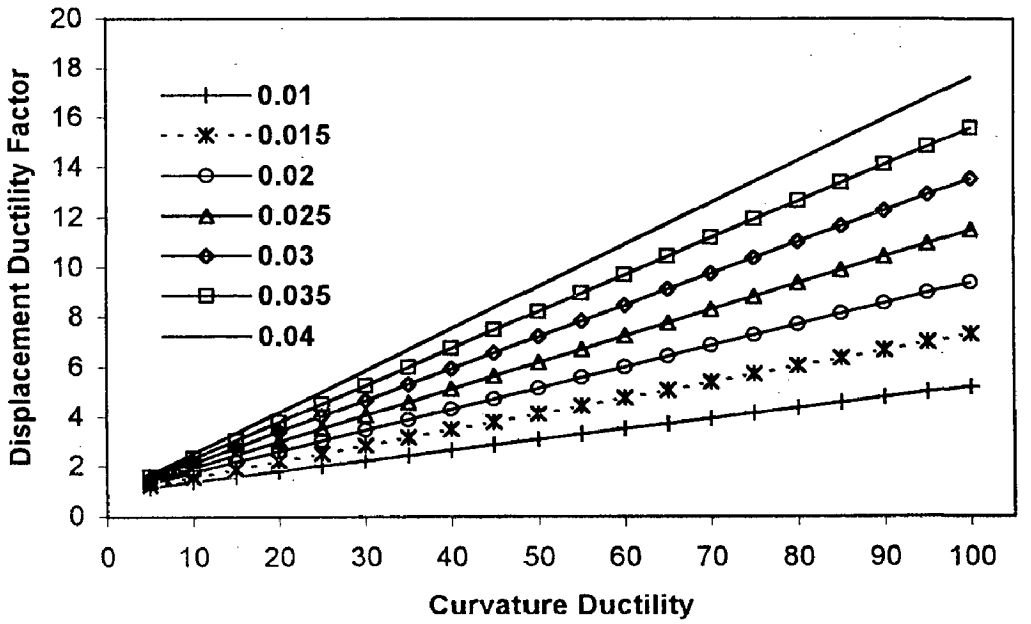

Fig.5.72 Change in Displacement Ductility factor with plastic hinge length (Coefficient C=0.7)

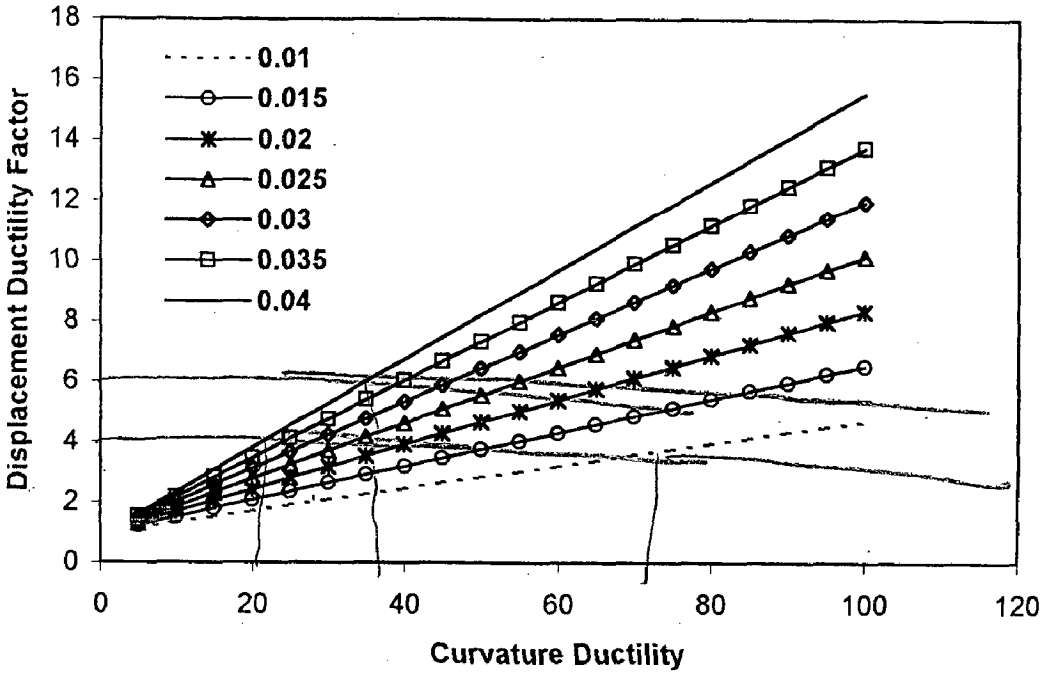

Fig.5.73 Change in Displacement Ductility factor with plastic hinge length
(Coefficient C=0.8)

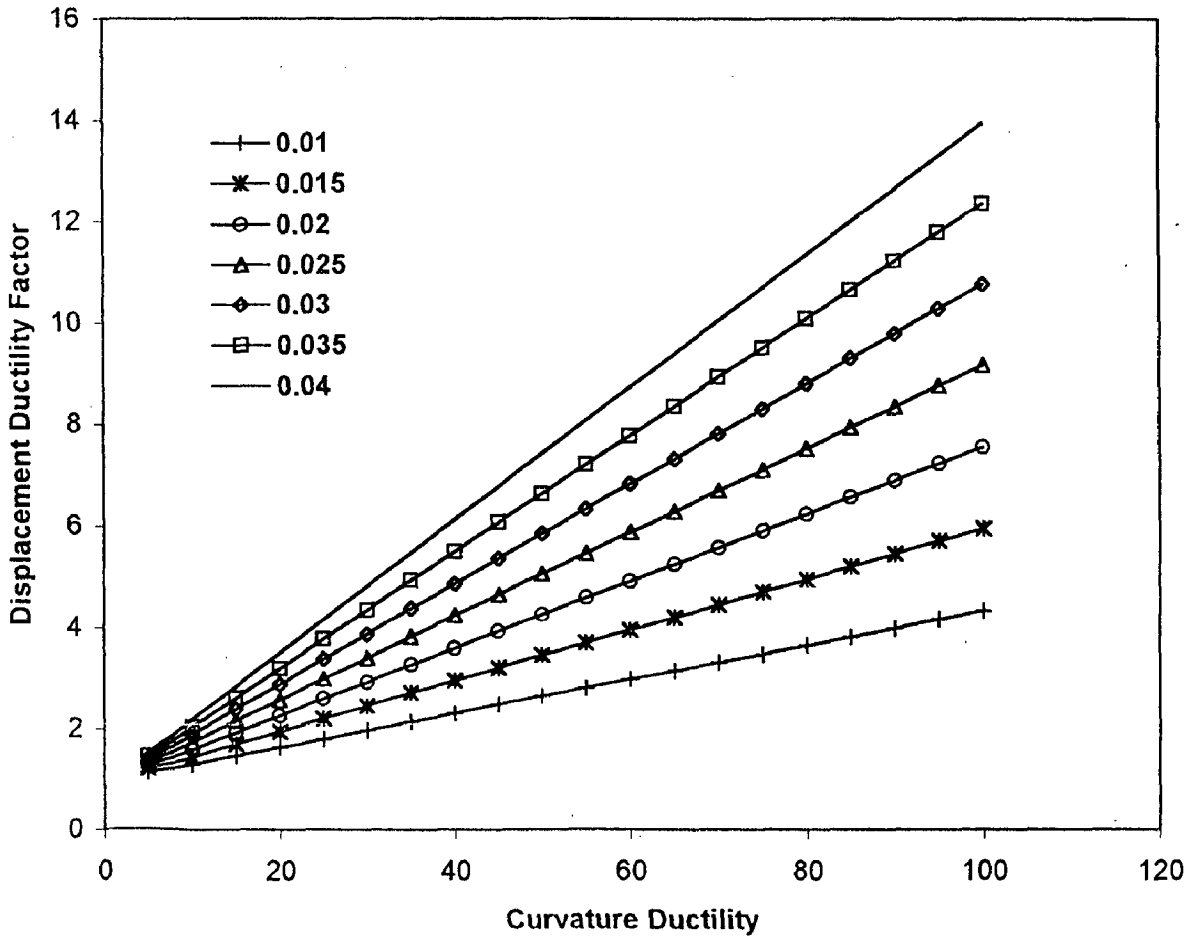

Fig.5.74 Change in Displacement Ductility factor with plastic hinge length
(Coefficient C=0.9)

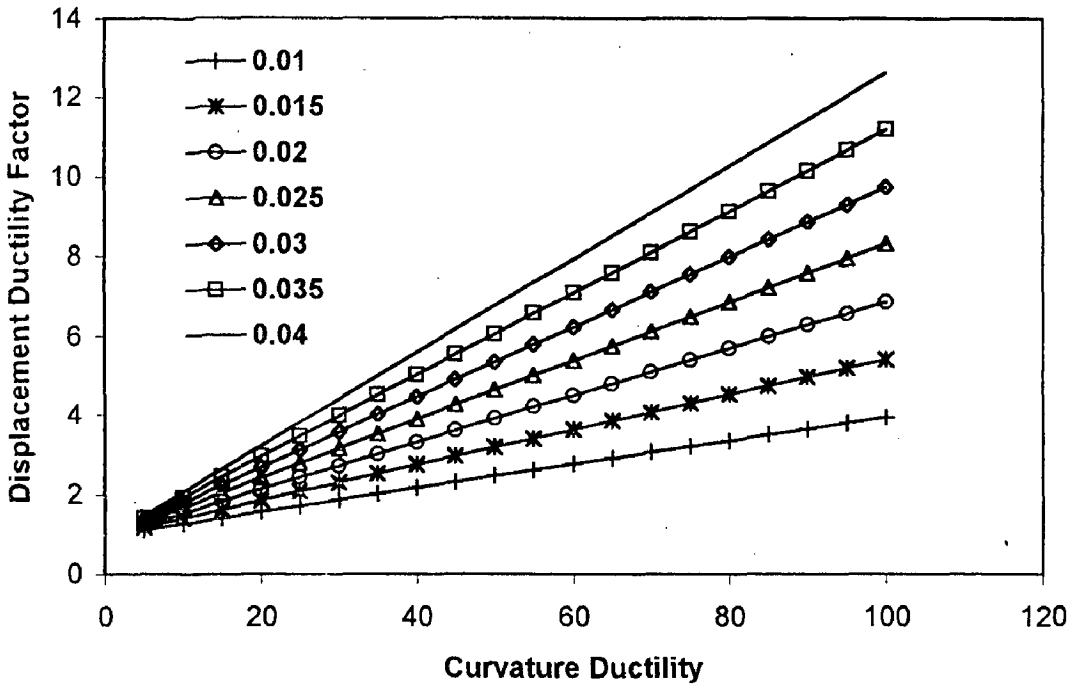

Fig.5.75 Change in Displacement Ductility factor with plastic hinge length (Coefficient C=1.0)

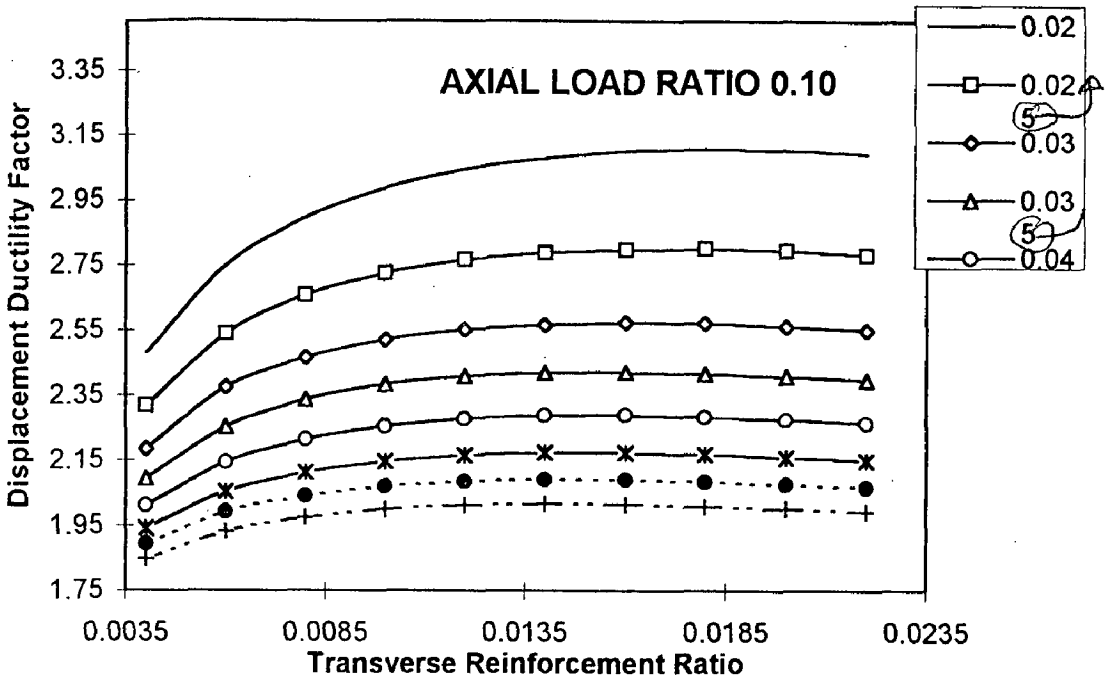

Fig.5.76 Change in Displacement Ductility factor with Transverse Reinforcement Ratio
(C=0.5,Lpr=0.02,Diameter Ratio 0.84)

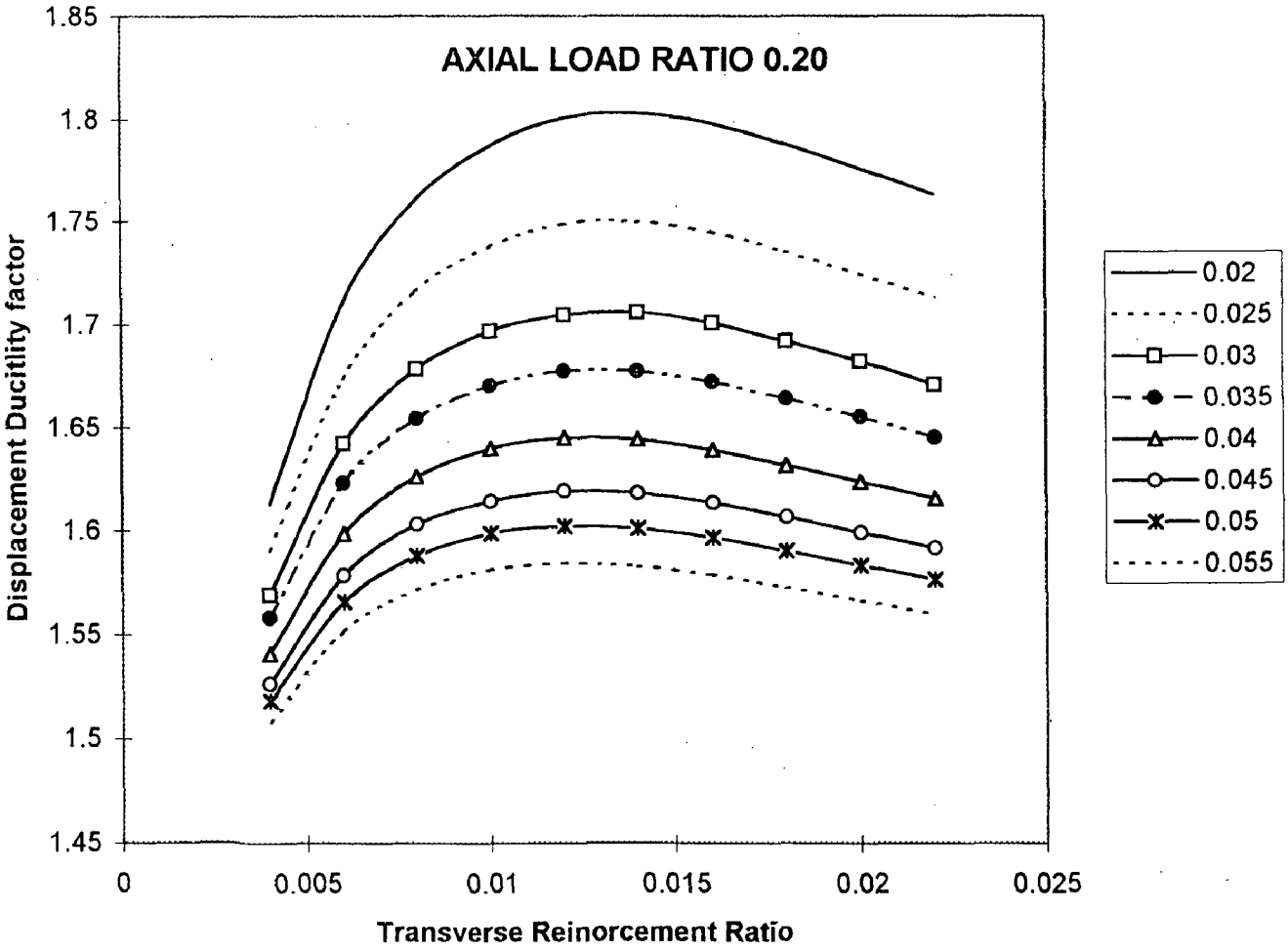

Fig.5.77 Change in Displacement Ductility factor with Transverse Reinforcement Ratio
(C=0.5,Lpr=0.02,Diameter Ratio 0.84)

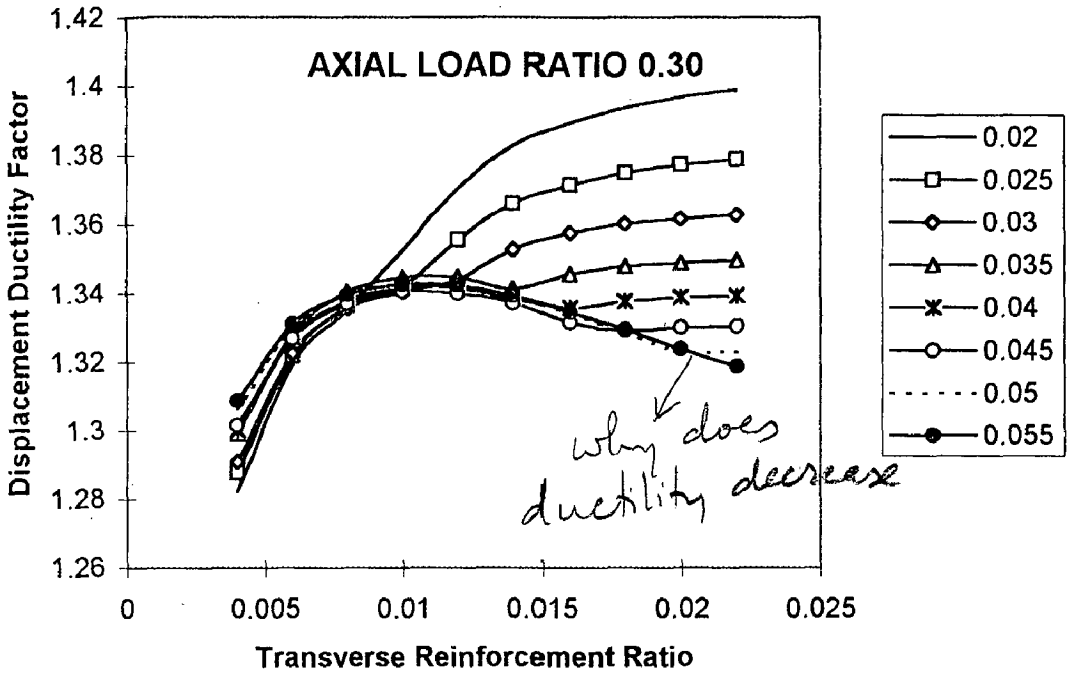

Fig.5.78 Change in Displacement Ductility factor with Transverse Reinforcement Ratio at constant Longitudinal Reinforcement Ratio
(C=0.5,Lpr=0.02,Diameter Ratio 0.84)

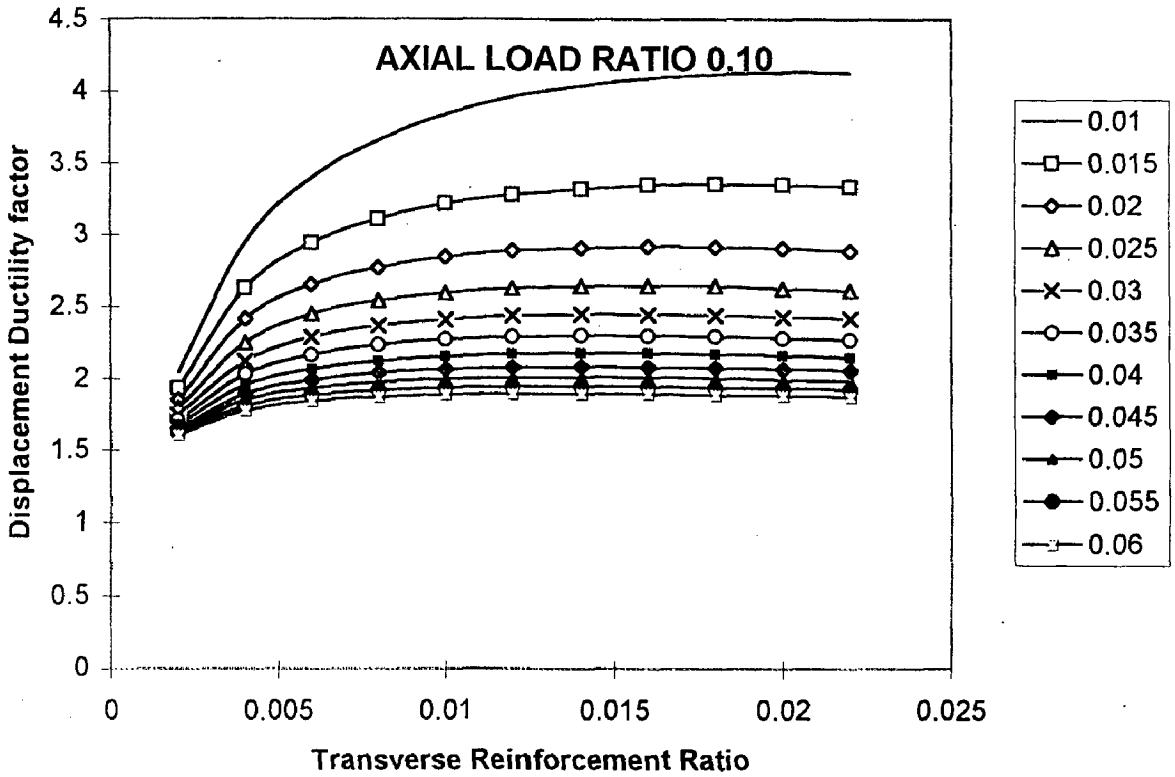

Fig.5.79 Change in the displacement ductility factor with transverse reinforcement ratio of 0.86 diameter ratio column section

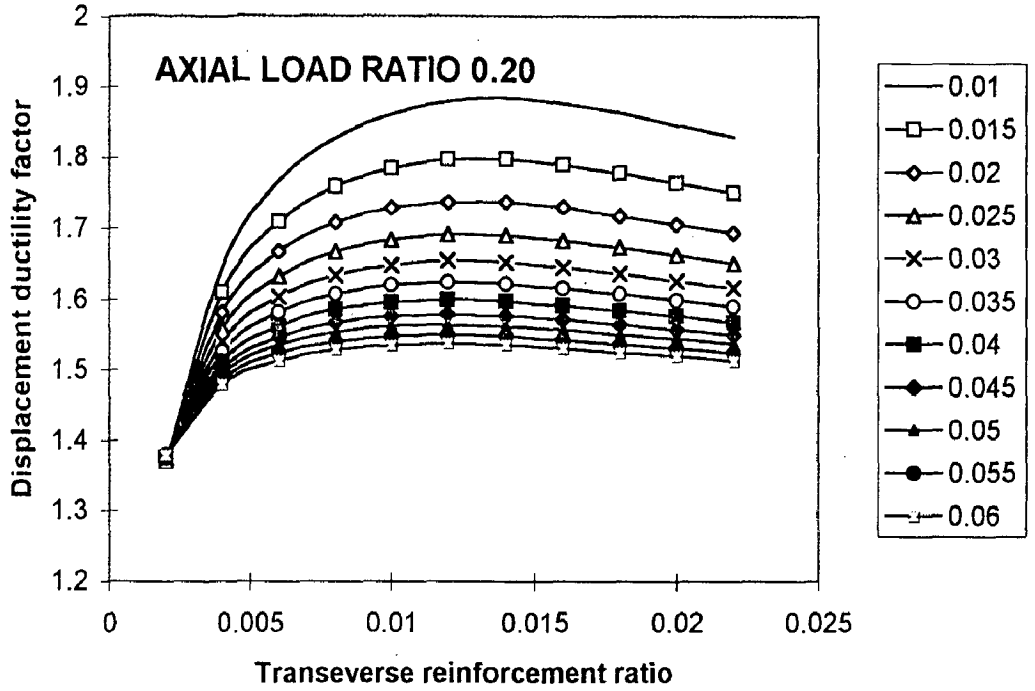

Fig.5.80 Change in the displacement ductility factor with transverse reinforcement ratio of 0.86 diameter ratio column section

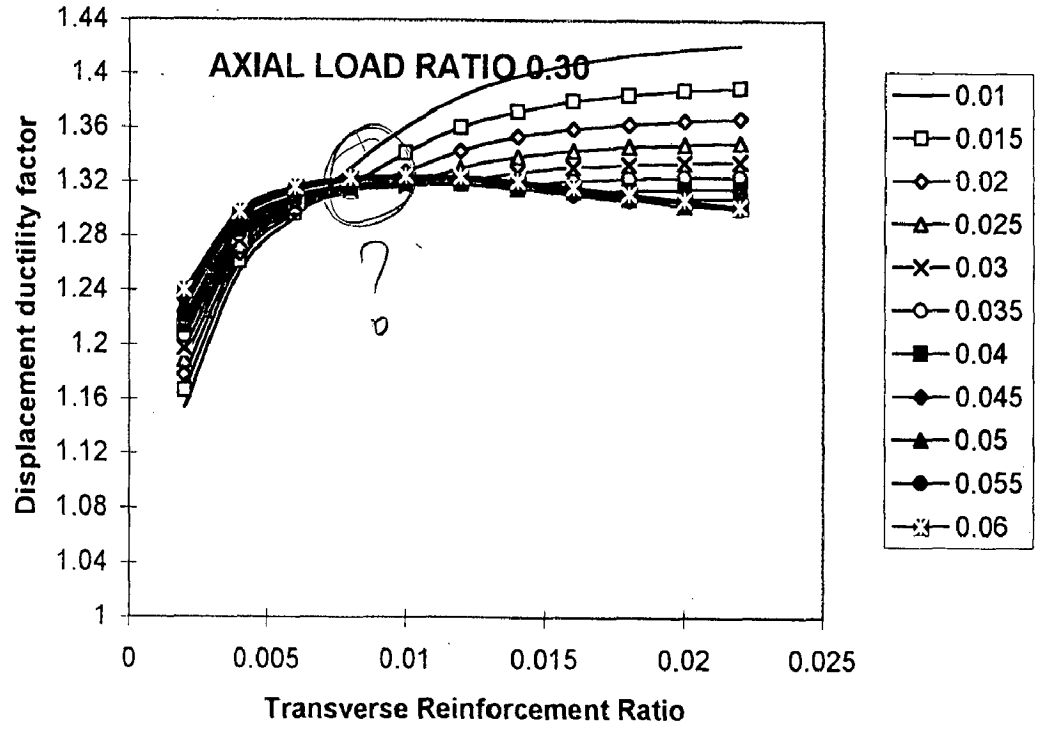

Fig.5.81 Change in the displacement ductility factor with transverse reinforcement ratio of 0.86 diameter ratio column section

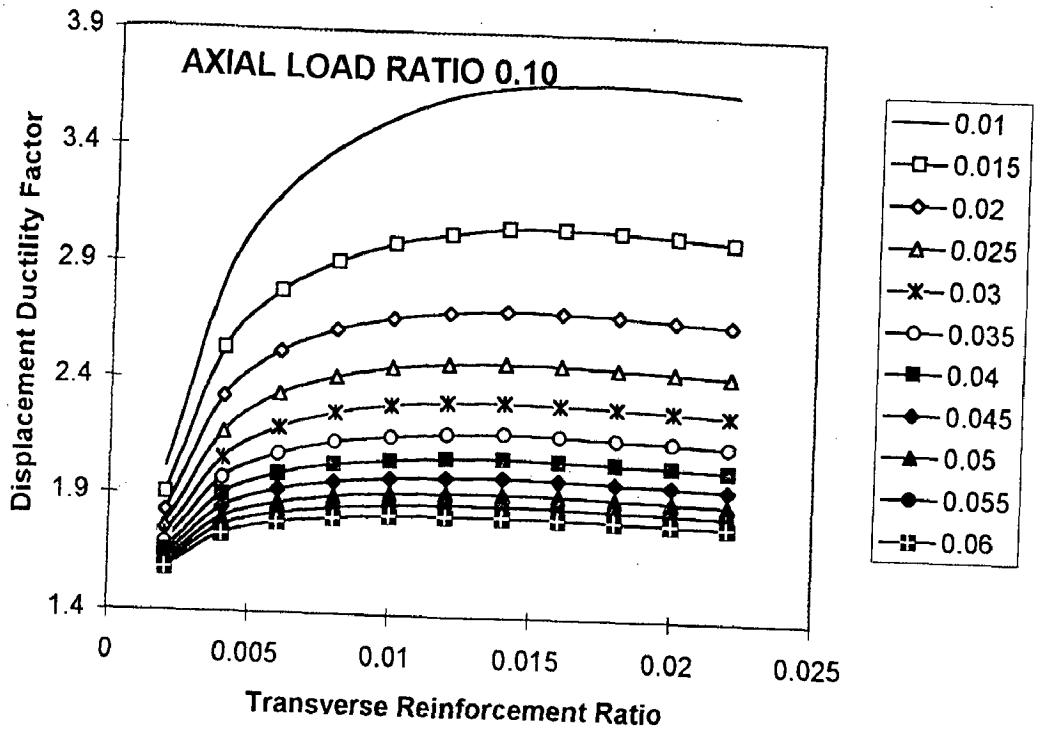

Fig.5.82 Change in the displacement ductility factor with transverse reinforcement ratio of 0.88 diameter ratio column section

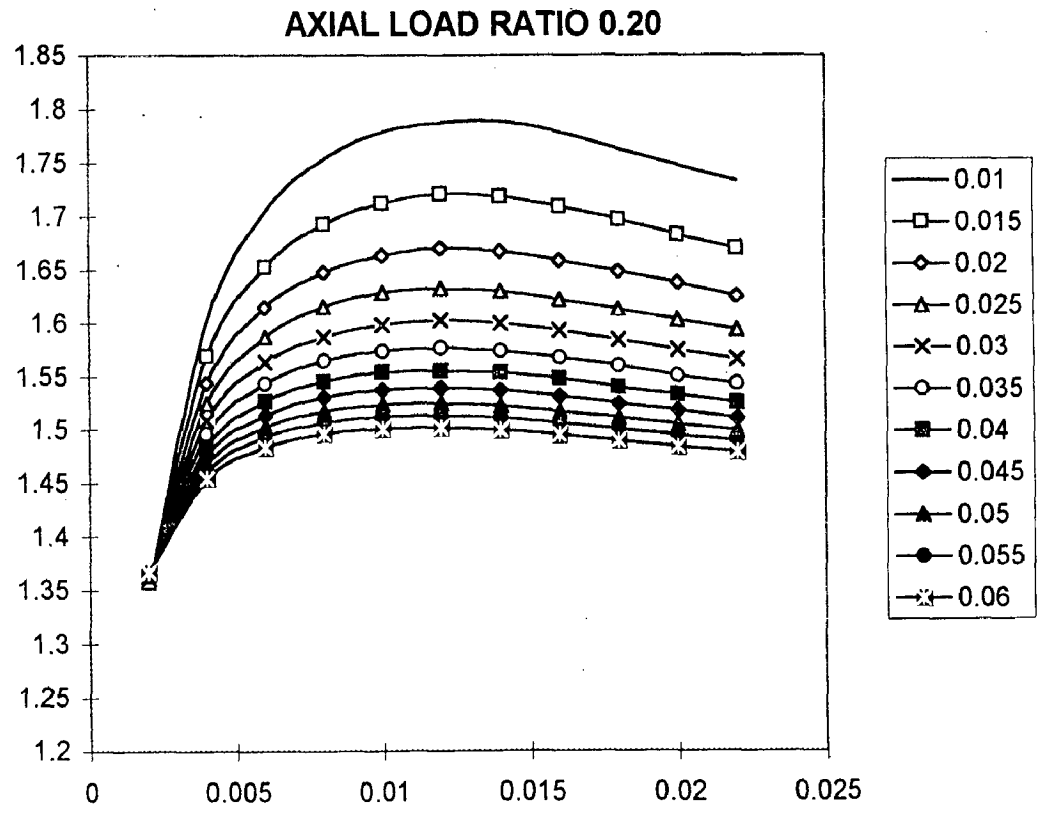

Fig.5.83 Change in the displacement ductility factor with transverse reinforcement ratio of 0.88 diameter ratio column section

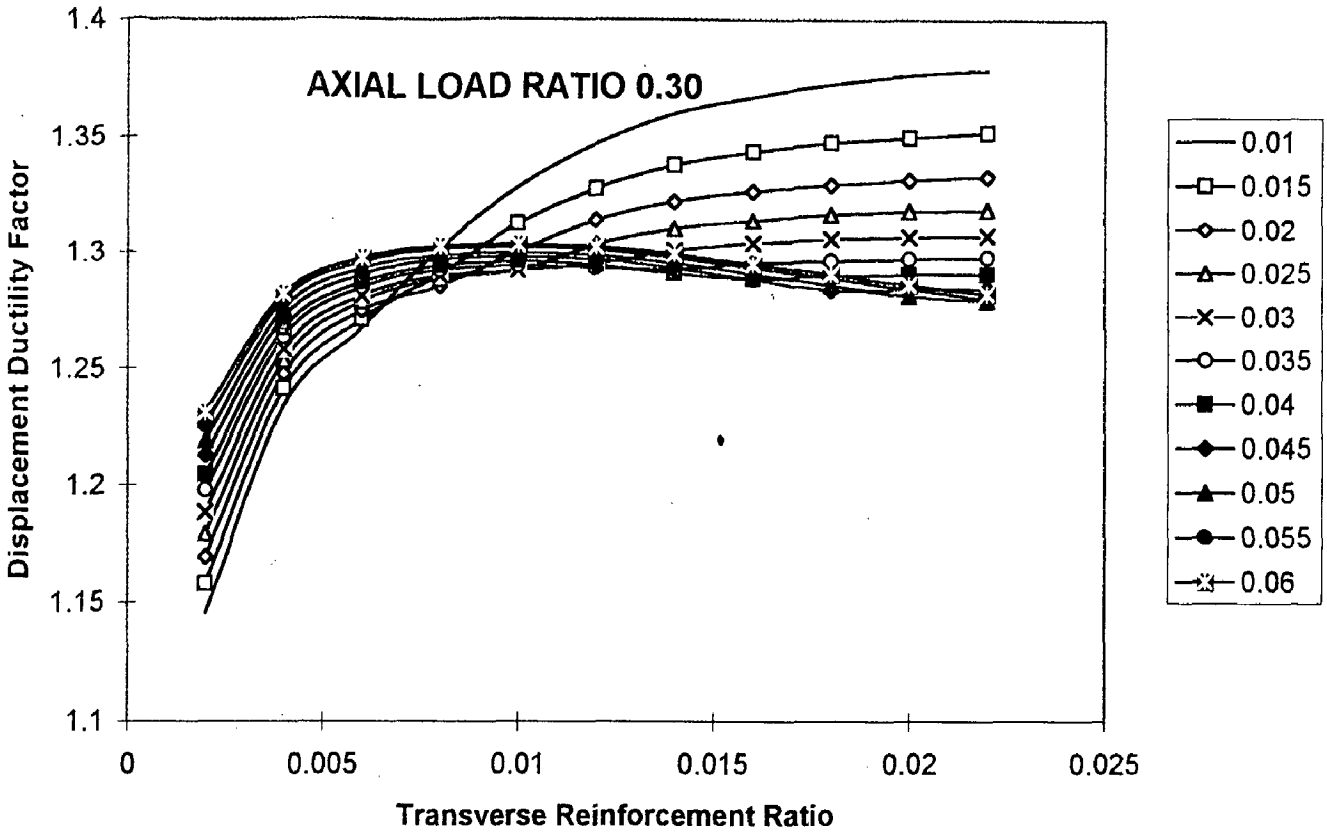

Fig.5.84 Change in the displacement ductility factor with transverse reinforcement ratio of 0.88 diameter ratio column section

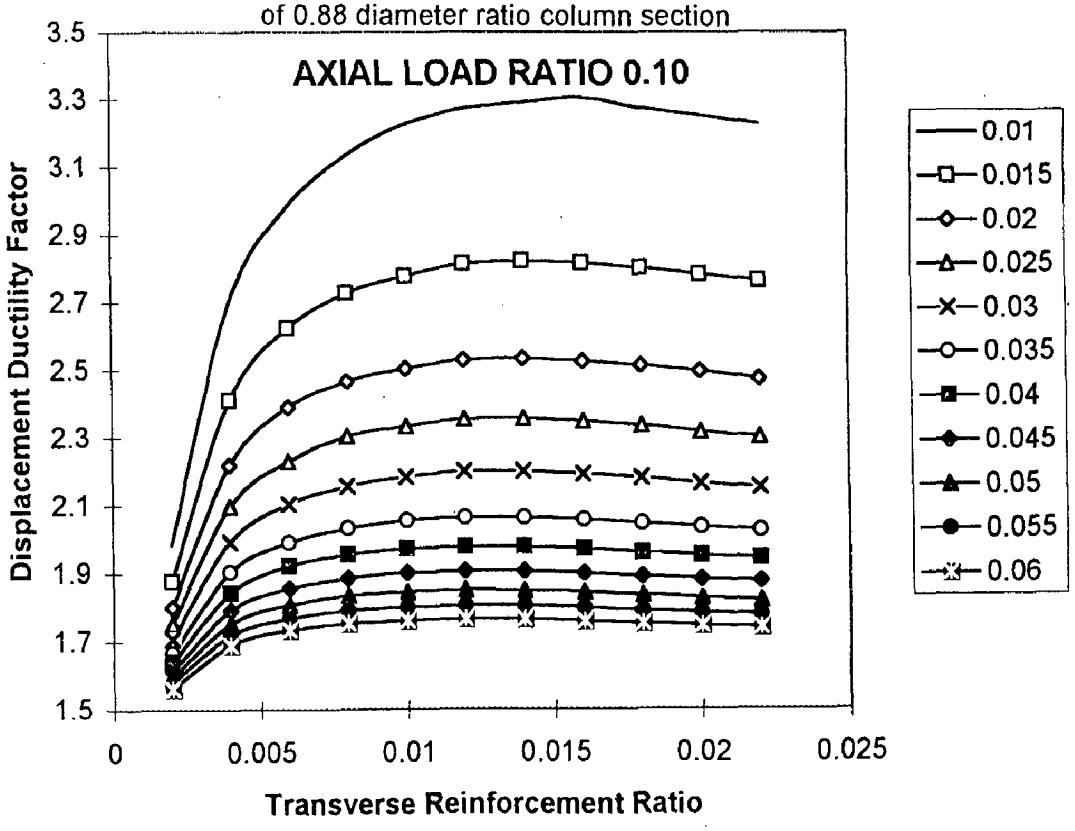

Fig.5.85 Change in Displacement ducitlity factor with transverse reinforcement ratio of diameter ratio 0.90

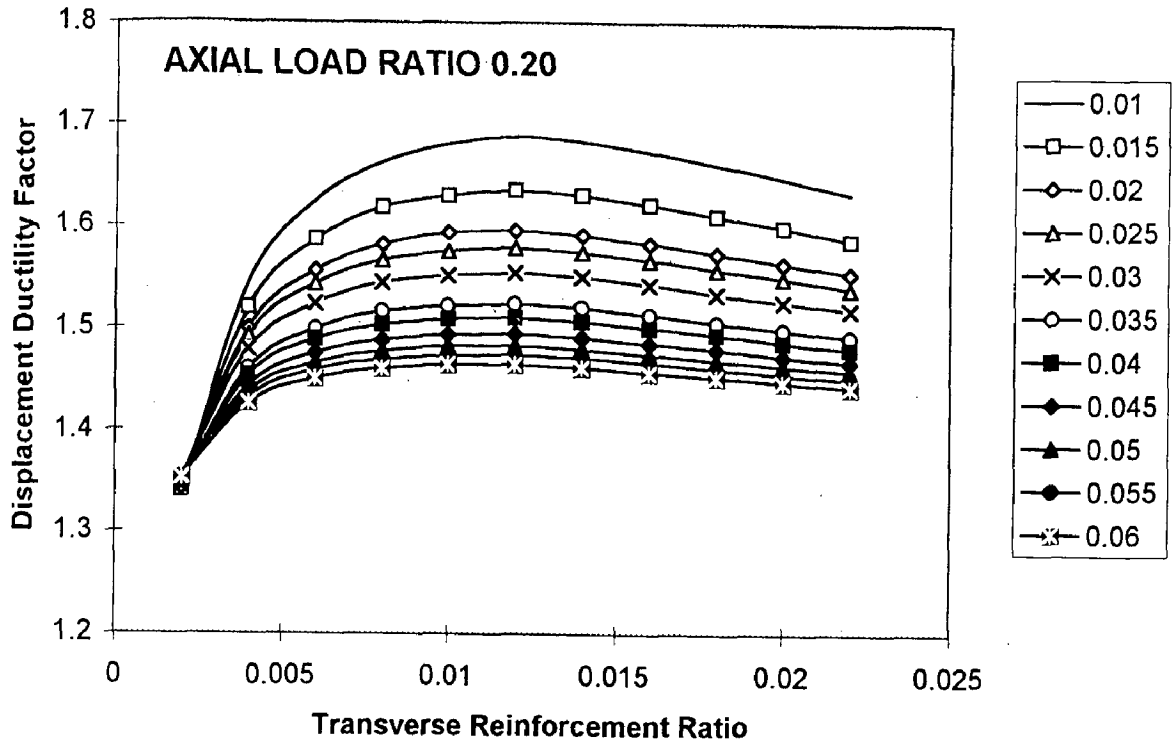

g.5.86 Change in Displacement ducitlity factor with transverse reinforcement ratio of diameter ratio 0.90

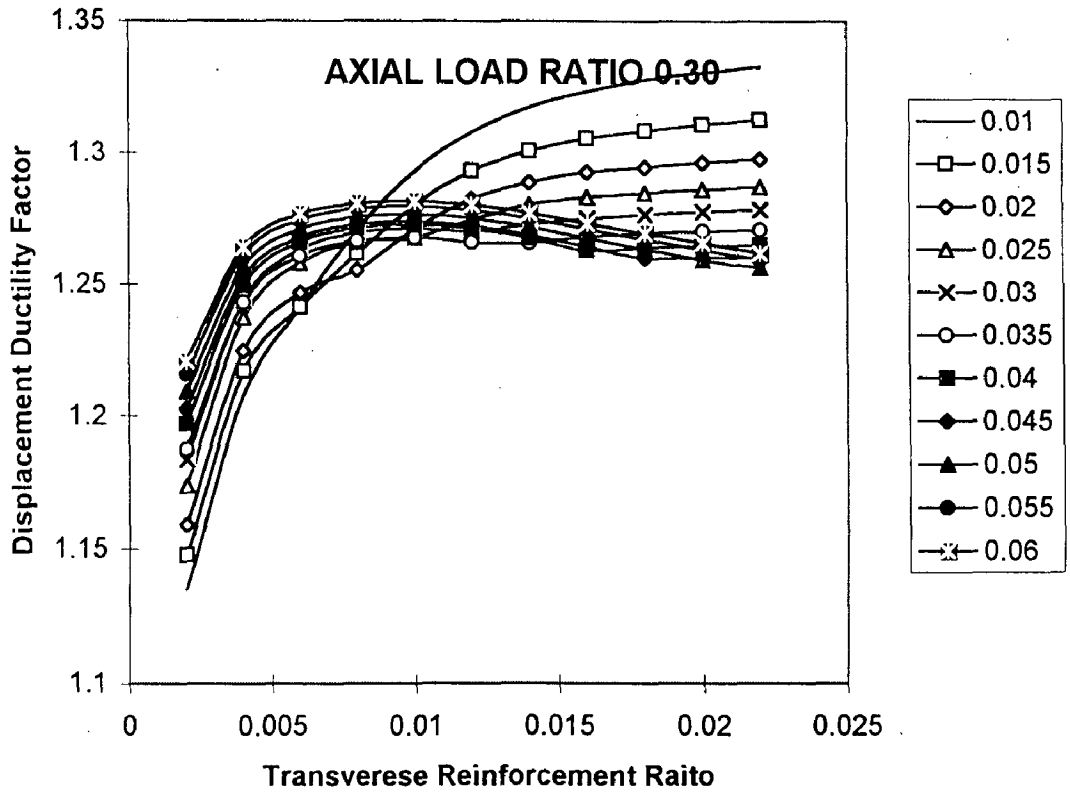

g.5.87 Change in Displacement ducitlity factor with transverse reinforcement ratio of diameter ratio 0.90

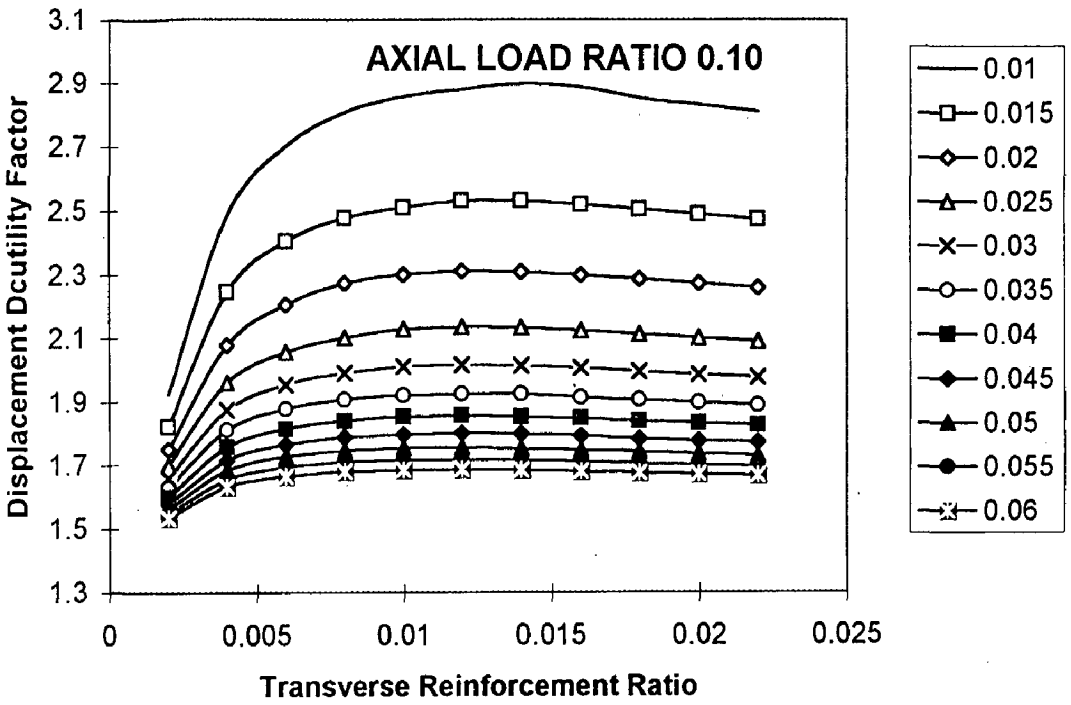

Fig.5.88 Change in Displacement ducitlity factor with transverse reinforcement ratio of diameter ratio 0.92

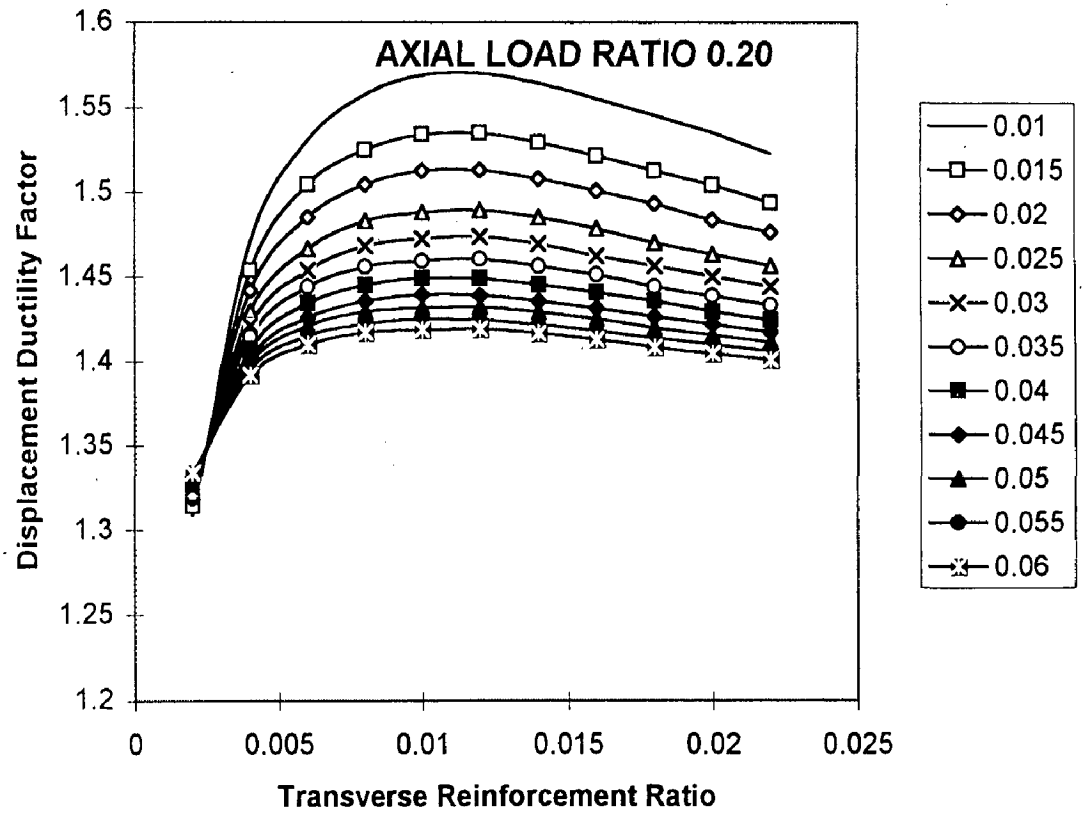

Fig.5.89 Change in Displacement ducitlity factor with transverse reinforcement ratio of diameter ratio 0.92

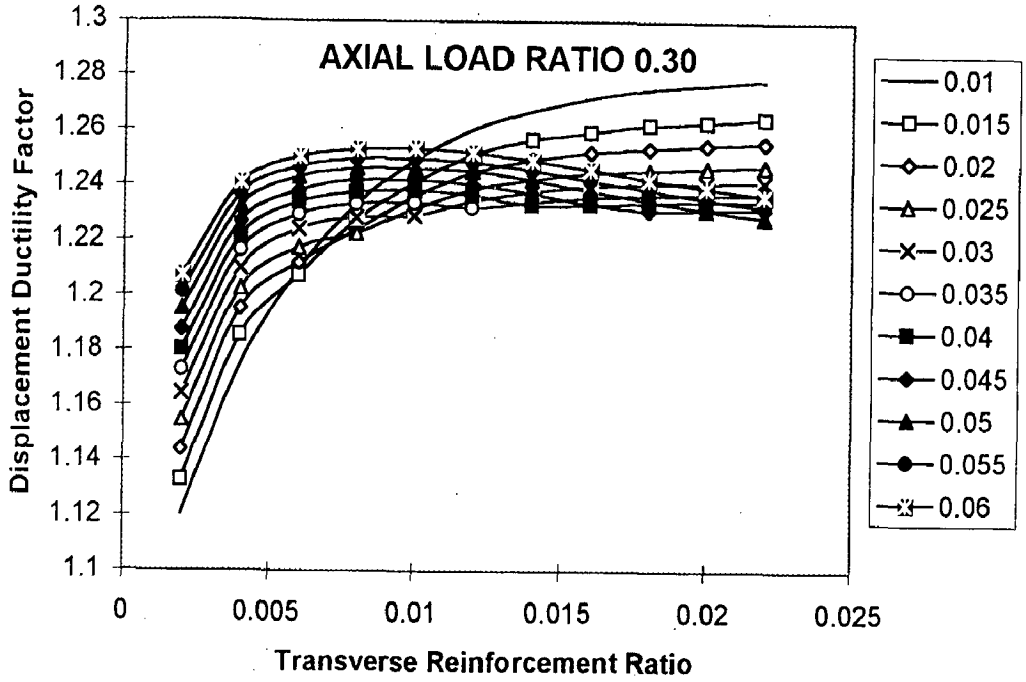

Fig.5.90 Change in Displacement ducitlity factor with transverse reinforcement ratio of diameter ratio 0.92

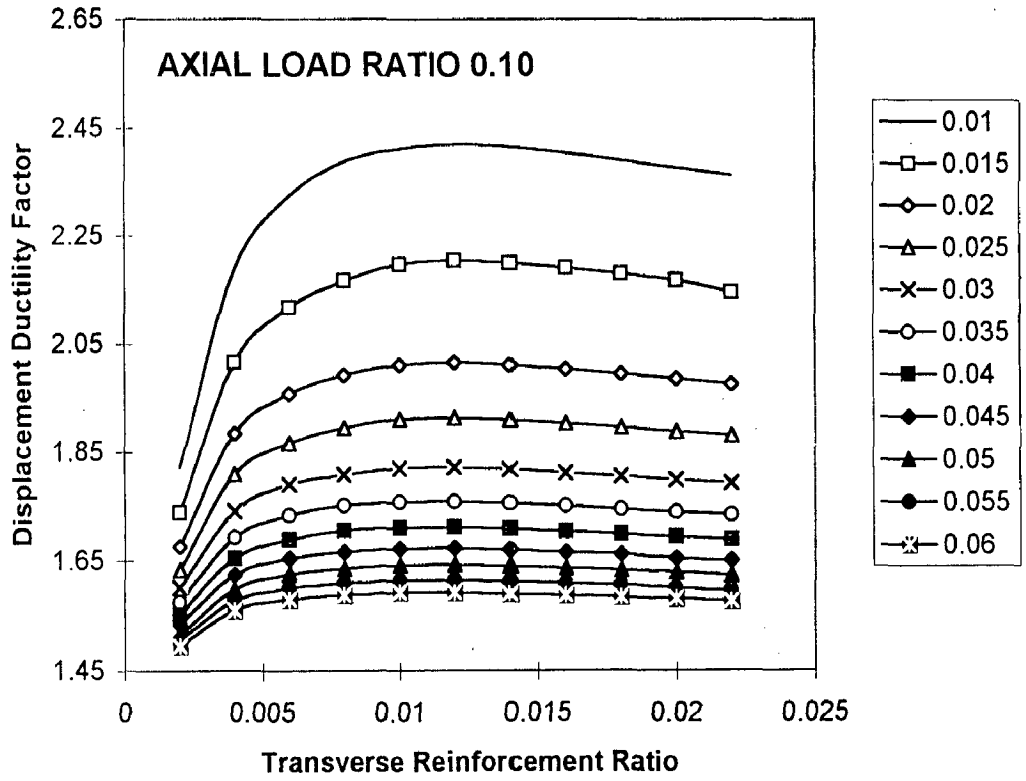

Fig.5.91 Change in Displacement ducitlity factor with transverse reinforcement ratio of diameter ratio 0.94

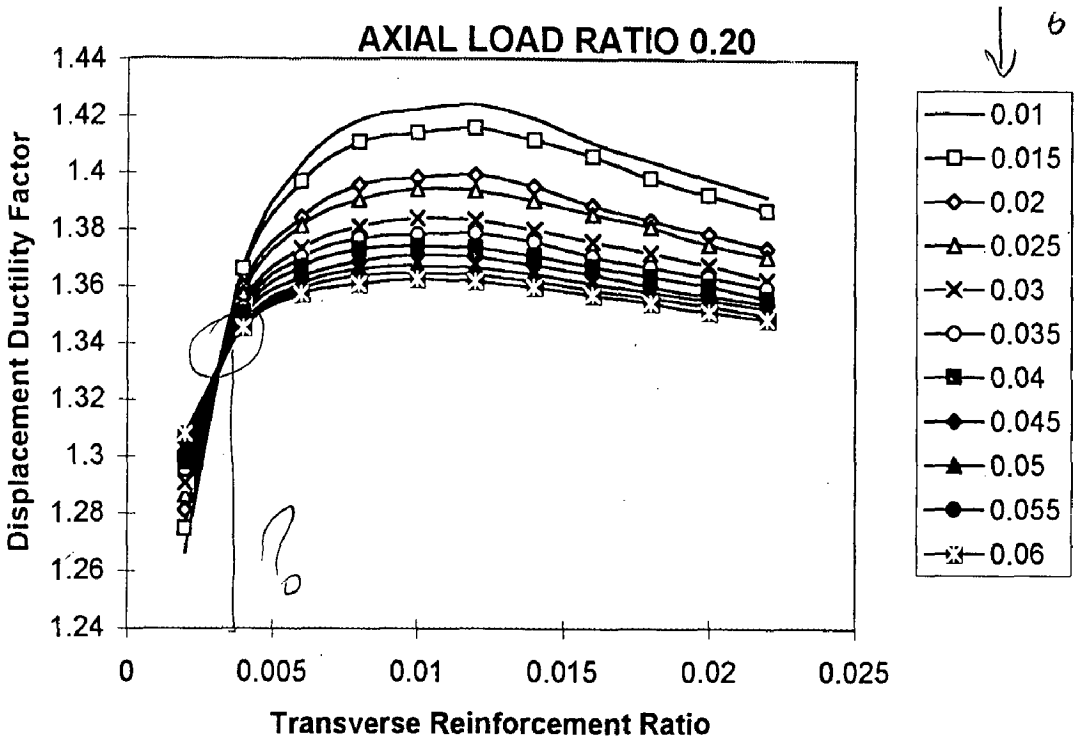

Fig.5.92 Change in Displacement ducitlity factor with transverse reinforcement ratio of diameter ratio 0.94

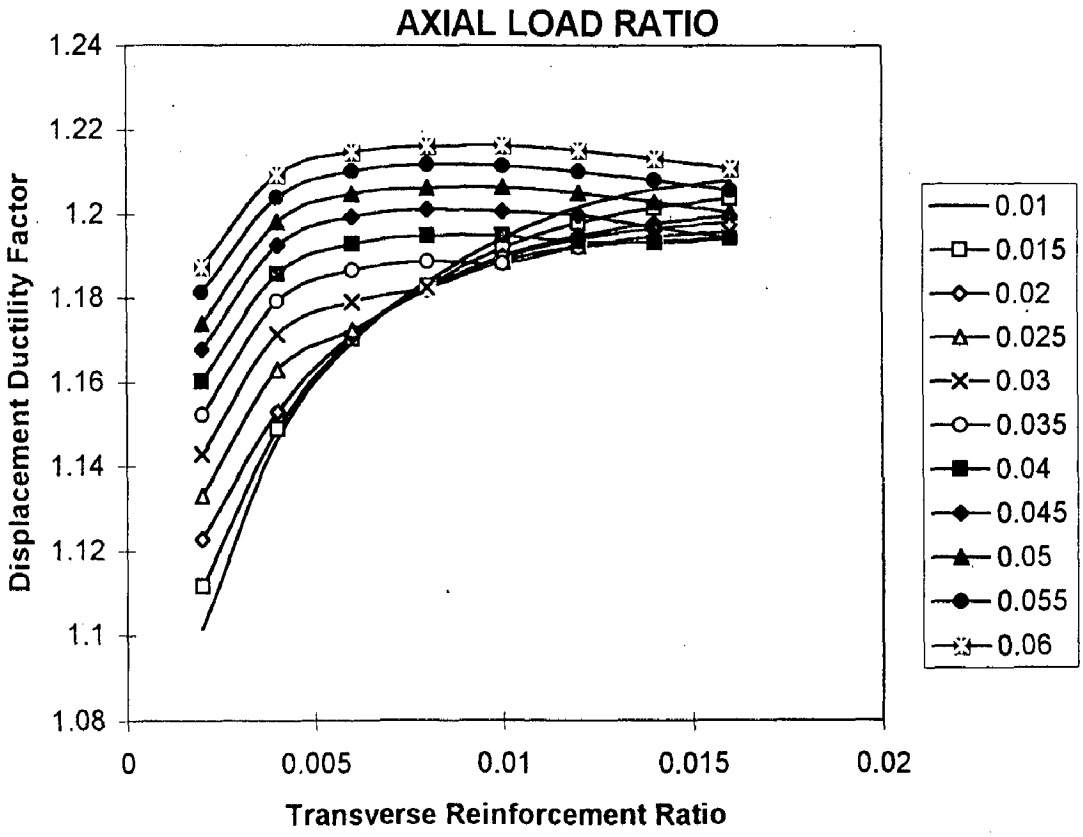

Fig.5.93 Change in Displacement ducitlity factor with transverse reinforcement ratio of diameter ratio 0.94